PROJECT SCOPE

A Satellite for Carbon Monoxide Pollution Evaluation

Cover Design by Mr. John Luchini

A Student Design Project
Department of Aerospace Engineering
The University of Michigan
April 1972

FOREWORD

Project SCOPE is one of a series of preliminary design feasibility studies conducted over the past seven years in Aerospace Engineering 483. Previous studies have included a Mars probe, Jupiter probe, solar probe, polar-orbiting meteorological and earth resources satellites, geostationary communications satellites, a teleoperator satellite and a lunar far-side communication satellite.

In this senior and graduate elective course, over a period of three months, the students develop a preliminary design based on a problem statement with specific constraints. In the current problem an experimental atmospheric pollution sensing satellite was specified. The interplay between sensors, control, launch vehicle, trajectory, communications, tracking, power, weight and volume, etc., was then investigated and the spacecraft configuration determined.

The students set up their project organization and meet two afternoons a week as a team and during weekends as sub-groups to coordinate the critical interface problems. Primary emphasis is placed upon team effort with a high degree of mutual interdependence.

Guest lectures are given by the faculty, university research specialists, industry and government specialists, and supplemented with small group conferences. The participant is given the opportunity to apply his previous theoretical and analytical course work to the highly redundant field of preliminary design. He is also in active contact with professional experts in the field. Despite the short time available, it has been found possible to select current problems of national interest and make significant contributions. Copies of the final report are distributed to industry and government for review and comment.

Professor Wilbur C. Nelson

SUMMARY

PROJECT SCOPE

SCOPE is a satellite designed to pioneer remote sensing of atmospheric carbon monoxide pollutants using state of the art satellite technology. A sensing mechanism now under development by General Electric will be used to take the measurements. The information will be recorded on one of two tape recorders and transmitted on VHF to the STADAN network once every orbit.

The sensing mechanism will require an orbit which is circular and has a lifetime of at least one year. The sensing mechanism requires a nominal orbit height of 320 nm. The orbit mode will be sun synchronous at an inclination of 97.7°. The satellite will be boosted into orbit from Vandenberg AFB with the Scout Launch Vehicle. Orbit trim will be accomplished with the aid of a rocket motor designed as part of the satellite.

The attitude control system employs sun sensors, earth horizon sensors, and a three axis stabilization system of momentum wheels. The required accuracy of 1° in nadir sensing mode and 0.05° in limb sensing mode is expected to be met when this attitude control system is used in conjunction with jet thrusters.

SCOPE weighs approximately 191 pounds. Its octagonal body is 40 inches high and 25 inches wide flat-to-flat. Two "V" type solar paddles extend perpendicular from its main body and will be used for powering the satellite in sunlight as well as provide power for recharging the NiCd batteries which are used for dark operation. Effective thermal control is accomplished with thermal insulation, a thermal conduction ring, and emmissive exterior paints.

SCOPE is designed to be launched in May 1975 at an estimated cost of approximately $5.4 million.

TABLE OF CONTENTS

FOREWORD

SUMMARY

1. INTRODUCTION 1

1.1 The Need for Carbon Monoxide Research by Satellite 1
1.2 Mission Description 1
1.3 Project Design Philosophy 2
1.4 Reference 2

2. EXPERIMENT PACKAGE 3

2.1 Introduction 3
2.2 Experimental System 3
2.3 Sensor Specifications 5
2.4 Operational Modes 8
2.5 Factors Affecting Experiment Performance 12
2.6 References 12

3. ATTITUDE CONTROL 14

3.1 Introduction 14
3.2 System Constraints and Operation 14
3.3 System Hardware 19
3.4 Attitude Sensing 24
3.5 Propulsion System 26
3.6 Component Specifications 28
3.7 References 28

4. ORBITAL ANALYSIS 30

4.1 Introduction 30
4.2 The Nominal Orbit Mapping in the Nadir Mode 30
4.3 Error Analysis 35
4.4 Propulsion System 43
4.5 References 46

5. LAUNCH VEHICLE 47

5.1 Introduction 47
5.2 Vehicle Description 47
5.3 Launch Sequence 47

5.4 Loading Factors 48
5.5 Payload Envelope 48
5.6 Launch Vehicle Systems 48
5.7 Launch Vehicle Range and Booster Splashdown 55
5.8 References 55

6. STRUCTURES 56

6.1 Introduction 56
6.2 Exterior Design 56
6.3 Interior Satellite Design 60
6.4 Weight Budget 65
6.5 References 65

7. COMMUNICATION SYSTEM 68

7.1 Introduction 68
7.2 Ground System 68
7.3 Onboard Communication System 72
7.4 Summary 80
7.5 References 81

8. POWER 83

8.1 Introduction 83
8.2 Mission Requirements 83
8.3 Solar Cells 87
8.4 Batteries 87
8.5 Complete System 90
8.6 References 90

9. THERMAL CONTROL 91

9.1 Introduction 91
9.2 Thermal Analysis 91
9.3 Passive Thermal Components 95
9.4 Auxiliary Thermal Control System 97
9.5 References 98

10. PROGRAM AND COST ANALYSIS 100

10.1 Introduction 100
10.2 Program Development Plan 100
10.3 Cost Analysis 101
10.4 Communication Network 101

10.5 Contract for Satellite 101
10.6 Contract for Launch Vehicle 101
10.7 Reference 101

11. MISSION SEQUENCE 104

11.1 Introduction 104
11.2 Mission Sequence 104

APPENDIX A 105
APPENDIX B 107
APPENDIX C 113
APPENDIX D 125
APPENDIX E 130
APPENDIX F 137
APPENDIX G 137

ACKNOWLEDGMENTS 156
SCOPE PROJECT TEAM 157

LIST OF FIGURES AND TABLES

Table 1.1	Mission Time Table	2
Figure 2.1	Schematic of Correlation Interferometer Apparatus	4
Figure 2.2	Interferometer Main Frame	6
Figure 2.3	Sink Mechanisms	9
Figure 2.4	Limb Mirror	11
Figure 3.1	Definition of Axes	15
Table 3.1	Attitude Control System Schematic	17
Figure 3.2	Orientation for Orbital Maneuvers	18
Figure 3.3	Location of Sensors	20
Figure 3.4	Yo-Yo Despin	22
Figure 3.5	Yo-Yo Despin Mechanism	23
Table 3.2	Attitude Control System Components	25
Figure 3.6	Location of Thrusters	27
Figure 4.1	Comparison of Non-Synchronous and Synchronous Orbital Planes	32
Figure 4.2	Plane and Ground Track	32
Figure 4.3	SCOPE Orbit	32
Figure 4.4	Ground Track-Polar Projection	33
Figure 4.5	Ground Track-Flat Earth Projection	34
Figure 4.6	Launch Day	36
Figure 4.7	Position of Maximum Viewing Altitude	36
Table 4.1	Apogee and Perigee Injection Errors	38
Table 4.2	ΔV Requirements	38
Figure 4.8	Apogee and Perigee Deviations due to Injection	39
Figure 4.9	Correction to Acceptable Ellipse	39
Table 4.3	Inclination Angle Errors	40
Figure 4.10	Errors in Inclination	41
Figure 4.11	Inclination Errors due to Injection	41
Figure 4.12	Plane Rotation	42
Table 4.4	Thruster and Fuel Specifications	43
Table 4.5	Fuel Weight and Burn Time	43
Figure 4.13	Propulsion System	45
Table 4.6	Weight Summary	46
Figure 5.1	Payload Envelope	49
Figure 5.2	Cross Section of Separation System	51
Figure 5.3	Stage Impact Areas	52
Figure 5.4	Stage Control Systems	53
Figure 5.5	Launch Sequence	54
Figure 6.1	Basic Payload Structure	57
Figure 6.2	Satellite Configurations	59
Figure 6.3	Paddle Boom Mechanism	61
Figure 6.4	Layout-Side View	62
Figure 6.5	Layout-Top View	63
Figure 6.6	Payload Attachment Collar	64
Table 6.1	Component Coordinates	66
Figure 7.1	Satellite Tracking and Transmitting Geometry	71
Figure 7.2	Communication System Block Diagram	73

Figure 7.3	One Cycle of Output Format	75
Table 8.1	Power Requirements	84
Figure 8.1	SCOPE Power Requirements-Nadir	85
Figure 8.2	SCOPE Power Requirements-Limb	86
Figure 8.3	Solar Paddle Folds	88
Figure 8.4	Power System Block Diagram	89
Chart 9.1	Temperature Budget	93
Figure 9.1	Radiation Zones	94
Figure 9.2	Solar Paddle Temperature Variations	96
Chart 10.1	SCOPE Development Schedule	102
Chart 10.2	SCOPE Cost Estimate	103

1
INTRODUCTION

1.1 THE NEED FOR CARBON MONOXIDE RESEARCH BY SATELLITE

High carbon monoxide levels in the atmosphere have resulted in the designation of carbon monoxide (CO) gas as a health hazard. Potentially, CO levels can create a global crisis and it is imperative that scientists learn more about its atmospheric concentrations. The rates at which the CO sources are putting concentrations in the atmosphere would tend to show that the present concentrations would be double those of four years ago. Apparently this has not been happening. The CO concentration levels have been rather stable for the past eight years implying that there exists some mechanism for absorbing CO and taking it out of the atmospheric environment. It is important for scientists to understand this mechanism and analyze its effectiveness, as well as find the locations of these sink mechanisms, as they are commonly called (Reference 1).

Since it is desirable to research the CO pollution problem on a global scale, a satellite is the logical vehicle for transporting a sensing system. This project report is a preliminary design and feasibility study of such a satellite. The project is called SCOPE, Satellite for Carbon Monoxide Pollution Evaluation, in the hope that it will aid scientists to effectively put the pollution problem in proper scope and make solutions easier and faster.

1.2 MISSION DESCRIPTION

SCOPE employs a carbon monoxide sensor proposed by General Electric in AIAA Paper No. 71-1120. At an orbital inclination of 97.7 ^{o} and an altitude of 320 nm the satellite is expected to have a life time of at least one year, and will be able to completely scan the earth's surface in less than three months. Two basic types of measurements will be made: a nadir mode which aims the sensor at the earth's surface and a limb mode which will scan through the atmosphere into the sun and obtain a profile of CO concentrations in the upper atmosphere. Both of these types of measurements are expected to aid immeasurably to the study of carbon monoxide.

A brief mission time table is outlined in Table 1.1. Mission sequence for SCOPE is shown in detail in Section 11 of this report; a complete discussion of the sensing sequence appears in Section 2.

May 1, 1975	Launch from Vanderberg AFB
May 1 - June 1	Vehicle outgassing and orbit trim maneuver
June 1 - Nov 23	Nadir viewing measurements - 6 mos.
Nov 23 - Nov 25	Limb viewing measurements
Nov 25 - Feb 21	Nadir
Feb 21 - Feb 23	Limb
Feb 23 - Mar 23	Nadir
Mar 23 - Mar 25	Limb
Mar 25 - May 1	Nadir

Table 1.1. Mission Time Table

1.3 PROJECT DESIGN PHILOSOPHY

SCOPE was designed so that the most advanced state of the art components could be used. They were chosen with regard to reliability, efficiency and cost so that an inexpensive, realistic system could be manufactured and be ready for launch in 1975. The anticipated cost for two such satellites is expected to be approximately $5.4 million.

1.4 REFERENCE

1. Grenda, R.N., Bortner, M.H., Carbon Monoxide Pollution Experiment (I). A Solution to the Carbon Monoxide Sink Anomaly, AIAA, Paper No. 71-1120, November 1971.

2
EXPERIMENT PACKAGE

2.1 INTRODUCTION

The sensor used onboard SCOPE is a modified Michelson interferometer currently being designed for carbon monoxide detection by General Electric. This correlation interferometer was selected due to its large capacity for data handling, light weight, and compactness. The interferometer has high stability requirements, however, no difficulties are anticipated in meeting them.

The sensor detects the 2.35 micron absorption band (4240-4340 cm^{-1}) of carbon monoxide for both its primary and secondary modes of operation, which are nadir viewing and limb viewing respectively. Measurements will be made in the concentration range from ten parts per billion to ten parts per million.

A radiometer has been added to the equipment package to obtain a temperature profile of the atmosphere and to determine the amount of atmosphere through which the incoming spectrum has passed.

2.2 EXPERIMENTAL SYSTEM

The incoming light, after having been separated by a spectral filter, is split at a beamsplitter. The split beams then travel toward two different mirrors where they are reflected back through the beamsplitter. The beams now recombine slightly out of phase causing an interference pattern. This interference pattern, known as an interferogram, is passed through a collecting lens which focuses it on the detector. The interferogram is then stored for later transmission to the ground.

To insure that the split beams travel through equal refractive thicknesses, a compensating plate is added into one beam path. The delay between the beams is also introduced in this path (see Figure 2.1) to form the interferogram. In normal laboratory interferometers this delay is usually achieved through a translation of one of the mirrors. The inaccuracy of translation makes such a mechanism impractical for satellite applications, thus the correlation interferometer of SCOPE incorporates an alternative method for creating the delay. The compensating plate mentioned previously rotates and scans the optical path difference. Hence, mirrors are rigidly fixed and system reliability is increased by reducing the susceptibility to vibrations and tilt.

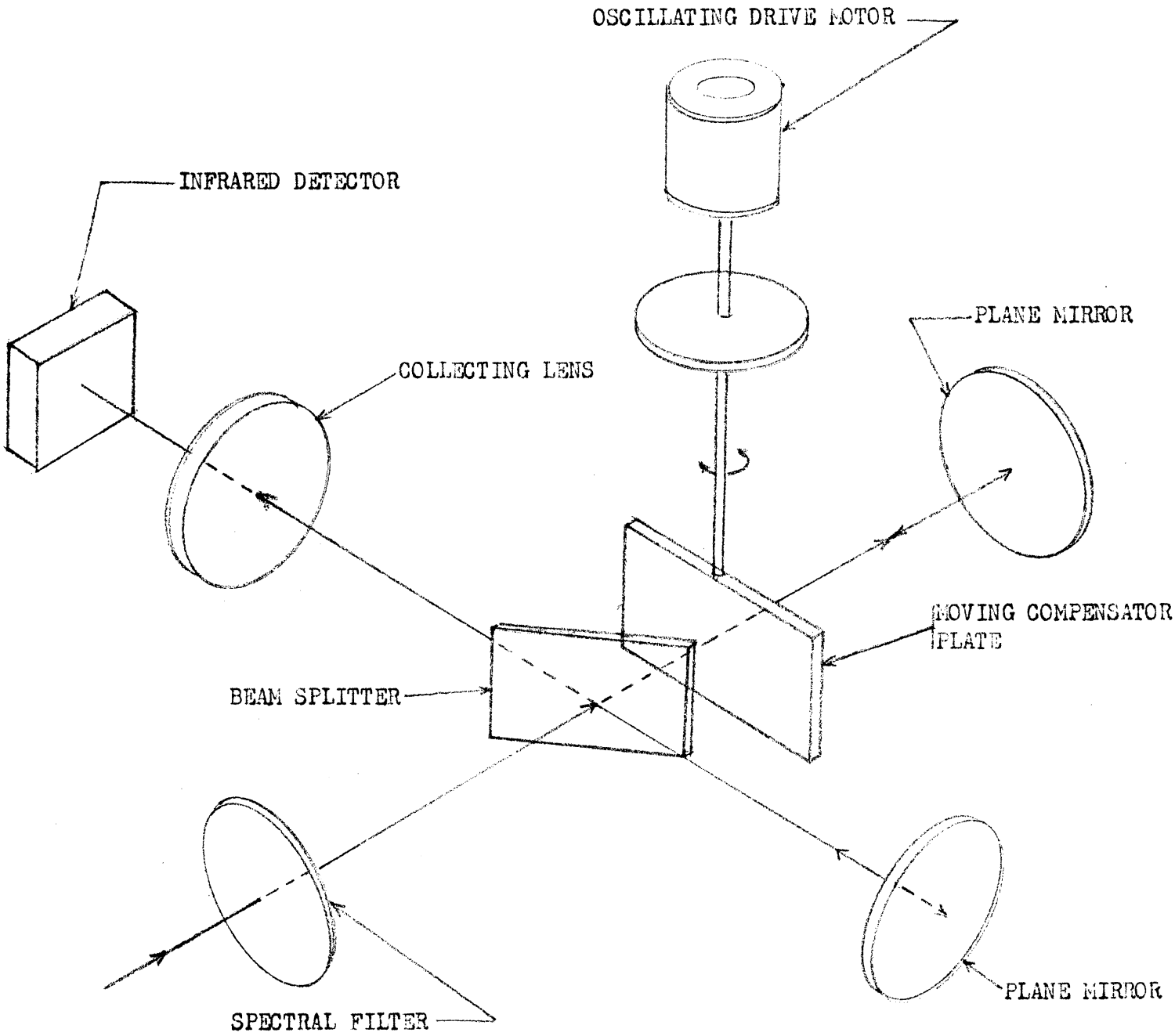

Figure 2.1 Schematic of Correlation Interferometer Apparatus

Radiometers measure the intensity of electromagnetic radiation within a given spectral interval. The radiometer onboard SCOPE yields information on the distribution of molecules along the line of sight.

The complete SCOPE package includes an interferometer, radiometer, and limb mirror assembly.

2.3 SENSOR SPECIFICATIONS

2.3.1 Structural Specifications

The weight breakdown is as follows:

sensor package (including radiometer, detector cooling, and frame)	35 lbs
limb mirror assembly (includes mirror, mirror frame, and servos)	2.3 lbs
total weight	37.3 lbs

The main frame of the interferometer is shown in Figure 2.2. It is constructed of fused titanium silicate and weighs 3.3 lbs. The various components of the interferometer are fit into this frame. When complete, the interferometer package is 13" in depth with a 8" x 6" viewing face. This includes the lead sulfide (PbS) detector. The radiometer has a 4" x 3" viewing face with a 6" depth.

The mirror which is deployed for limb measurements will be made of polished beryllium. Beryllium is suggested because of its lightness, high melting point, modulus of elasticity which is about one third greater than steel, nonmagnetic quality, and low thermal expansion. The mirror's dimensions are 3.25" x 15" x 0.1".

2.3.2 Thermal Specifications

SCOPE's non-operating thermal range is 0° to 50°C. During operation, the maximum thermal range is 0° to 50°C with a tolerance of 10°C. Heat dissipation is 5 watts. Included is the heat released by the cooling of the PbS detector to $195^{\circ} \pm 1^{\circ}$K. The detector cooling is accomplished by a thermoelectric cooler which is oriented to the cold side of the spacecraft.

2.3.3 Power Specifications

Operation of SCOPE's instruments requires 28 volts with a 10% tolerance. Power required by the sensor varies due to the several operational

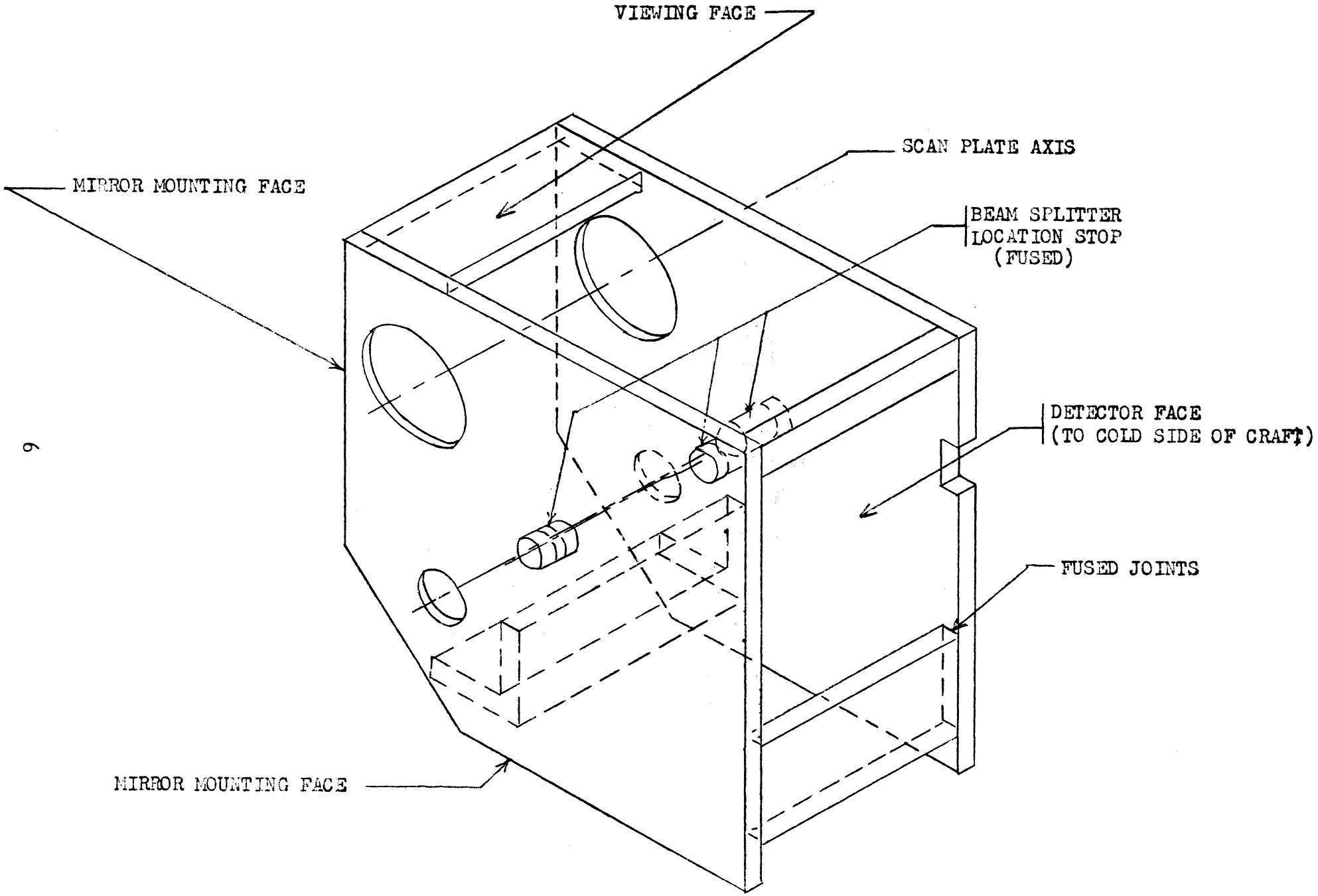
VIEWING FACE
SCAN PLATE AXIS
MIRROR MOUNTING FACE
BEAM SPLITTER
LOCATION STOP
(FUSED)
DETECTOR FACE
(TO COLD SIDE OF CRAFT)
FUSED JOINTS
MIRROR MOUNTING FACE

modes the package will experience. While on the dark side of the earth, where no measurements are to be taken, 5 watts of power are required to keep the unit on standby. During nadir operation on the light side of the earth, 15 watts of power are necessary. For deployment of the limb mirror and the stopping down of the satellite field of view, 25 watts are required. These power specifications include the radiometer operation.

2.3.4 Flight Characteristics

The experiment directivity is $\pm 30^{\circ}$ from nadir. The stability requirement is 2° per minute. A pointing accuracy of 1° is required for nadir viewing while an accuracy of 0.05° is required for limb viewing. The necessary accuracy of attitude determination is 0.5° and the required orbital tracking accuracy is 1 nautical mile.

2.3.5 Instrument Characteristics

SCOPE's interferometer package has a nadir field of view of 7° (0.12 radian). Its aperture is 6.6 cm in diameter. A field stop to a field of view is 0.5° will be used for the limb mode.

The radiometer has a 3 cm diameter aperture with a 0.5° field of view.

The 2.35 micron absorption band was selected for carbon monoxide measurements. This band is advantageous because atmospheric and ground temperatures, as well as emissivity, are not required for processing data. Additionally, measurements at this band are interpreted directly in terms of carbon monoxide densities. The disadvantage in choosing this band is that the interferogram picked up at the detector is a combination of carbon monoxide (CO), methane (CH_4), and water vapor (H_20), as methane and water vapor both strongly overlap this band. However, this is not a problem, for when the interferogram is processed on the ground, the carbon monoxide, methane, and water vapor effects are separated.

2.3.6 Data Handling

The amount of data handled is 1200 bits per second. This digital output includes experimental data, housekeeping, plus a small contingency factor. The breakdown is as follows:

data rate:	15 bits per word
spectrum scan:	64 sample points x 15 bits per word = 960 bits per
scan rate:	1 scan per second second
housekeeping:	10 words = 150 bits per second
radiometer:	1 word = 15 bits per second
contingency:	5 words = 75 bits per second

2.3.7 Signal Processing

Signal processing will have as its goal the measurement of one or more of the parameters which comprise the particular structure of the input spectrum. These parameters include such items as profiles and quantities of various atmospheric absorbers in the optical path and the temperature and pressure structure along the path.

As the interferogram itself is a function of both the delay setting and structure of the spectrum, signal processing theory is applied and a weighting function or linear filter is applied to the interferogram to make the measurement. The basic method followed in generating a set of data for use in determining a suitable weighting function for the carbon monoxide, methane, water vapor mixture is detailed in Reference 1. It has been found that any set of weighting functions obtained using carbon monoxide densities in the mid to low range and water density and temperature conditions which span their range of use are adequate for determining amount of carbon monoxide.

Measurements will be made in the concentration range from ten parts per billion to ten parts per million.

2.4 OPERATIONAL MODES

2.4.1 Nadir Viewing (earth viewing)

As shown in Figure 2.3, there exists numerous possible sink mechanisms, most of which are located on the surface of the earth. For this reason, SCOPE has selected nadir viewing as its primary mode of operation.

At a nominal altitude of 320 nautical miles, the 7^{o} field of view will cover an area of 39.34 nautical miles squared. With a good deal of overlap, particularly over land masses, the surface of the earth will then be mapped in approximately 88 days.

2.4.2 Limb Viewing (solar viewing)

The possibility of a transport of carbon monoxide to the upper atmosphere cannot be ignored. Therefore, SCOPE is equipped to measure vertical carbon monoxide profiles from the earth's surface to an altitude of 43.1 nautical miles (80.0 km) as the spacecraft travels from the light side to the dark side of the earth at the south pole.

Rather than rotate the spacecraft, which would add thermal problems as well as additional fuel, it was decided to run the limb experiment utilizing a mirror which would be external to the spacecraft and deployed

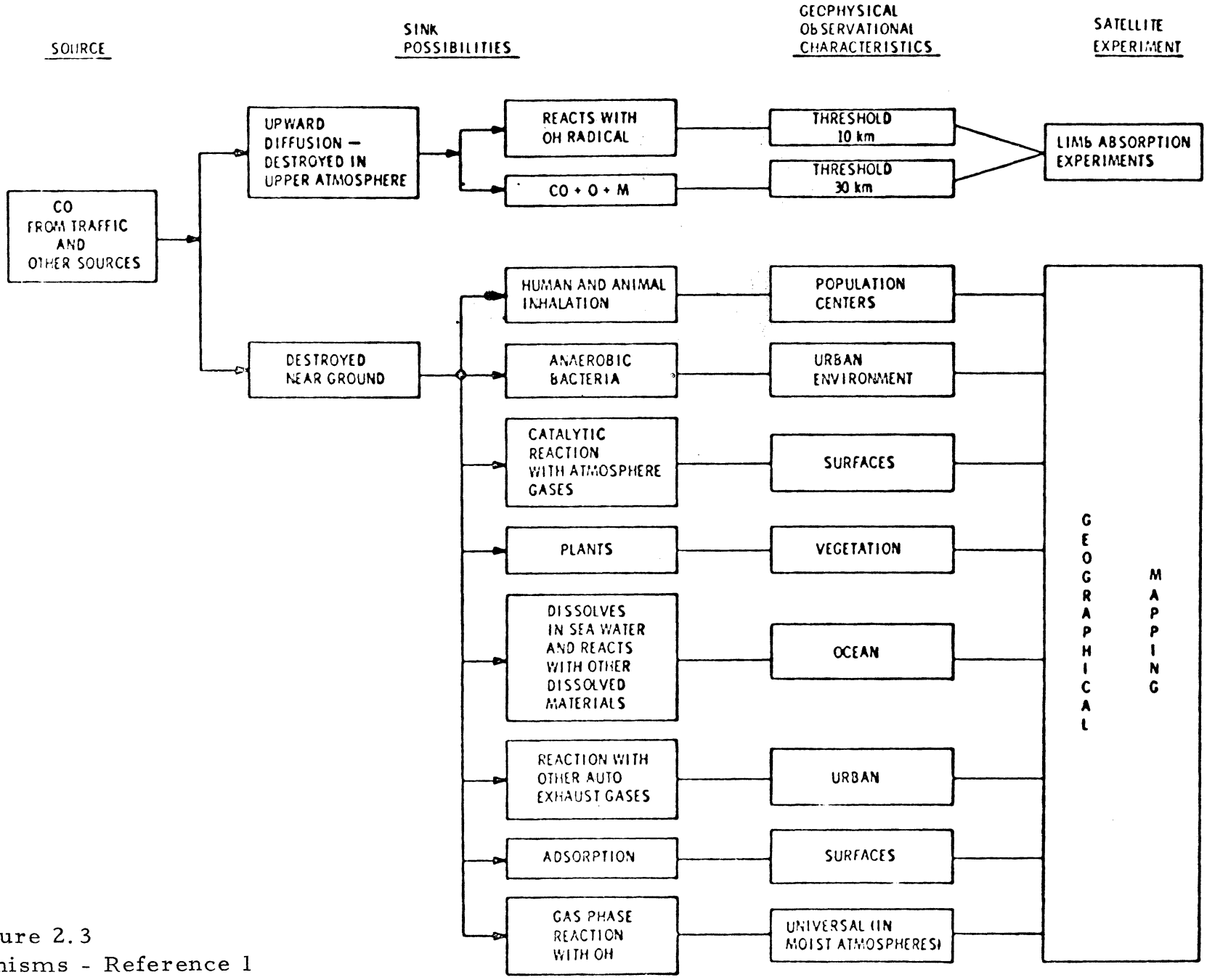

Figure 2.3
SinkMechanisms - Reference 1

only for limb measurements. While the spacecraft is in the nadir mode of operation, the mirror assembly will be stored in a recession on the underside of the craft.

When limb measurements are to be taken, the aperture of the equipment package must be stopped down to give a field of view of 0.5^{o} The onboard sun sensors must then lock onto the sun. After the confirmation of this operation, the mirror assembly will be raised to an angle of 45^{o}. The assembly is then rotated 90^{o} as to arrive at the configuration of Figure 2.4. Elevation and rotation servos should have vernier adjustments to correct for mirror errors. Using the procedure outlined in Appendix A, the total time required for the taking of carbon monoxide measurements is 28.9 seconds.

Mirror deployment should be controlled from the ground so as to provide researchers with maximum opportunity to switch modes of operation as the situation warrants. A suggested timeline is given in Section 2.4.3.

2.4.3 Mission Timeline

As mentioned previously, carbon monoxide measurements taken during nadir mode is the primary mission objective. With this in mind, SCOPE will follow the time line shown below. This time line takes into account possible seasonal variations in carbon monoxide concentration both on the ground and in the atmosphere.

Two days of limb measurements are deemed sufficient as the data is obtained from the same locale on each orbit.

May 1, 1975 launch date

May 1 - June 1 outgassing

Date	Mode of Operation
June 01 - Nov. 23	nadir
Nov. 23 - Nov. 25	limb
Nov. 25 - Feb 21, 1976	nadir
Feb. 21 - Feb. 23	limb
Feb. 23 - Mar. 23	nadir
Mar. 23 - Mar. 25	limb
Mar. 23 - on	nadir

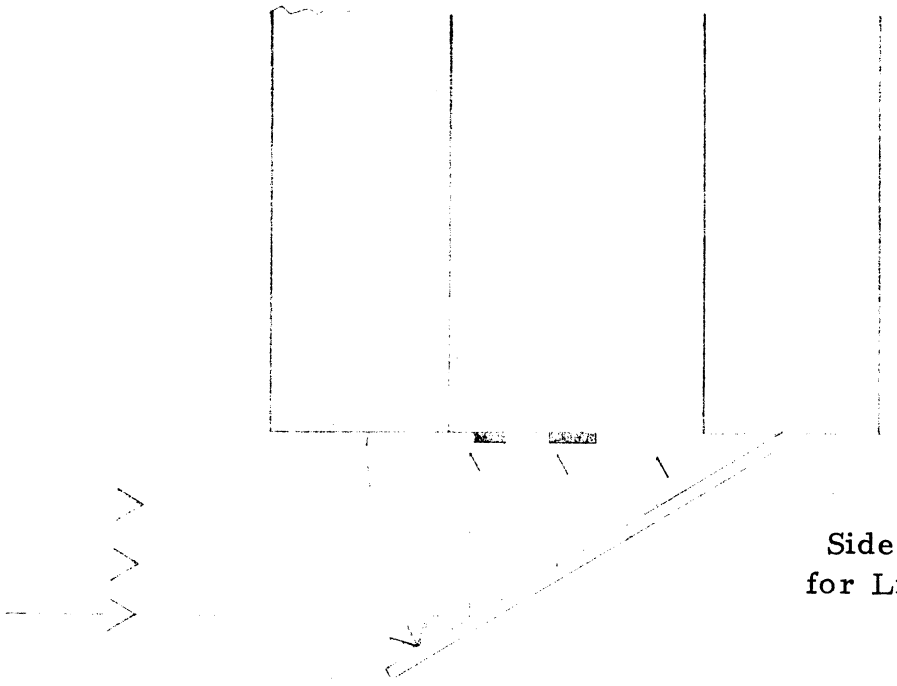

Side View of Satellite
for Limb Mirror Deployment

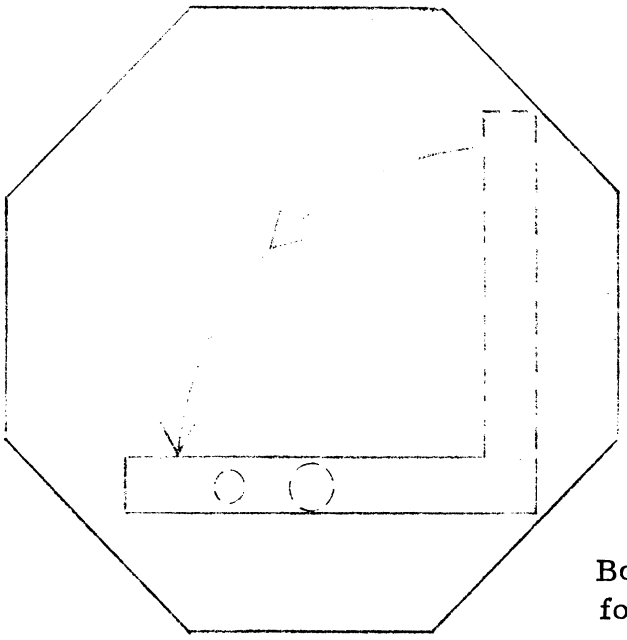

Bottom View of Satellite
for Limb Mirror Deployment

Figure 2.4

2.5 FACTORS AFFECTING EXPERIMENT PERFORMANCE

2.5.1 Launch Shock Acceleration

The G load due to acceleration during launch is a prime concern for the success of the mission as the high G's experienced could possibly damage the package. Therefore, shock mounting of the experiment package is advisable.

2.5.2 Limb Mirror Failure

Two types of limb mirror failure have been considered in SCOPE's design. The first is failure of deployment of the mirror for limb measurements. In this case, SCOPE's prime mission of nadir mapping would still be accomplished and continue.

Another failure possibility is that the mirror will not retract to its stored (nadir) position after being used for limb viewing. Such a failure, according to the mission timeline, cannot occur until after the major portion of the nadir mapping has been completed. Hence, constrainment to the limb mode for the remainder of the mission would not eliminate much of the primary data.

2.5.3 Scanning Drive Motor Failure

The heart of SCOPE's sensor unit is the oscillating scan drive motor. Its failure would disable the entire package. Although a redundant drive unit could be included, the performance of existing units has proven dependable and reliable enough for the required one year mission lifetime.

2.5.4 Cloud Cover

Cloud cover acts as an optical barrier to SCOPE's interferometer. For this reason, SCOPE uses a radiometer to measure the atmosphere through which the incoming light has passed. In the event of radiometer failur the Nimbus satellite system could be used in determining cloud cover thicknes

2.6 REFERENCES

1. R. N. Grenda, M. H. Bortner, P. J. LeBel, J. H Davies, R. Dick, "Carbon Monoxide Pollution Experiment - (I). A Solution to the Carbon Monoxide Sink Anomaly", AIAA paper no. 71 - 1120 from Joint Conference on Sensing of Environmental Pollutants, Palo Alto, Calif. Nov. 8-10, 1971

2. Goldstein, H. W., private communication Jan. 20, 1972

3. Mertz, L. Transformations in Optics, Wiley, New York, 1965, p. 63.

4. Wolfe, William L. Handbook of Military Infrared Technology, Washington D.C., Office of Naval Research, Dept. of Navy, 1965, pp. 331-332, 458-477, 520-566, 758-761.

5. Holter, Marvin R., "Imaging with Non Photographic Sensors", Remote Sensing, Washington, D. C., National Academy of Science, 1970, pp. 73-159.

6. Cooper, Charles F., Potential Applications of Remote Sensing to Ecological Research, Third Symposium on Remote Sensing of Environment, Feb. 1965.

7. Ludwig, C. B., et al, "Study of Air Pollutant Detection by Remote Sensors", N69-31961, General Dynamics Corporation, San Diego, Calif. July, 1969.

8. Casey, W. L., "The Importance of Elemental Registration and Calibration in Orbital Earth Resources Multi-Spectral Imaging", AIAA paper no. 68-1075 from AIAA Fifth Annual Meeting and Technical Display, Philadelphia, Pa., October 21-24, 1968.

3
ATTITUDE CONTROL

3.1 INTRODUCTION

The purpose of an attitude control system is to maintain a desired orientation based upon the requirements of SCOPE. Such a system is important in obtaining accurate data from the nadir and limb experiments and for exercising orbital trim maneuvers. The proposed attitude control system for Project SCOPE consists of three momentum wheels working in conjunction with thrusters needed for unloading of the wheels and rotational maneuvers. Attitude sensing is accomplished by a system of rate gyros, a rate-integrating gyro, earth-planar scanners, and sun sensors.

3.2 SYSTEM CONSTRAINTS AND OPERATION

3.2.1 Definition of Axes

Before further discussion, two sets of reference coordinate frames should be defined: one for the purpose of defining the moments of inertia (body-fixed) and the other for the purpose of relating the satellite to its orientation in space (earth-fixed).

The body-fixed system (x, y, z) is a right-handed coordinate system with its origin at the satellite's center of gravity. The y-axis is parallel to the axis of the solar panels. The z-axis is the axis of symmetry of the satellite. The x-axis completes the right-handed system.

The earth-fixed system (roll, pitch, yaw) is also a right-handed system with its origin at the satellite's center of gravity. The +X or Roll axis coincides with the direction of flight. The +Z or Yaw axis coincides with the local vertical. The +Y or pitch axis is normal to the orbital plane and completes the right-handed system.

The two systems coincide for nadir-viewing mode if an ideal sun-synchronous orbit is achieved (Figure 3.1).

3.2.2 System Requirements

The requirements for the attitude control system are the following:

1. The attitude control system must provide attitude pointing accuracy of at least 1^{o} on all three axes for nadir viewing.
2. It must obtain and maintain pointing accuracy of less than 0.05^{o} on pitch and yaw during limb viewing.

Figure 3.1
Definition of Axes

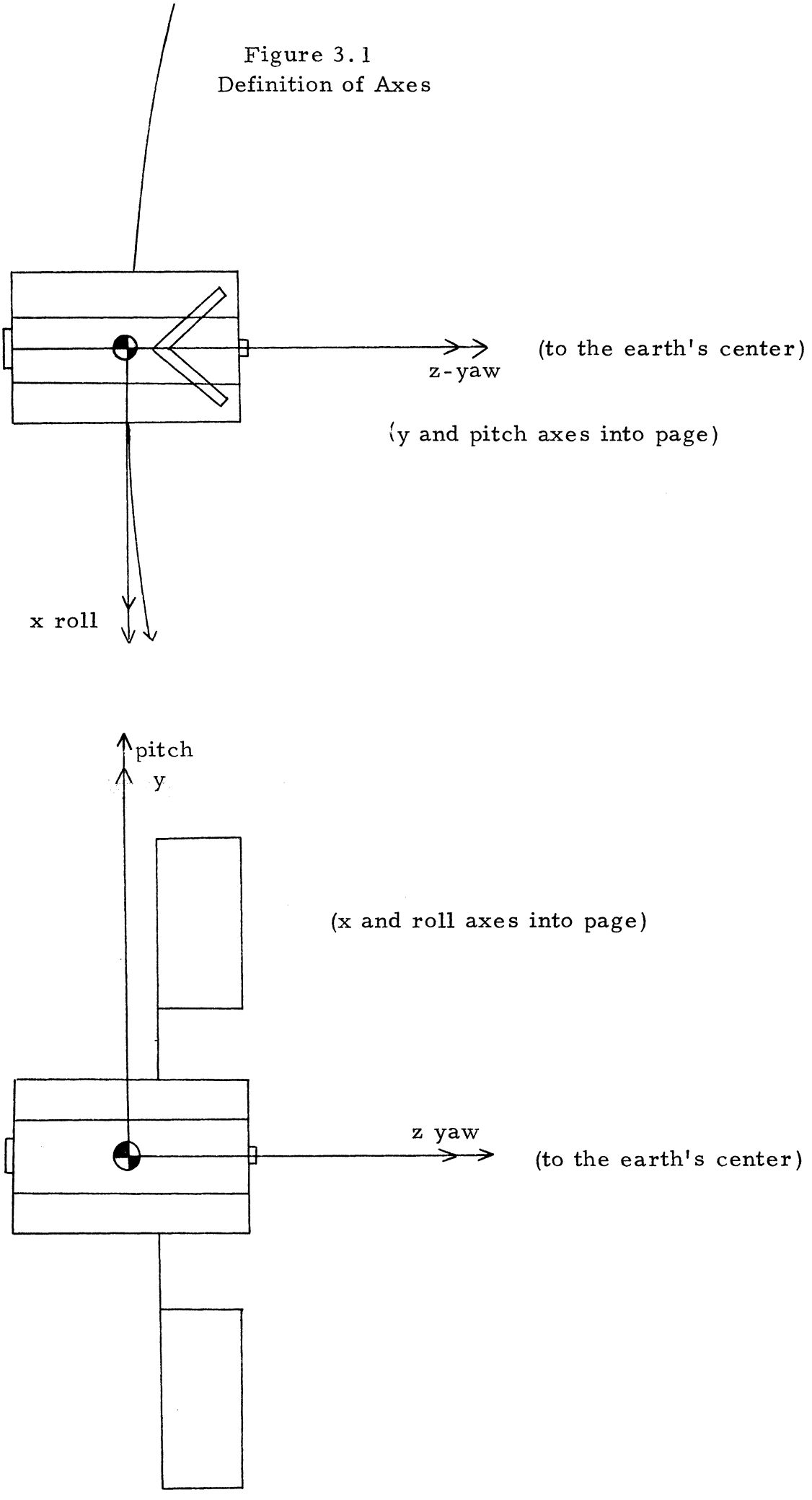

3. The system must provide proper attitude orientation for orbital trim maneuvers and must be able to perform rotational maneuvers
4. The system must be lightweight, low in power consumption, and reliable.

Four different systems were considered.

A. Gravity-gradient systems are reliable in that they are passive systems but they are of too low accuracy to meet the system requirements.
B. Spin-stabilization systems are not accurate enough (for limb viewing) and are not physically possible because of the need for solar panels.
C. The mass-expulsion system is accurate enough but is of high weight.
D. Three-axis stabilization with momentum wheels using reaction jets for unloading requires low fuel and is highly accurate.

Based on the above analysis, a three-axis, momentum wheel system was chosen.

3.2.3 System Description

The attitude control system is an active feedback control system. Attitude information is provided by a system of solar and earth sensors and gyroscopes. Any errors will result in the actuation of signals by an on-board programmer to the proper momentum wheels. The wheels apply a torque to the vehicle, returning it to its proper attitude. Each of the system components and their corresponding functions are described below. An overall block diagram of the system is shown in Table 3.1.

Spacecraft orientation for orbital maneuvers is shown in Figure 3.2. A planar scanner provides pitch and roll sensing. Yaw sensing is provided by a rate-integrating gyro which is set from information obtained by a wide-angle sun sensor. Control is maintained by the momentum wheels and rotations are performed by the reaction jets. The final -90^{o} rotation into nadir attitude is sensed by two planar scanners.

Nadir attitude is sensed in pitch and roll by the second planar scanner. Yaw attitude is sensed by two wide-angle sun sensors while the craft is on the sun-lit side of the earth. A rate gyro will help provide coarse yaw data while on the dark side.

For limb viewing, the system will switch from an earth-sensing mode to a solar sensing mode. The switch will occur each orbit in which limb viewing is performed at least 5 1/2 minutes before viewing begins. Pitch

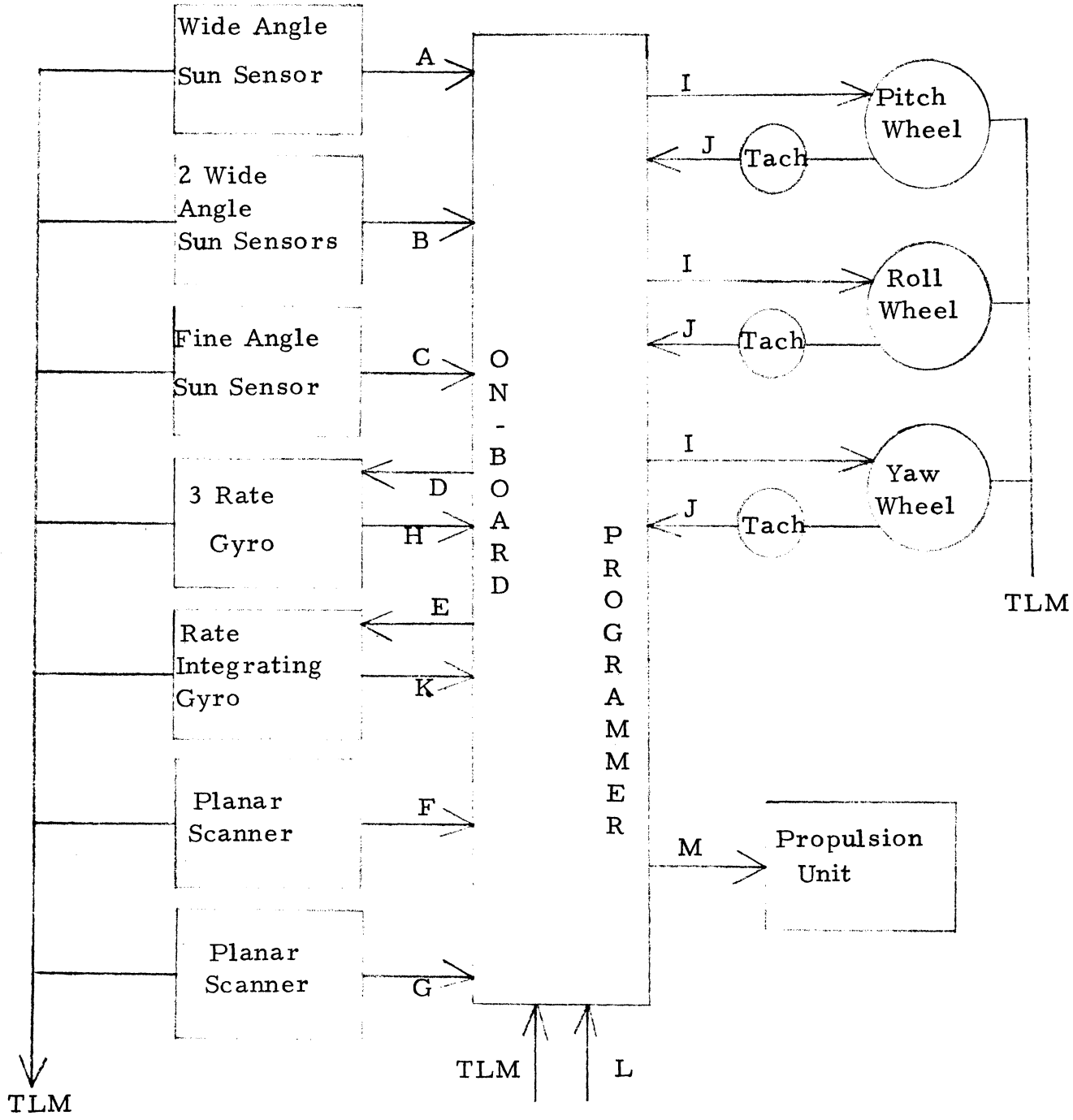

A - Yaw Data (orbital trim)
B - Yaw Data (nadir-viewing)
C - Pitch and Yaw Data (limb-viewing)
D - Pitch, Roll, and Yaw Rates
E - Yaw Data (orbital trim)
F - Roll and Pitch Data (orbital trim)
G - Roll and Pitch Data (nadir-viewing) Roll Data (limb-viewing)
H - Reset Gyros
I - Momentum Wheel Drive Command
J - Tachometer Data
K - Reset Rate-Integrating Gyro
L - Override Computer Commands
M - Thruster Control Commands
TLM - Telemetry

Table 3.1

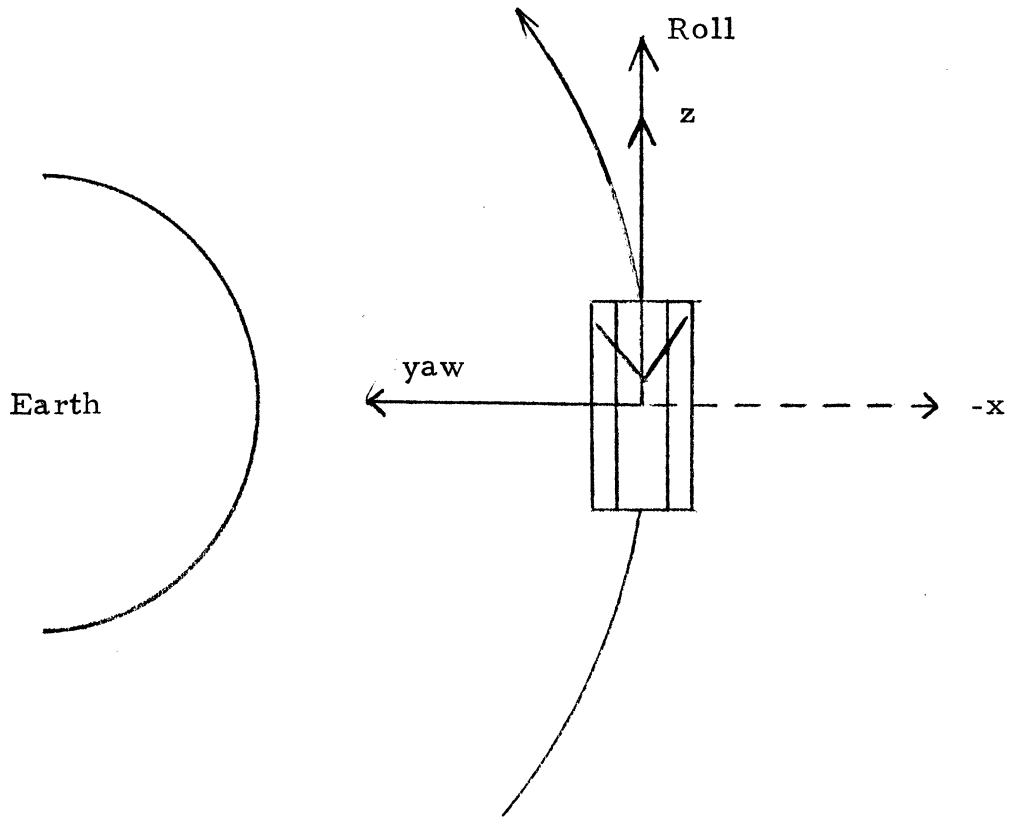

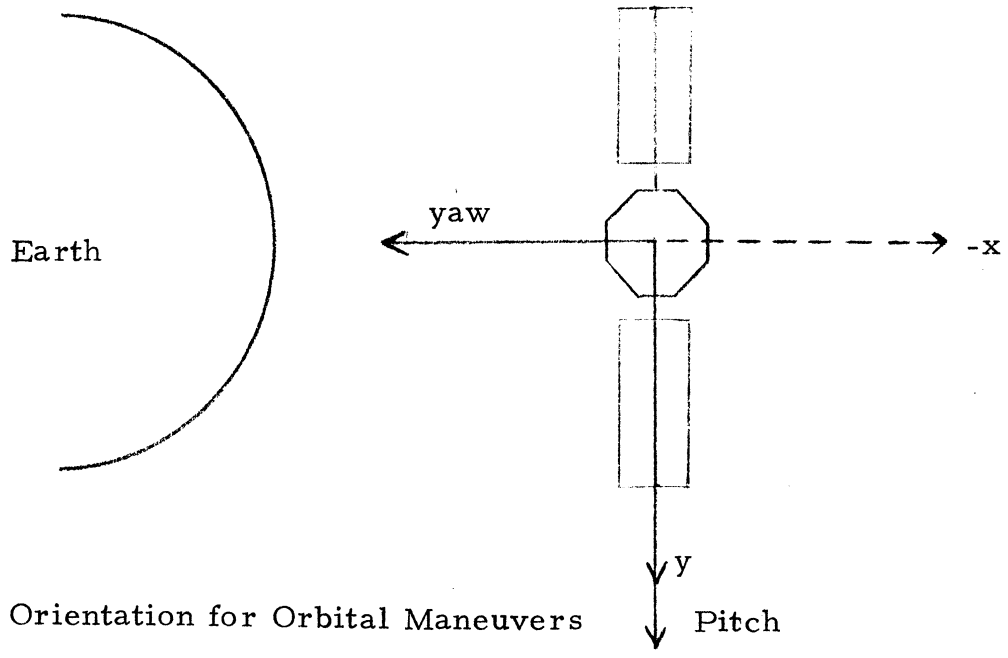

Figure 3.2 Orientation for Orbital Maneuvers

and yaw attitude information are obtained by a fine sun sensor. The planar scanner still provides roll attitude information. After limb data is taken, the system returns to earth-sensing mode.

Location of the sensors is shown in Figure 3.3.

3.3 SYSTEM HARDWARE

3.3.1 Momentum Wheels

Vehicle attitude is controlled by three momentum wheels. One is located along each of the three axes. The wheels are basically a momentum exchange device. A disturbing torque acting upon the satellite results in a change in satellite angular momentum and thus a change in satellite attitude. The sensing devices detect these changes, inform the programmer which in turn signals the appropriate wheels. The rotor of the wheel accelerates creating a counter-acting torque such that the total momentum of the satellite remains unchanged.

The wheels, however, cannot store an infinite amount of momentum. When wheel saturation occurs, appropriate thrusters are fired which disperses the momentum loaded in the wheels. After unloading, the system reverts to the original procedure.

The sizing of the wheels is dependent upon known disturbing torques' magnitude and frequency. The wheels must be able to counteract these torques without undergoing frequent unloading.

The wheels used in Project SCOPE have a momentum storage capacity of 0.4 ft-lb-sec at 1250 rpm. They are each driven by a brushless DC motor which turns the rotor. The rate of the wheel speed is measured by a tachometer.

3.3.2 Yo-Yo Despin Mechansim

When the heat shield separates from the spacecraft and the fourth stage has finished its final burn, SCOPE and the fourth stage (still connected) will be spinning at approximately 120 rpm. This 120 rpm spinning rate must be reduced to approximately 0 rpm for two basic reasons. One is to enable proper orbit injection attitude for orbit trim of the delta V motor burns, and also because the SCOPE C0 scanning procedure requires an earth-oriented non-spinning platform.

To remove the spin from the spacecraft we have a choice of passive or active system. An example of the active system is cold gas and hot gas retro device. This appears unattractive because the initial spin rate as well

Figure 3.3 Location of Sensors

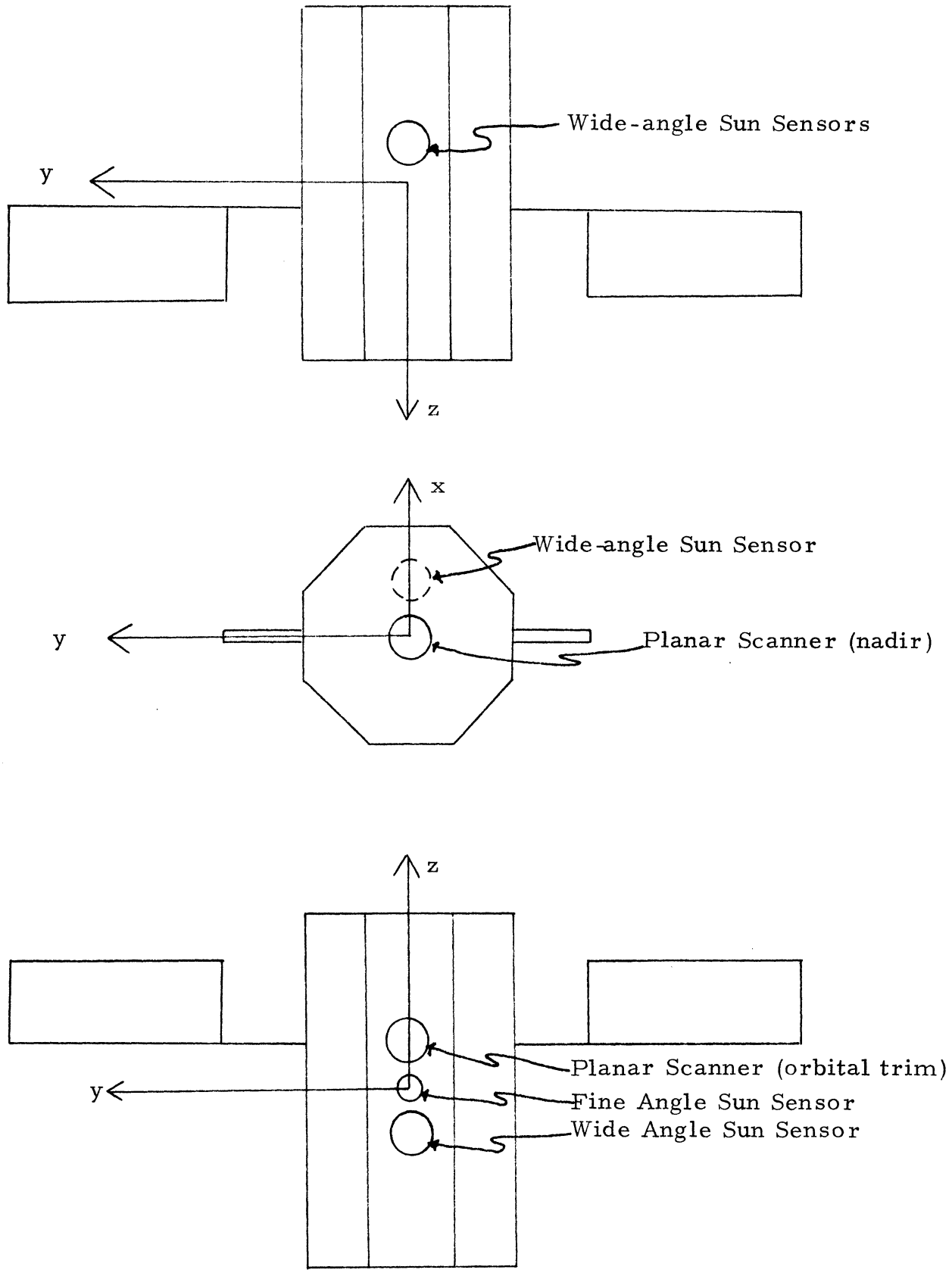

as the moment of inertia must be known accurately. At present, the initial spin rate is not known accurately and these systems would tend to decrease reliability and increase both cost and weight of the spacecraft. Another active system that was considered is despinning by thrusters. Thrusterswill be used in attitude control, and the weight penalty due to the additional fuel needed by the thrusters would be moderate. However, despinning by thrusters would also require that an accurate initial spin rate be known.

There are two passive means of despinning the spacecraft, which come under the realm of Yo-Yo depsin. The Yo-Yo consists primarily of two cables with a weight on one end of each cable and the other end fixed initially to the spacecraft. First is the stretch Yo-Yo for despinning a spacecraft to a specified spin rate. Second is the rigid Yo-Yo which also despins a spacecraft to a specified spin rate. We have chosen the latter because it is less complex and when the final spin rate approaches zero (which it does in our case) the cable length and weight of the end weight become independent of the initial spin rate (Reference 5).

The Yo-Yo despin is of simple construction. There are two cables, each being long enough to wrap around SCOPE 1 1/2 times with a diameter of 1/16". This cable was chosen because a long thin cable reduces the error in the calculation of the mass of the end weight and produces a final spin rate close to zero. A long cable also reduces deceleration of the spacecraft which in turn assures safety of on-board equipment. The strength of the cable is well within design limits of the spacecraft (see Appendix B.6). One end of each cable is fixed to half-cylinder shaped weights, while the other end of each cable is connected to a ring which is looped around a hook until despinning is terminated. The Yo-Yo system will be located at that end of SCOPE which will put the system clear of the solar panels and all other obstructions (see Figure 3.4). This will enable the weights to have a clear path during despin. Since the Yo-Yo will be activated by means of the Scount Interface Connector Package, the despin is necessary prior to fourth stage separation.

The operation of the Yo-Yo system is fairly simple. First a signal is sent from the fourth stage to the pyrotechic thrusters in SCOPE. These two thrusters are located on opposite sides of the vehicle. When they have received their signals they will release the hold down clamps. Once the clamps release the end weights, a spring will propel them away from the spacecraft (see Figure 3.5). The end weights swing away, at the same time decelerating the spacecraft to approximately 0 rpm. After the deceleration is terminated, the rings connecting the cables to the anchor hooks will slide off, thus separating the Yo-Yo system from SCOPE.

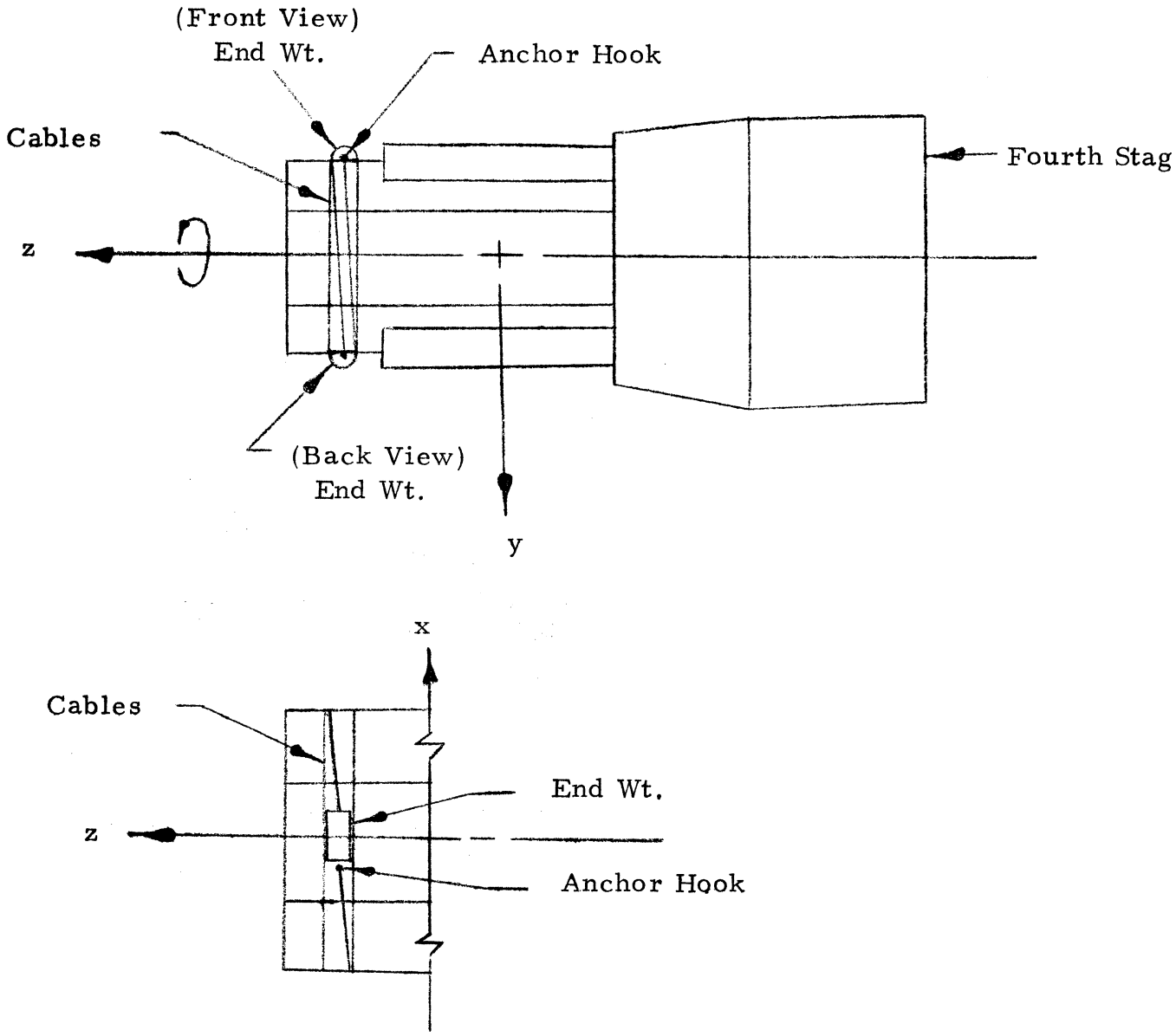

Figure 3.4 Yo-Yo Despin

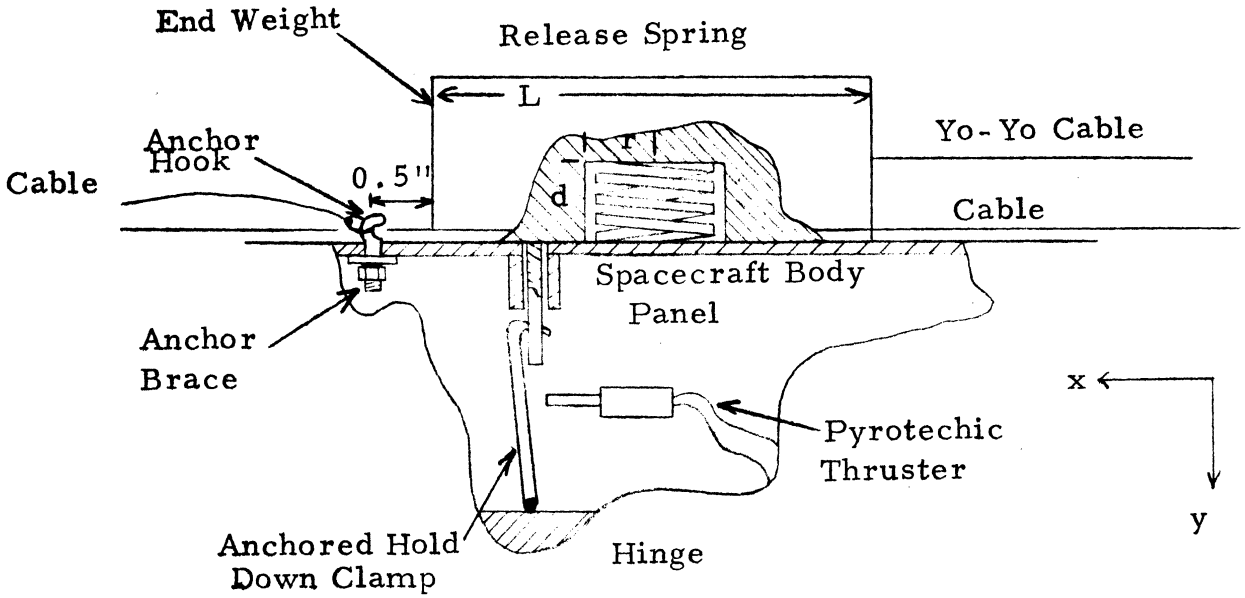

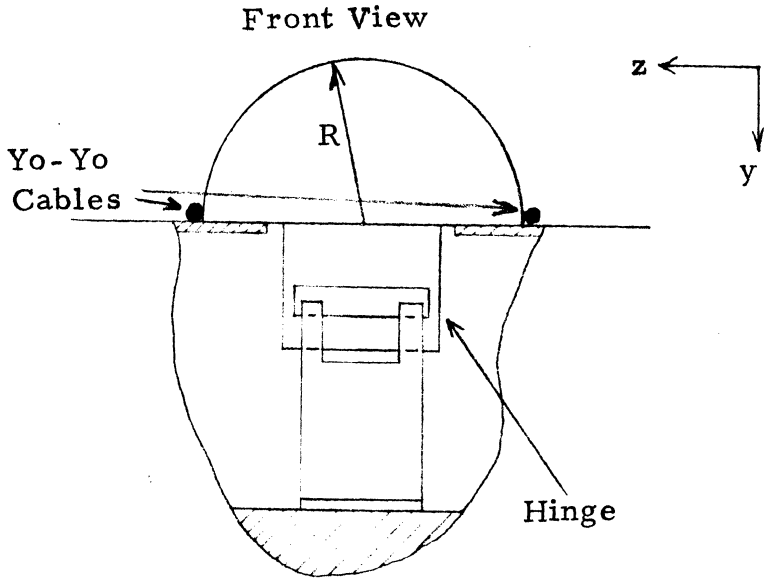

L = 2 in
R =0.853 in
r =0.50 in
d =0.3 in

Figure 3.5 Yo-Yo Despin Mechanism
z axis is into page for this view

Design Parameters:

L = each cable length 118"
W_o = weight of each end weight .344 pounds
W_1 = each cable weight .102 pounds
t = time to despin .853 seconds
T = maximum tension in cable 22.8 pounds
a = maximum deceleration 25 radians/sec^2

End weight dimensions: half cylinder

length 2"
radius .853"
hollow for spring .06 in^3
density .283 lb/in^3

Cable: 1/16 in dia steel .000864 lb/in

3.4 ATTITUDE SENSING

The sensing equipment consists of two infrared earth planar scanners, three wide angle solar sensors, one fine angle solar sensor, a rate-integratin gyro, and a package of three rate gyros, (see Table 3.2).

3.4.1 Planar Scanners

The planar Scanner makes use of the discontinuity in infrared radiatio emitted between earth and space. The unit contains four infrared radiation detectors whose fields of view are rotated synchronously in two perpendicular planes from space across the earth's horizon. Thus the two field of view in each plane make equal angles with the primary axis of the scanner. If pointing error exists, the field of view of one detector will cross the horizon before the field of view of the second detector crosses the horizon. Since the scanning rate is constant, the time difference in crossing opposite horizor in one scanning plane is directly proportional to the error in that plane (Reference 7).

Two planar scanners are used. One scanner is mounted near the -x axis and will provide pitch and roll sensing data during orbital maneuvers. The second scanner is located on the z axis and will provide pitch and roll attitude information during nadir viewing and roll information during limb viewing. The scanners give attitude information to within 0.1^o at all times. Both scanners will work together for sensing attitude during the 90^o rotation from orbital trim orientation to nadir mode orientation.

Table 3.2

Component	Weight	Power	Comments
Momentum Wheels (3) Bendix #1778600	4.6 lbs	4.6 watts	Momentum Storage Capacity = 0.4 ft-lb-sec at 1250 rpm
Fine Angle Sun Sensor Bendix #1771878	0.08 lbs	0	Null accuracy = 1 arc-min Field of view = 5^{o}
Wide Angle Sun Sensor (3) Bendix #1771858	0.15 lbs	0	Null accuracy = 0.1^{o} Field of view = 180^{o}
Planar Scanner (2)	3.0 lbs	3.5 watts	Accuracy = 1^{o}
Rate-Integrating Gyro Honeywell GG49	1.0 lbs	3 watts	
Rate Gyro (3) Honeywell GG440 Gnat	0.24 lbs	3.5 watts	
Yo-Yo			
End Weights (2)	0.688 lbs		
Cables (2)	0.204 lbs		
Springs	0.50 lbs		
Thruster Actuators	0.10 lbs		
	1.5 lbs total		

Total weight of attitude control system = 25.8 lbs

3.4.2 Solar Sensors

Two wide angle solar sensors provide yaw information during nadir viewing. These sensors are located near the x and -x axis. Each sensor has a 180° field of view, thus providing spherical coverage. They each have a null accuracy of 0.1°. A third wide angle sun sensor is located near the -z axis and provides yaw data needed to set the rate-integrating gyro for orbital maneuvers. This sensor can also be used to provide yaw information during nadir-viewing for approximately 1/2 orbit.

A fine angle sun sensor is located on the -x axis and provides yaw and pitch attitude data during limb viewing. This sensor has a 5° field of view and a null accuracy of $\pm$ 1 arc-min.

3.4.3 Gyroscopes

A rate-integrating gyro is located on the -x axis and will provide yaw data during orbital trim. A package of three rate gyros are supplied. These are used to obtain the error rates of deviation. This data can be analyzed by the programmer to provide yaw data on the dark side. They also improve the accuracy of the system, as well as decreasing the steady-state error and increase the response of the system.

3.5 PROPULSION SYSTEM

3.5.1 System Description

A propulsion system is needed for momentum wheel unloading and rotational maneuvers. A system of twelve Hamilton Standard TCA thrusters is proposed. Each thruster produces 0.055 lb of thrust and has a specific impulse of 207 sec. at 80 psia supply pressure. A monopropellant system is utilized with hydrazine (N_2H_4) as the fuel and gaseous nitrogen as a pressurant. The pressurization system used is the same as the one used for orbital trim burns. Therefore, a pressure regulator is added to reduce the supply pressure to 80 psia. A description of the system may be found in Section 4.4.

3.5.2 Fuel Budget

Two pounds of fuel is supplied for attitude control purposes. This is well over the amount required. Derivation of fuel needed for momentum wheel unloading and rotational maneuvers can be found in Appendices B.4 and B.5.

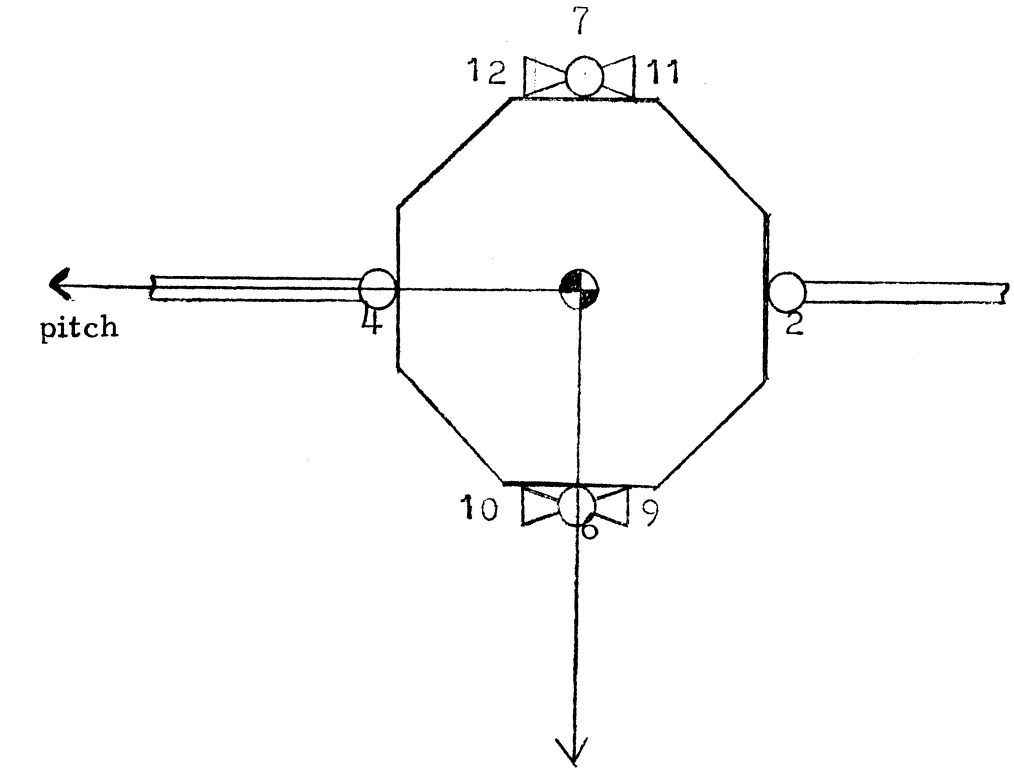

Thruster	Rotational Mode
1-4	+ roll
2-3	- roll
5 7	+ pitch
6-8	- pitch
9-12	+ yaw
10-11	- yaw

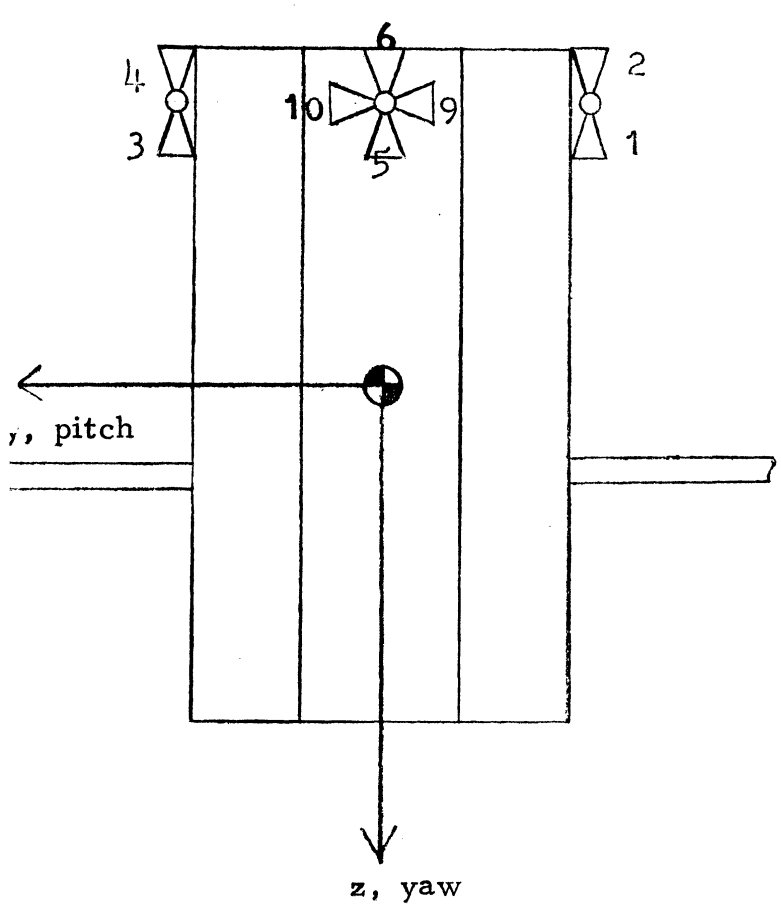

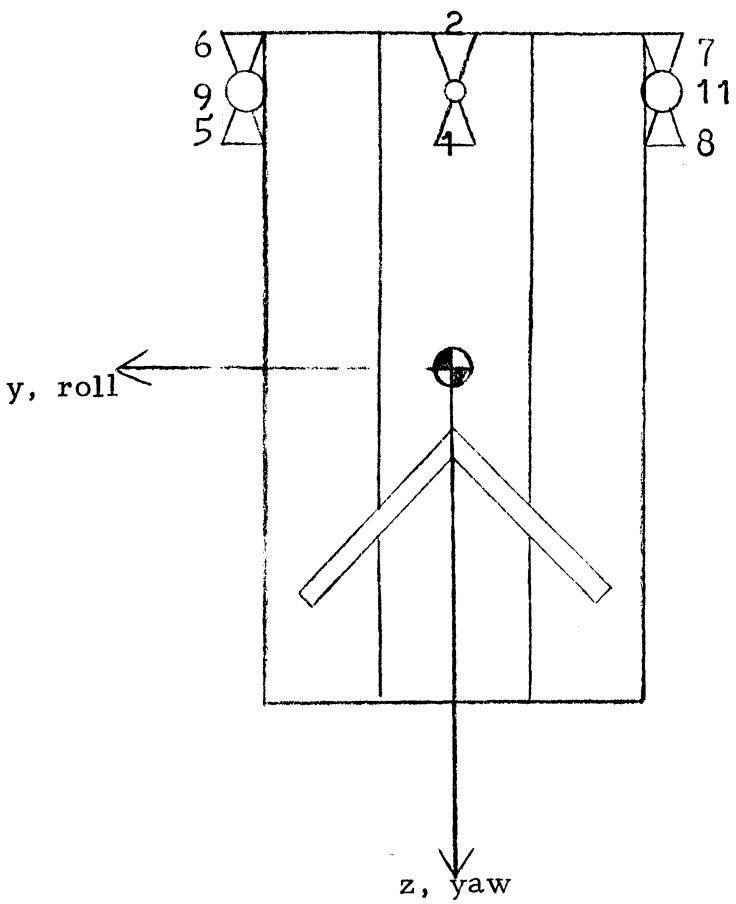

Figure 3.6 Location of Thrusters

3.5.3 Location of Thrusters

Thruster placement is shown in Figure 3.6. Thrusters 1-4 are used for $\pm$ x rotations and for unloading of the x-axis momentum wheel, 5-8 for $\pm$ y rotations and unloading of the y-axis wheel, and 9-12 for $\pm$ z rotations and unloading of the z-axis wheel.

For minimum fuel use, while obtaining maximum torques, the thrusters are to be located as far from their corresponding axes as possible. On this basis, thruster locations shown in Figure 3.6 were chosen.

3.6 COMPONENT SPECIFICATIONS

Component specifications including power requirements and weight are given in Table 3.2.

3.7 REFERENCES

1. Beusch, J. U., "Three-Axis Attitude Control of a Synchronous Communications Satellite", AIAA Paper 70-456, April 1970.

2. Corliss, W., Scientific Satellites, NASA SP-133, 1967.

3. Crandall, S. H., and Dahl, N. C., Introduction to the Mechanics of Solids, McGraw-Hill, 1959, p. 204-205.

4. Dinter, H. A., Inertial Sensors Theory and Application, Honeywell Report AM-62-2, July 1967.

5. Eide, D. G. and Vaughn, C. A., "Equations of Motion and Design Criteria for the Despin of a Vehicle by the Radial Release of Weights and Cables of Finite Mass", Langley Research Center, NASA TND-1012, January 1962.

6. Fedor, J., "Analytical Theory of the Stretch Yo-Yo for Despin of Satellites", Goddard Spacecraft Center, NASA TND-1676, April 1963.

7. Hatcher, N. M., "Development of a Proposed Infrared Horizon Sensor for Use in Spacecraft Attitude Determination", NASA TND-2995, September 1965.

8. Leondes, C. T., Guidance and Control of Aerospace Vehicles, McGraw-Hill, 1963.

9. Project MEDUSA - Michigan Educational and Utility Satellite for Alaska, A Student Design Project, The University of Michigan, Department of Aerospace Engineering, April 1970.

10. Project OBSERVER, A Student Design Project, the University of Michigan, Department of Aerospace Engineering, December 1968.

11. Project SCANNAR - Satellite Communications and Aircraft Navigation for the North Atlantic Region, A Student Design Project, The University of Michigan, Department of Aerospace Engineering, April 1970.

12. Sabroff, A. E., "Advanced Spacecraft Stabilization and Control Techniques", AIAA Paper 67-878, October 1967.

4
ORIBTAL ANALYSIS

4.1 INTRODUCTION

In choosing the nominal orbit for SCOPE there were three primary constraints to be considered. The first was scan width. General Electric, the sensor developer indicated that as a worst case the scan width on the surface of the earth should be no greater than 50 statute miles. This constrained the altitude to a low earth orbit of approximately 300 nautical miles. The second constraint was involved with mapping. For complete global coverage a polar orbit was needed. The third constraint involved the lifetime of the satellite. Since cloud cover hampers data gathering in the nadir mode, four complete coverages of the earth were deemed necessary to ensure at least one data gathering at each point on the earth's surface. Hence at least a year's lifetime was needed.

4.2 THE NOMINAL ORBIT. MAPPING IN THE NADIR MODE

4.2.1 Nominal Orbit Characteristics

The important constraints operating on the orbit characteristics are these:

a) Lifetime. A nominal lifetime of one year is desired.

b) Sensor requirements. One of the sensor's chief constraints on the orbit is the maximum acceptable width for its scan on the earth's surface. General Electric has indicated that for acceptable operation in the nadir mode, the seven-degree field of view of the sensor would subtend a scan width no greater than fifty statute miles, thus placing a maximum on the acceptable altitude of approximately 409 statute miles or 355 nautical miles (nm).

c) Mapping. The greater the inclination of the satellite orbit to the equator, the greater the latitude and therefore the greater the total earth area which will pass under the satellite's view during nadir viewing.

On the basis of these constraints, a nominal orbit was chosen which has these characteristics: a 320 nm circular retrograde orbit inclined 97.7° to the equator, and is sun-synchronous. Launch site for such an orbit would be Vandenberg Air Force Base in California, since its location facilitate near-polar launches.

Given the vehicle's drag-weight parameter, a 320 nm orbit yields a nominal lifetime of ten years. Given the uncertainty of lifetime calculations, it was felt that accepting a worst case of one order of magnitude error is

necessary in lifetime calculations (see Appendix C. 1). A 320 nm orbit is thus safely within both the maximum altitude established by the sensor requirements, and the minimum altitude necessary to ensure a full year's lifetime.

It was decided to use a retrograde orbit which is nearly polar, but offset slightly in order to obtain sun-synchronization. The resulting orbital plane, then, would maintain a constant orientation with respect to the earth-sun line. Figure 4. 1 indicates the difference between a polar (non-synchronous) orbit, which rotates 360^{o} with respect to the earth-sun line each year, and a sun-synchronous orbit, which has been given a precession rate calculated to exactly cancel this rotation (see Appendix C. 2).

The advantages of the sun-synchronous orbit include the simplicity of its constant orientation and the fact that the local time of day of the satellite is nearly constant. Thus, a particular time of day may be chosen based on ground measurements of CO quantity as a function of time of day, and the most fruitful hunting grounds chosen for survey (see Figures 4. 2 and 4. 3).

A disadvantage is that the sun-synchronous orbit fails to provide coverage of earth areas greater than 82.3^{o} north and south latitude during nadir viewing. The area lost to view is, however, so small and so seldom available due to cloud cover, that the loss of it would seem not to outweigh the advantages of the chosen orbit.

4. 2. 2 Mapping

The ground track of the satellite during the first three revolutions is shown in Figures 4. 4 and 4. 5.

The satellite sensor, while in nadir-viewing mode, will attempt a systematic mapping of CO quantities across the earth's surface. In order to determine the time necessary for this mapping, several factors need to be known, including the inclination of the orbit, the width of the sensor's scan across the earth's surface, and the nature of the ground track.

With all of the above considerations in mind, and given the nominal conditions of a satellite in 320 nm orbit having an angle of view of 7^{o}, it has been determined that a mapping survey can be completed within 1305 revolutions, or 87. 5 days. Such a survey would cover each available point on the earth's surface at least once. Unavailable points would be those whose latitude is greater than the inclination of the satellite's orbit; in SCOPE's case, 82.3^{o}, (see Figure 4. 5).

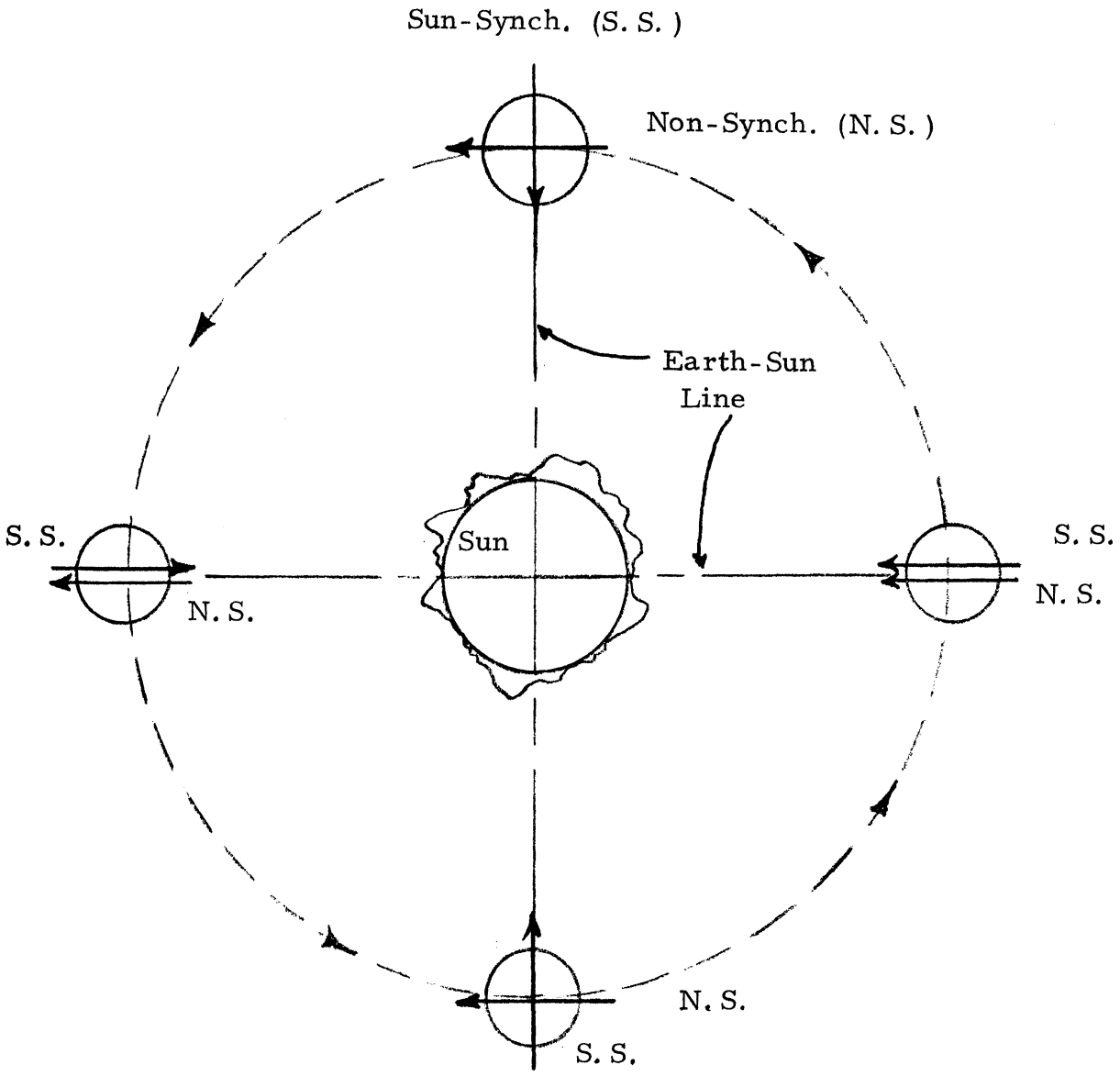

Figure 4. 1 Comparison of Non-Synchronous Orbital Plane with Desired Sun-Synchronous Plane. Both are Polar for Clarity, seen edge on.

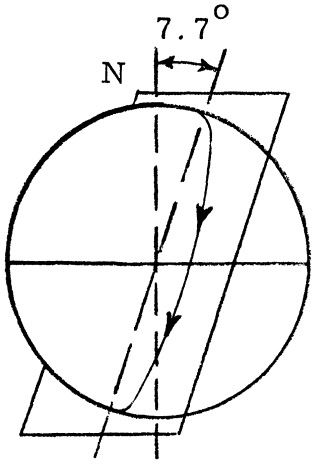

Figure 4. 2 Plane and Ground Track of 82. 3° Retrograde Orbit.

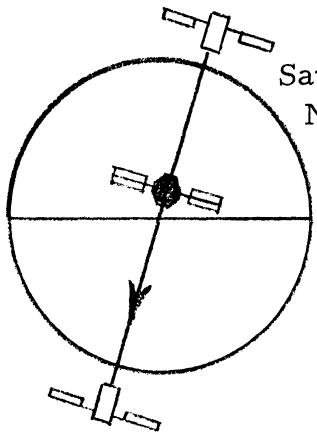

Figure 4. 3 SCOPE Orbit, as seen edge-on from the sun.

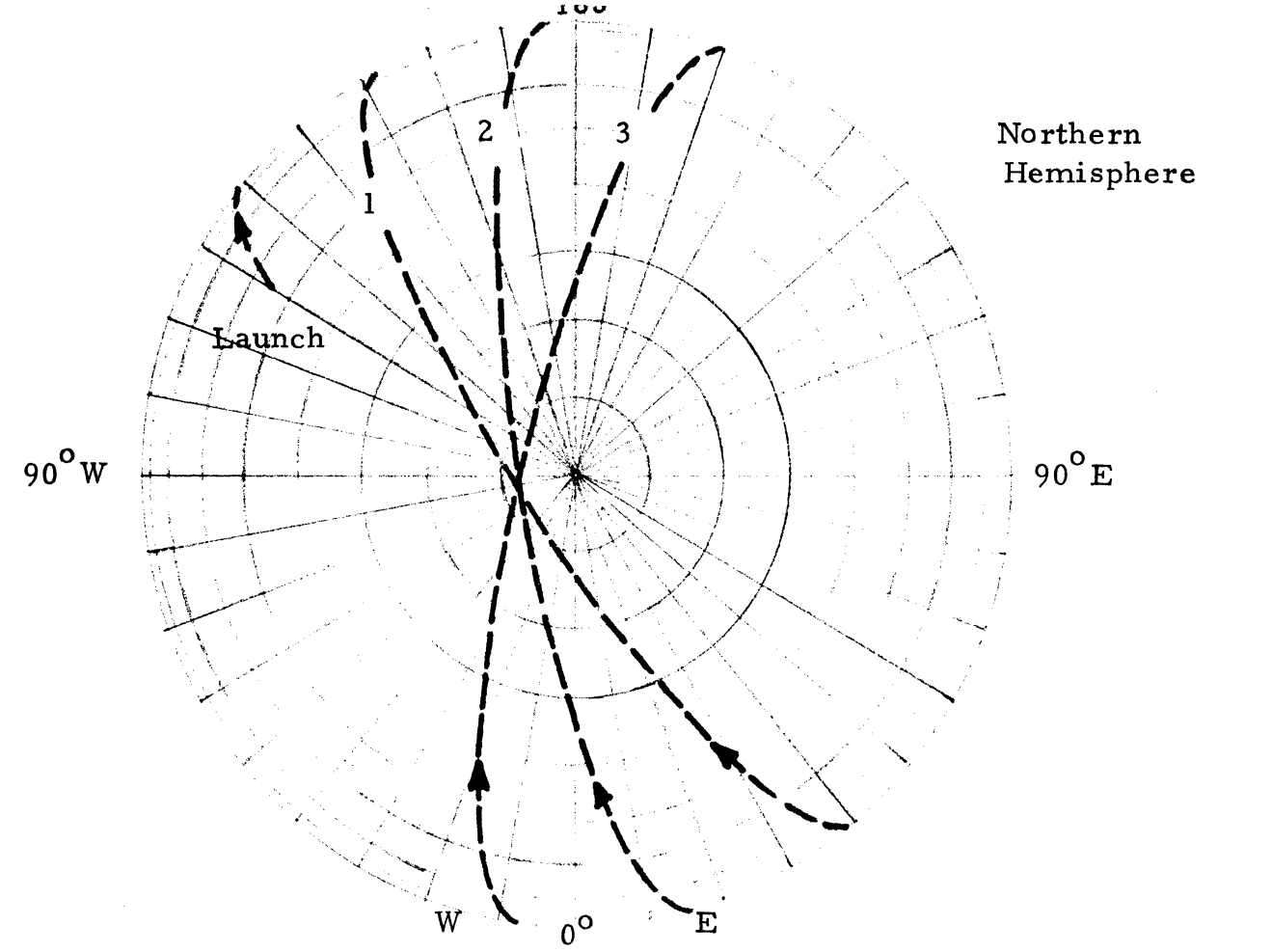

Figure 4.4 Ground Track for First Three Revolutions, Polar Projection

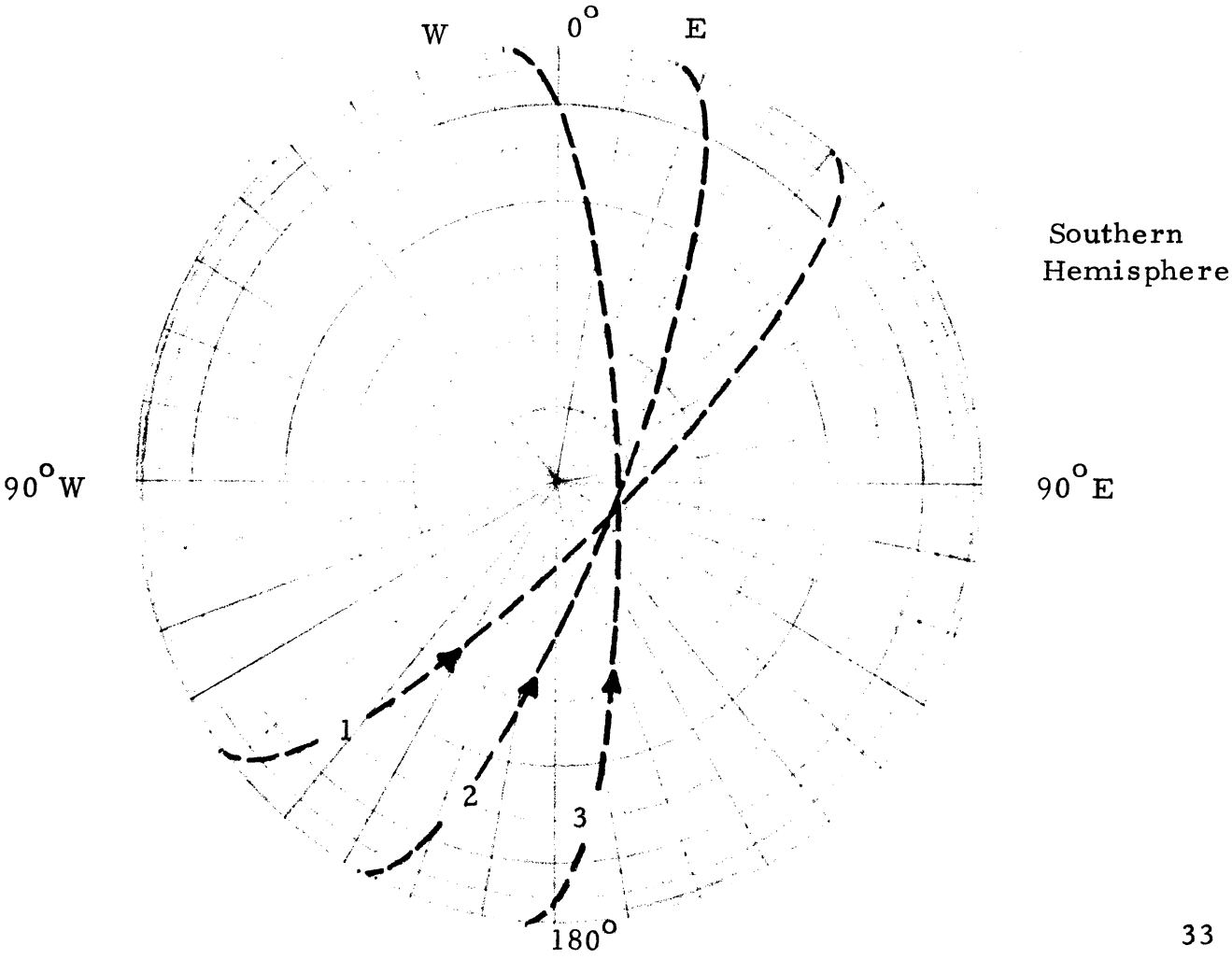

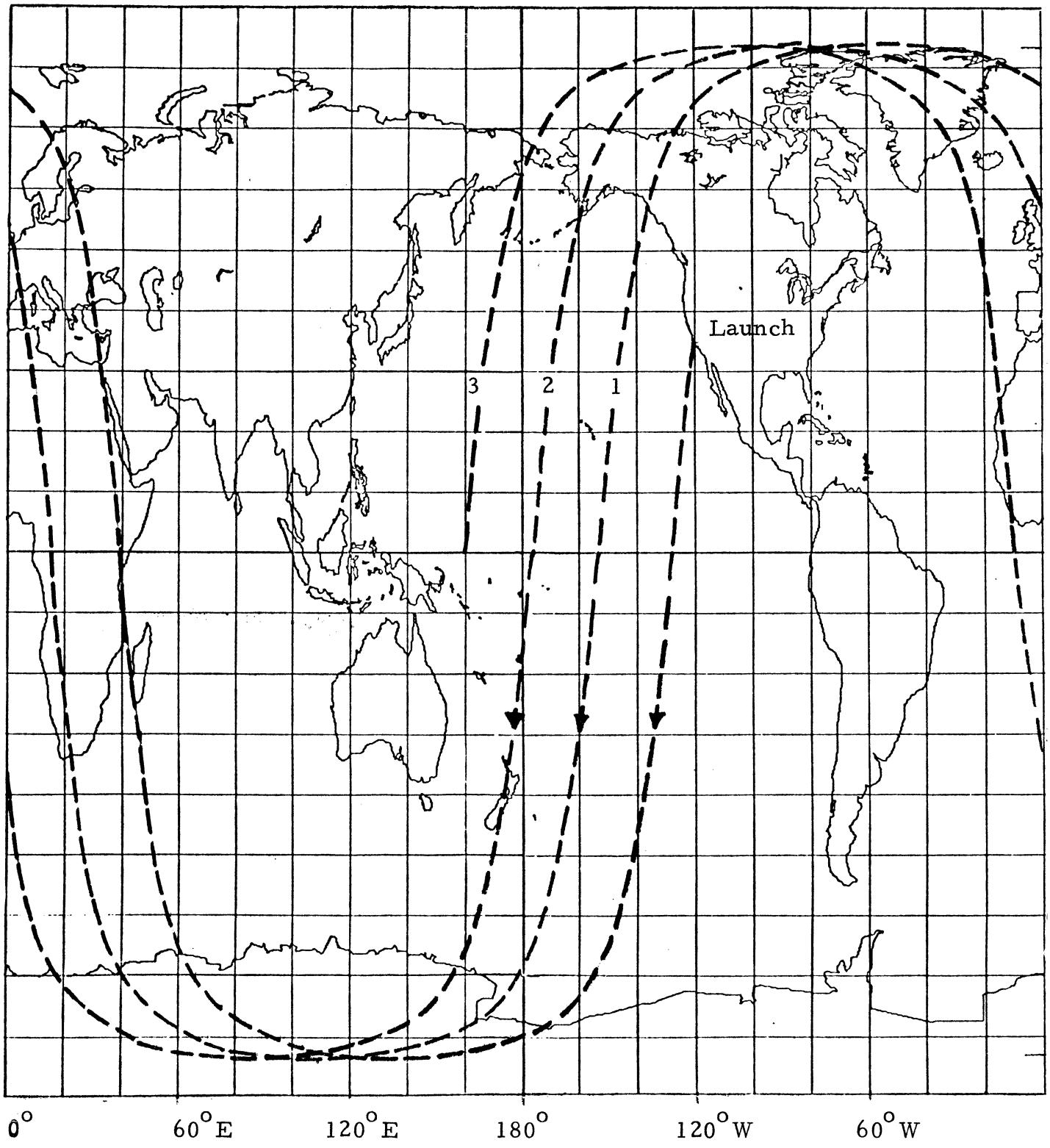

Figure 4.5 Ground Track for First Three Revolutions, Flat Earth Projection

Cloud cover is an additional problem relating to the mapping project. The sensor does not function acceptably over cloud-covered areas, so the mapping surveys will have to be duplicated a certain number of times in order to ensure that all points are not only surveyed once, but once when unclouded. The worst situation exists in the greater latitudes, where there is as much as a 75% chance of cloud cover at certain times of the year (see Reference 2, p. II-25). Thus it is assumed that four complete mapping surveys will be necessary to ensure at least one valid reading for each point on the earth's surface between 82.3° north and south latitude (see Appendix C 4).

4.2.3 Launch Windows

The launch trajectory of the Scout vehicle from Vandenberg Air Force Base is arranged so as to inject payload into orbit at 15° N latitude, and at perigee in the vehicle's orbit.

It is desirable to have perigee of the orbit in the ecliptic plane on the daylight side of the earth (see the theory of the acceptable ellipse, Section 4.3.1), and to have the perigee point of the orbit fall exactly on the earth-sun line. Thus it is desirable to launch on a day when the line of 15° N latitude intersects the ecliptic at one point: at noon, on the earth-sun line (see Figure 4.6). A satellite injected into orbit at 15° N latitude in such a situation will (if the orbit is sun-synchronous) fulfill the requirements listed above.

An optimum trajectory would require that the satellite be launched while the launch site is in the orbital plane. Thus the optimum launch time will be on 1 May or 11 August, near noon at the launch site--since as the ecliptic plane "climbs" in latitude toward a maximum at the summer solstice and later, as it descends again, it will both times cross the 15° N latitude line.

4.3 ERROR ANALYSIS OF ORBIT INJECTION

4.3.1 Apogee and Perigee Deviations

Nominally a circular orbit of 320 nm is desired for SCOPE. In order to obtain the nominal orbit, there are three conditions which must be met at orbit injection (fourth stage burn-out). The altitude at burn-out must be 320 nm, the velocity must be 24,820 ft/sec (local circular velocity) and the flight path angle must be zero (see 4.3.3 for yaw errors).

The Scout launch vehicle, however, is not accurate enough to meet these stringent conditions, thus the resulting orbit will not be circular but elliptical. Because of the elliptical shape there arise two problems of importance. First, if the perigee is too low the lifetime of the satellite

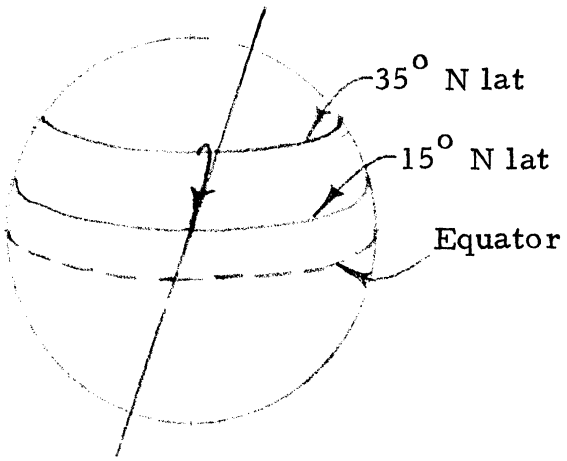

Figure 4.6 Launch on Day When Line of 15° N lat Intersects Earth-Sun Line

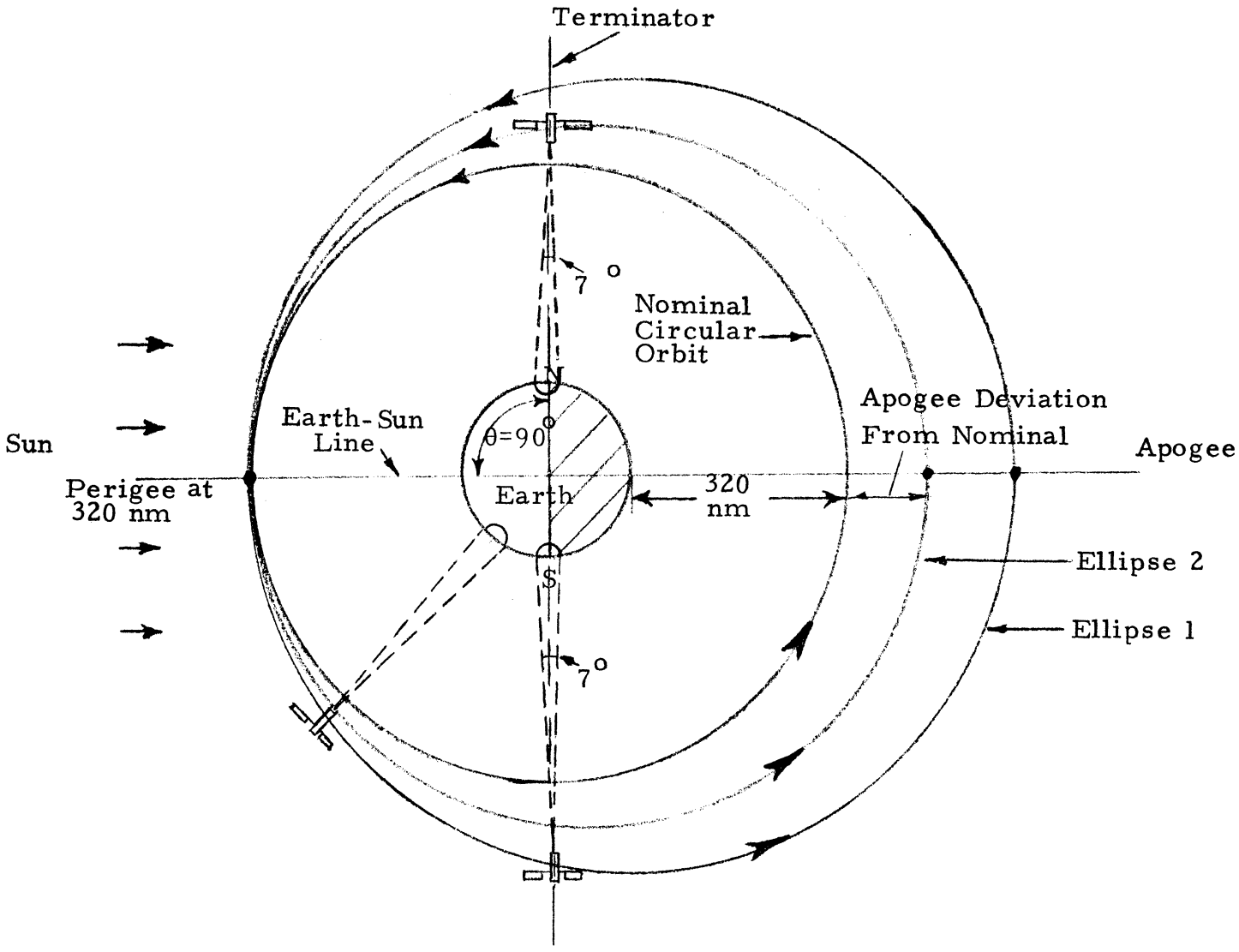

Figure 4.7 Position of Maximum Viewing Altitude

could be severely reduced. Secondly, if the apogee is too high the resulting data from the CO detector will become meaningless because the area of the earth's surface that the detector scans will be too large.

This does not mean that all ellipses are unacceptable. Consider Figure 4.7. The sensor cannot operate in the dark, therefore the altitude is not restricted to the right of the terminator. Hence when the satellite is at the terminator it is at the highest point of its orbit during which it can scan the earth.

Because the maximum viewing altitude of SCOPE has been established as 355 nm it is only necessary to impose this restriction when the satellite is at the terminator (the latus rectum). Therefore since the latus rectum and the perigee are known, the apogee is defined (see Appendix C.5), and calculations show this altitude to be 379.4 nm.

Therefore, if

1. Apogee and perigee are on the earth-sun line
2. Perigee is at 320 nm (on sun side)

then an acceptable ellipse will be defined as one whose apogee altitude is less than or equal to 379.4 nm.

4.3.2 Orbital Corrections

LTV has indicated in graphical form the probability that a certain magnitude of error will result from launch. This graph occurs in Figure 4.8 (see Reference 3 p. 5-48) and consists of three probability contours on a graph whose ordinate and abscissa indicate the appropriate apogee and perigee deviations. These contours have the value of 99.7%, 95% and 68% probability (hereafter called 3σ, 2σ and 1σ respectively).

To calculate the velocity increments (ΔV) needed to correct an injection ellipse to either a circle or an acceptable ellipse, six points were chosen from Figure 4.8 and the appropriate errors analyzed. This was done in an attempt to establish a worst case, and to use this worst case to establish the amount of fuel needed for orbit corrections. The following six points were chosen:

Table 4.1

Apogee and Perigee Injection Errors

Error Probability	Case	Apogee Deviation (nm)	Perigee Deviation (nm)
3σ	1	+171	-10
3σ	2	+100	-100
2σ	3	+128	-9
2σ	4	+80	-72
1σ	5	+82	-4
1σ	6	+52	-51

As seen from Table 4.1, the apogee error is usually above nominal and the perigee error is usually below nominal. Although this does not always have to be the case, it is more likely that this configuration would occur as depicted in Figure 4.9. After analyzing this configuration it was decided that two burns were needed to efficiently correct the orbit (the Hohmann transfer method - see Reference 2 p. II-49). The first burn (at apogee) is posigrade and places the perigee of the ellipse at nominal altitude. The second burn (at perigee) is retrograde and transfers the satellite to either an acceptable ellipse or a circular orbit.

The ΔV's for both burns have been calculated and are shown in Table 3.2 (see Appendix C.6):

Table 4.2

ΔV Requirements

Case	Type of error Correction	Burn #1 posigrade at Apogee	Burn #2 retrograde at Perigee	Total ΔV
1	circularize	15.8 (fps)	283.5 (fps)	299.3 (fps)
2	ellipse	164 (fps)	67.8 (fps)	231.8 (fps)
3	circularize	14.3 (fps)	211 (fps)	225.3 (fps)
4	circularize	103 (fps)	132.5 (fps)	235.5 (fps)
5	circularize	6.4 (fps)	135.9 (fps)	142.3 (fps)
6	circularize	82.4 (fps)	86.3 (fps)	168.7 (fps)

In choosing between correction to acceptable ellipse or circularization, circularization was given top priority because of life-time and mapping considerations. However in case 2 (Table 4.2) correction to acceptable ellipse was chosen because circularization exceeded SCOPE's capability. This capability was established, because of volume requirements within SCOPE, at a ΔV of 306 ft/sec. For further details see Section 4.4.3.

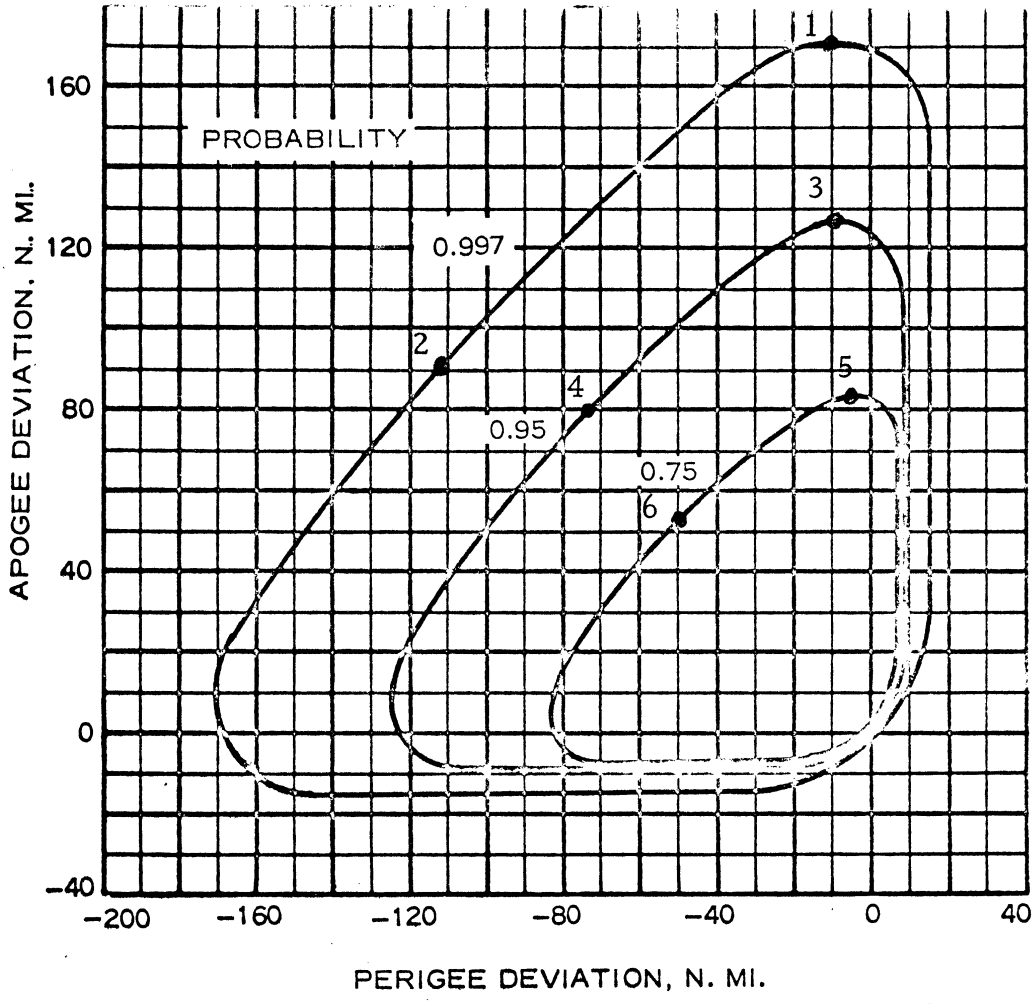

Figure 4.8 Apogee and Perigee Deviations Due to Injection

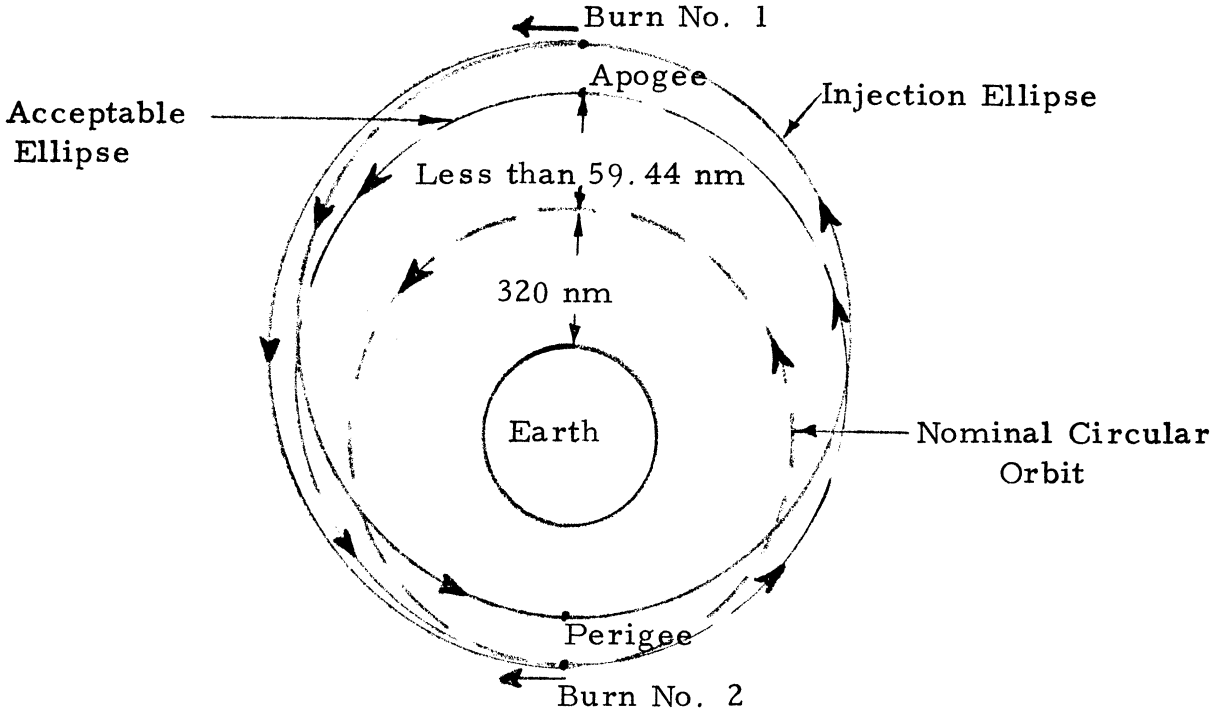

Figure 4.9 Correction to Acceptable Ellipse

4.3.3 Inclination Errors

Aside from the injection errors discussed in Section 4.3.1, there are also injection errors in yaw (see Figure 4.10). As can be seen from Figure 4.10, an error in yaw at injection results in an equal error in inclination. In order to correct these errors in inclination a dog-leg maneuver is required. This burn can only be made at two locations - at the injection point or one half revolution away (for purposes of efficiency).

LTV has expressed these errors due to launch in graphical form. Figure 4.11 (see Reference 3 p. 5-46) shows that with SCOPE's nominal inclination angle a one standard deviation of $\pm 0.6^{\circ}$ can be expected, and the dog-leg maneuver associated with this error requires a ΔV of 264.5 ft/sec (see Appendix C.7). This capability, however, is beyond SCOPE's capability for two reasons. First, priority was given to establishing either an acceptable ellipse or circular orbit. In order to accomplish this, Table 4.2 states 300 ft/sec is required. Thus only 6 ft/sec remains for the dog-leg maneuver--clearly inadequate. Secondly, this error is only one standard deviation. If it was decided to correct the inclination errors, an error at least twice as large would have to be assumed for safety. This also means doubling the ΔV required to 529 ft/sec which, by itself, is greater than SCOPE's capability.

The result of having dropped dog-leg capability is that SCOPE may not be in a sun-synchronous orbit. In other words, the orbital plane could rotate with respect to the earth-sun line. By using the errors predicted in Figure 4.11, the rotations have been calculated and expressed in Table 4.3 (see Appendix C.2):

Table 4.3

Inclination Angle Errors

Error ($^{\circ}$)	Plane rotation ($^{\circ}$/rev)	Plane rotation ($^{\circ}$/year)
+0.6	0.0050 west	27.2 west
+1.2	0.0104 west	56.7 west
-0.6	0.0048 east	26.2 east
-1.2	0.0108 east	58.85 east

An example of this rotation appears in Figure 4.12. It should be noted here that a slightly non sun-synchronous orbit does not destroy data gathering capability in either limb or nadir modes.

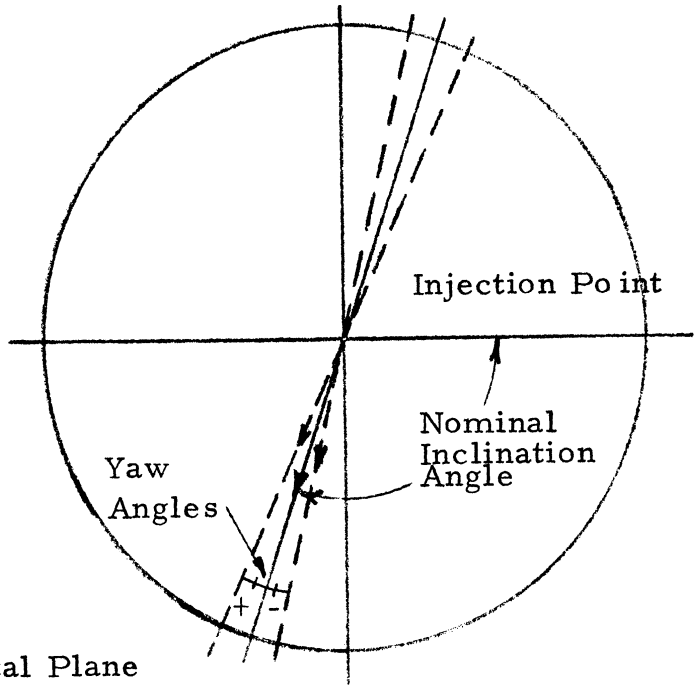

Resulting Orbital Plane with Possible Errors in Yaw

Figure 4.10 Errors in Inclination

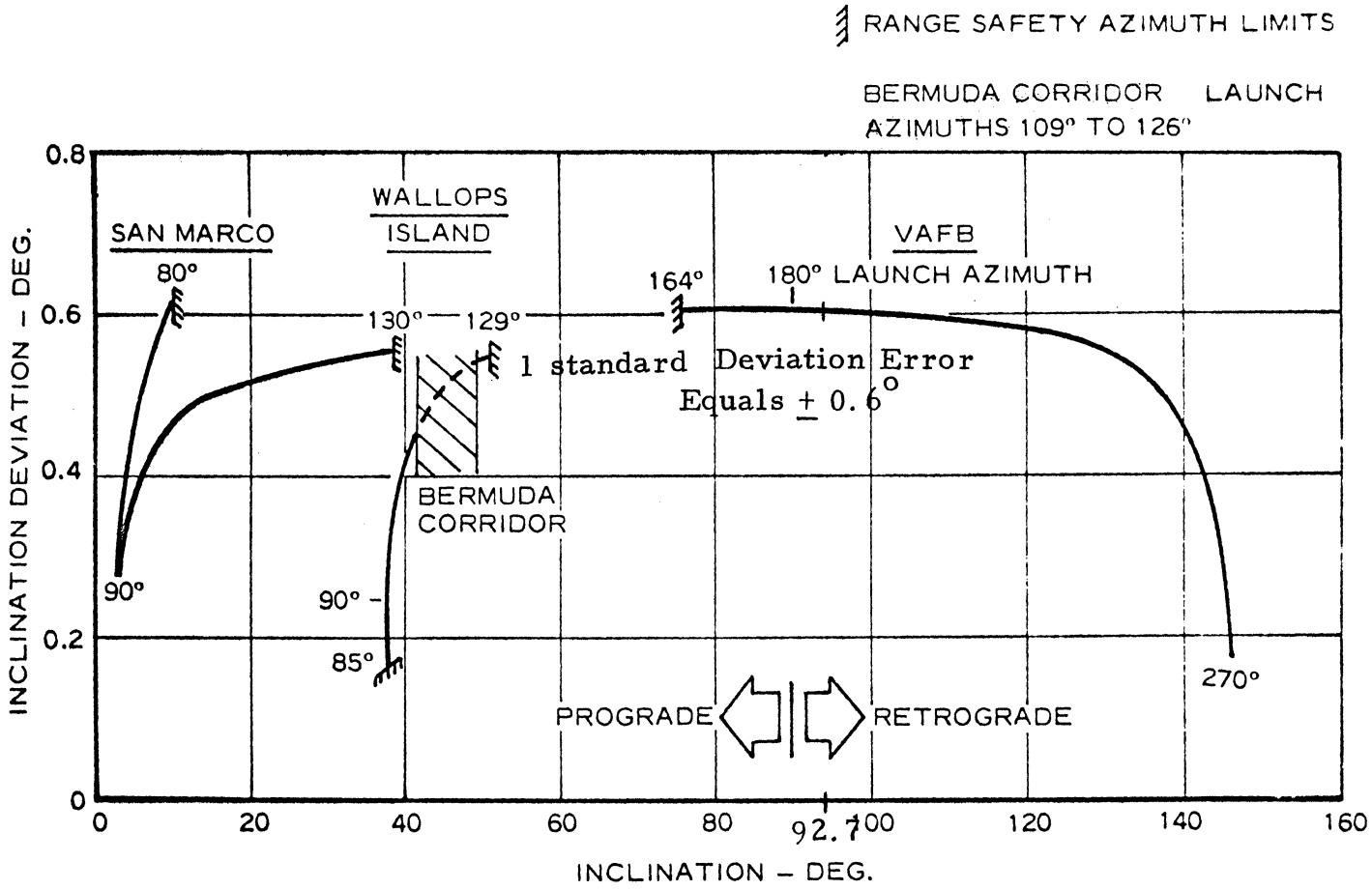

Figure 4.11 Inclination Errors Due to Injection

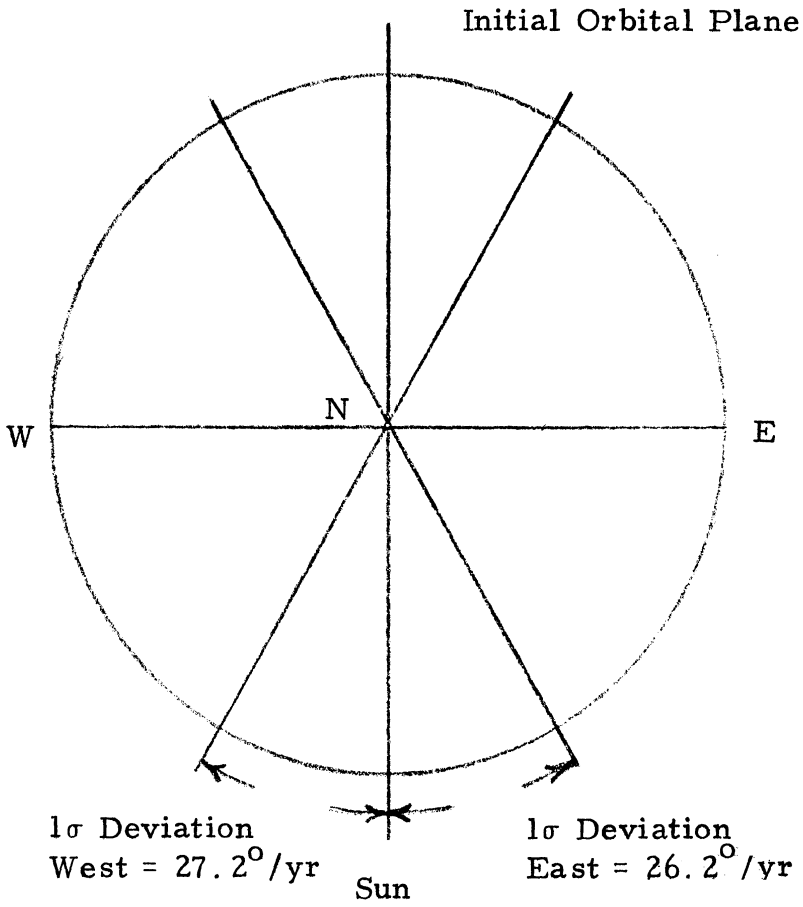

Figure 4.12 Plane Rotation

4.3.4 Errors Involved in Thruster Operation

The error involved in thruster operation occurs mainly because the thruster vector has a nominal deviation from center line. Therefore, the thrust will not pass through the satellite's center of gravity - thus causing a torque to be produced. Since accurate pointing is necessary for both burns, the reaction jets will be used to produce a cancelling torque. Calculations of the torque arrising from an assumed 0.25^{o} misalignment (see Reference 5, p. 137), and the resulting momentum imparted to the satellite, appear in Appendix C.8.

4.4 PROPULSION SYSTEM

4.4.1 Thruster

A schematic of the propulsion system is shown in Figure 4.13. Thruster and fuel specifications are as follows:

Number of thrusters	1 - Hamilton Standard REA-16-5
Total thrust	5-lbf
Specific impulse	220 sec at 300 psia
Power	14 watts
(see Reference 4, p C-69)	
Fuel	Hydrazine (N_2H_4) and Shell 405 catalyst
Density (N_2H_4)	62.7 lb/ft^3
Freezing point (N_2H_4)	36^{o}F (neat)
Boiling point (N_2H_4)	236.3^{o}F

Table 4.4

Since the final weight of SCOPE is 205.9-lbs (190.9 + 15 contingency), and the specific impulse is 220 sec, the approximate time involved, total impulse, and fuel required for each case shown in Table 4.2 have been calculated as (see Appendix D.6):

	Burn 1			Burn 2			Total		
Case	ΔT	I	Fuel	ΔT	I	Fuel	ΔT	I	Fuel
1	20.3	101.5	0.46	364.0	1820.0	8.28	384.3	1921.5	8.74
2	210.5	1052.5	4.79	87.1	435.5	1.98	297.6	1488.0	6.77
3	18.37	91.85	0.42	271.0	1355.0	6.17	289.4	1447.0	6.59
4	132.2	661.0	3.01	170.1	850.5	3.88	302.3	1511.5	6.88
5	8.22	41.10	0.19	174.5	872.5	3.97	182.7	913.5	4.16
6	105.8	529.0	2.41	110.8	540.0	2.52	216.6	1083.0	4.93

Table 4.5 ΔT = sec fuel = lbs
I = lbf-sec

The times are approximate because the thruster does not continuously supply 5-lbf. Since the fuel flow is provided by pressurized gas, as the fuel supply decreases so does the gas pressure. Hence the flow rate of the fuel decreases.

4.4.2 Latch Valves

Latch valves (manufactured by Carlton 2217-001-2) have been supplied in order to isolate any component of the propulsion system should it fail. As can be seen from Figure 4.13, either tank, the 5-lbf thruster or any single set of reaction jets can be removed from the system.

The latch valves operate in an on-off mode. A pulse of 54 watts (1.93 amps - see Reference 4, p. C-71) opens or closes the valve. After orbit injection, the latch valves will be opened sequentially and remain open. A pressure transducer was included into the system for two reasons. First, it is a valid test of the integrity of the system. If a tank fails or a thruster does not shut off at the proper time, the pressure transducer will register fuel flow (through dropping pressure) at a time in the flight program when there should be none - allowing either the tanks or an opened thruster to be isolated by closing a latch valve. Secondly, by monitoring the pressure drop, and knowing the relation between thrust and pressure, the impulse (thrust x time) can be regulated to specific amounts.

4.4.3 Tanks

As shown in Figure 4.13, the tanks are spherical in geometry with a spherical membrane separating the nitrogen gas from the hydrazine. A two to one nitrogen-hydrazine volume ratio was decided upon to limit the decrease in pressure of the nitrogen gas. The initial gas pressure will be 300 psia (at 50°F) and hence the final pressure will be approximately 200 psia

Limitations were placed on the tank diameter since the tanks were to be placed between the torsion tube and the skin of the satellite. This restriction allows an inside diameter of 9.51 in or a volume of 0.1745 ft^3 for the hydrazine. This volume relates to 10.95 lb of hydrazine, two pounds of which will be used to power the reaction jets for attitude and control leaving 8.95 lb for orbit correction. Therefore the capability of the 5-lbf thruster is limited to 306 ft/sec (see Appendix C.9).

4.4.4 Propulsion System Breakdown

The quantity and weight of the various propulsion system components are listed in Table 4.6.

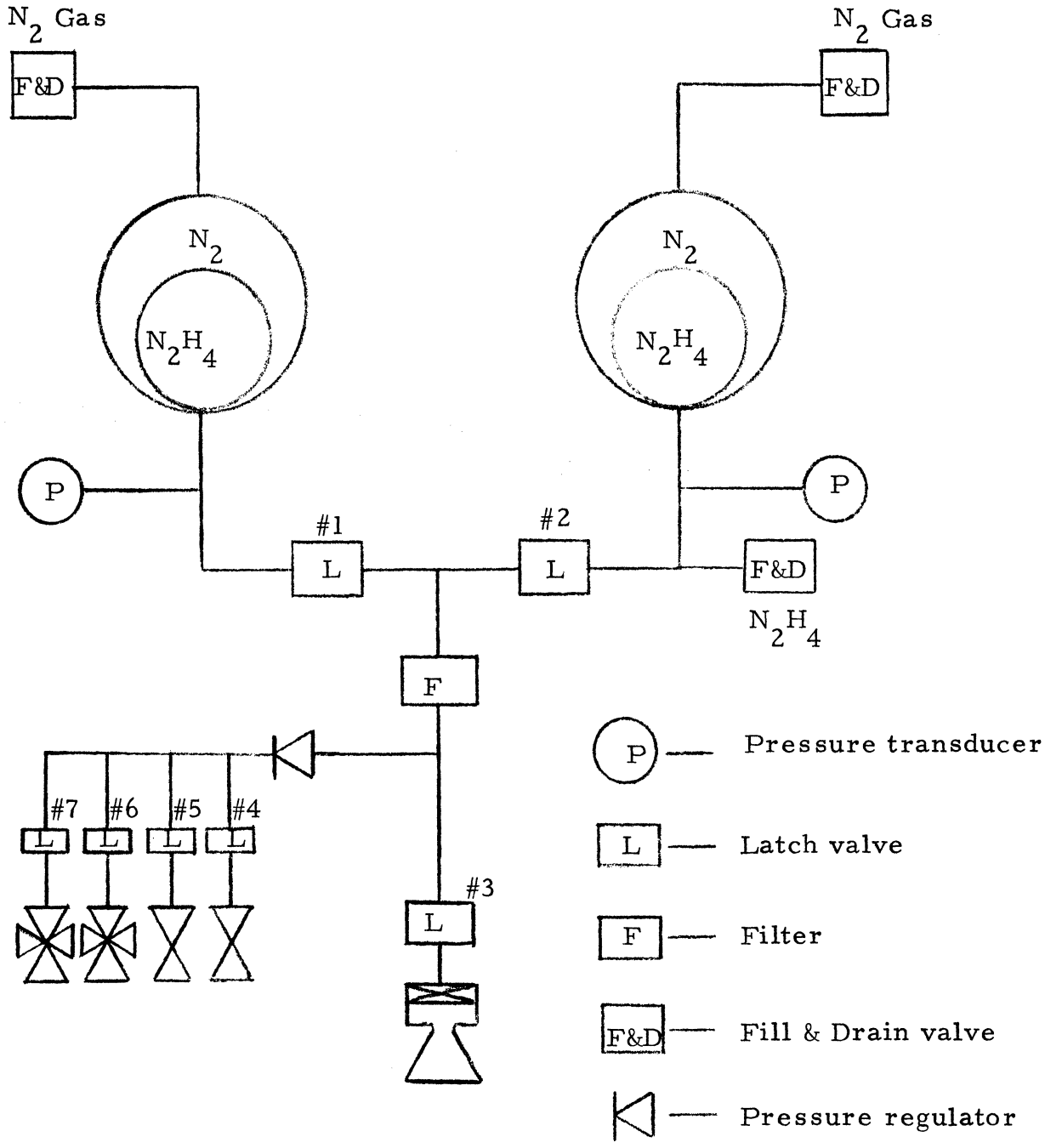

Figure 4.13 Propulsion System

Table 4.6

Item	Quantity	Total Weight
Latch valve	7	4.21
Feed and drain valve	3	0.6 (Ref. 7)
Fuel filter	1	0.4 (Ref. 7)
Pressure transducer	2	0.6 (Ref. 7)
Pressure regulator	1	1.0 (est.)
5-lbf thruster	1	0.87
0.055-lbf thruster (jet)	12	1.0 (Ref. 4)
Tank	2	5.5 (Ref. 7)
Hydrazine	-	10.95
Nitrogen gas	-	0.538
Wiring and connectors	-	1.0 (Ref. 7)
Tubing	-	2.5 (Ref. 7)
Total	29	29.0

4.5 REFERENCES

1. Wolverton, Raymond W., ed., Flight Performance Handbook for Orbital Operations, John Wiley and Sons, New York, 1961.

2. Space Planner's Guide, USAF Systems Command, 1965.

3. Scout User's Manual, LTV Corporation

4. Small Applications Technology Satellite, Program and Spacecraft Study Report, Goddard Space Flight Center, Greenbelt, Maryland, 1970.

5. Project SCANNAR, University of Michigan Aerospace Engineering Design Project Report, Ann Arbor, April 1970.

6. Donnay, J. D. H., Spherical Trigonometry, Interscience Publishers, New York, 1945.

7. Earth Observatory Satellite Definition Phase Report, Goddard Space Flight Center, Greenbelt, Maryland, 1971.

5
LAUNCH VEHICLE

5.1 INTRODUCTION

Project SCOPE necessitates being able to reliably and economically inject a 190.9 pound payload into a circular orbit of altitude 320 nautical miles. With this in mind, the Scout launch vehicle was chosen because of its low cost and history of reliable and successful launches. Its record shows 52 successful launches out of 55 from 1963 through 1971. The last twenty have been successful and much research is in progress to improve the accuracy and payload capabilities in the future (Reference 1). The Scout configuration that was chosen, known as the Scout D, is capable of launching a 320 pound payload into a 320 nautical mile circular polar orbit (Reference 2). The Scout D is a relatively inexpensive booster costing approximately 2.2 million dollars. This cost includes the launch vehicle, launch facilities, and payload interfacing service.

5.2 VEHICLE DESCRIPTION

The Scout D is the smallest and least expensive launch vehicle available in the United States. It is a four stage solid propellant rocket booster which includes its own telemetry system and attitude control capability to insure injection into orbit at the proper attitude. The Scout D provides a lift-off thrust of 130,000 pounds, stands 74.25 feet, and its weight on the launch pad less the payload is approximately 47,500 pounds (Reference 3). The Scout vehicle offers three different size heatshields and a standard separation system to provide for reliable separation of the payload from the spent fourth stage booster. The restraints on the satellite design imposed by the Scout D include a size limitation of the spacecraft due to the heatshield and separation mechanism. The significant details affecting SCOPE include the usable payload envelope, the vehicle-payload interfacing, the payload environment, and quantitative measurements of the Scout D performance such as acceleration and spin rates. These and other more detailed specifications are readily obtainable and do prove compatible with our satellite design.

5.3 LAUNCH SEQUENCE

After lift-off and first stage burnout, there usually occurs a short coast period. A coast period of five seconds minimum follows second stage burnout. The heatshield is ejected during this coast phase just prior to third stage ignition. Sometimes a non-optimum trajectory is flown, depending upon the mission, to dissipate excess performance. Following third stage burnout, the control system orients the vehicle to the proper attitude for fourth stage ignition. Following a long third stage coast phase

of between 200 and 600 seconds depending upon the mission, the payload plus fourth stage are spun up and separated from the expended third stage to provide stability for the fourth stage burning at the proper attitude. The fourth and injection stage is then ignited to provide the necessary velocity for injection into orbit. After fourth stage burnout, the fourth stage signals the satellite to activate the despin mechanism. After the payload plus spent fourth stage are despun, the payload is separated from the expended fourth stage and is then in its orbit. The times of the launch sequence are included in the mission timetable, (see Figure 5.5)

5.4 LOADING FACTORS

The acceleration loadings during launch are a maximum at 28 seconds after fourth stage ignition, and for a 225 pound payload which is approached with SCOPE's 190.9 pound payload plus 33.1 pound separation system, this maximum is 15 g's axial acceleration. The tests that the SCOPE payload is required to pass include (Reference 4):

a) axial acceleration of 22.5 g's for three minutes
b) lateral acceleration of 3 g's for one minute
c) spin rate of 180 revolutions per minute
d) shock and vibration tests as specified by the Scout contractors, LTV Aerospace

All other axial accelerations during launch will be much lower than the maximum.

5.5 PAYLOAD ENVELOPE

The size restraint imposed by the decision to use the Scout 34 inch diameter, -40 nose station heatshield is shown in Figure 5.1 (Reference 5).

The SCOPE payload is designed such that the solar paddles extend downward around the fourth stage motor case. Therefore special detailed coordination with the Scout contractor is essential to orient the payload properly when attached to the launch vehicle.

5.6 LAUNCH VEHICLE SYSTEMS

Details of other Scout systems influenced the design of the SCOPE satellite. Among these systems are the separation mechanism, the interface connector package, and the spin-up motors.

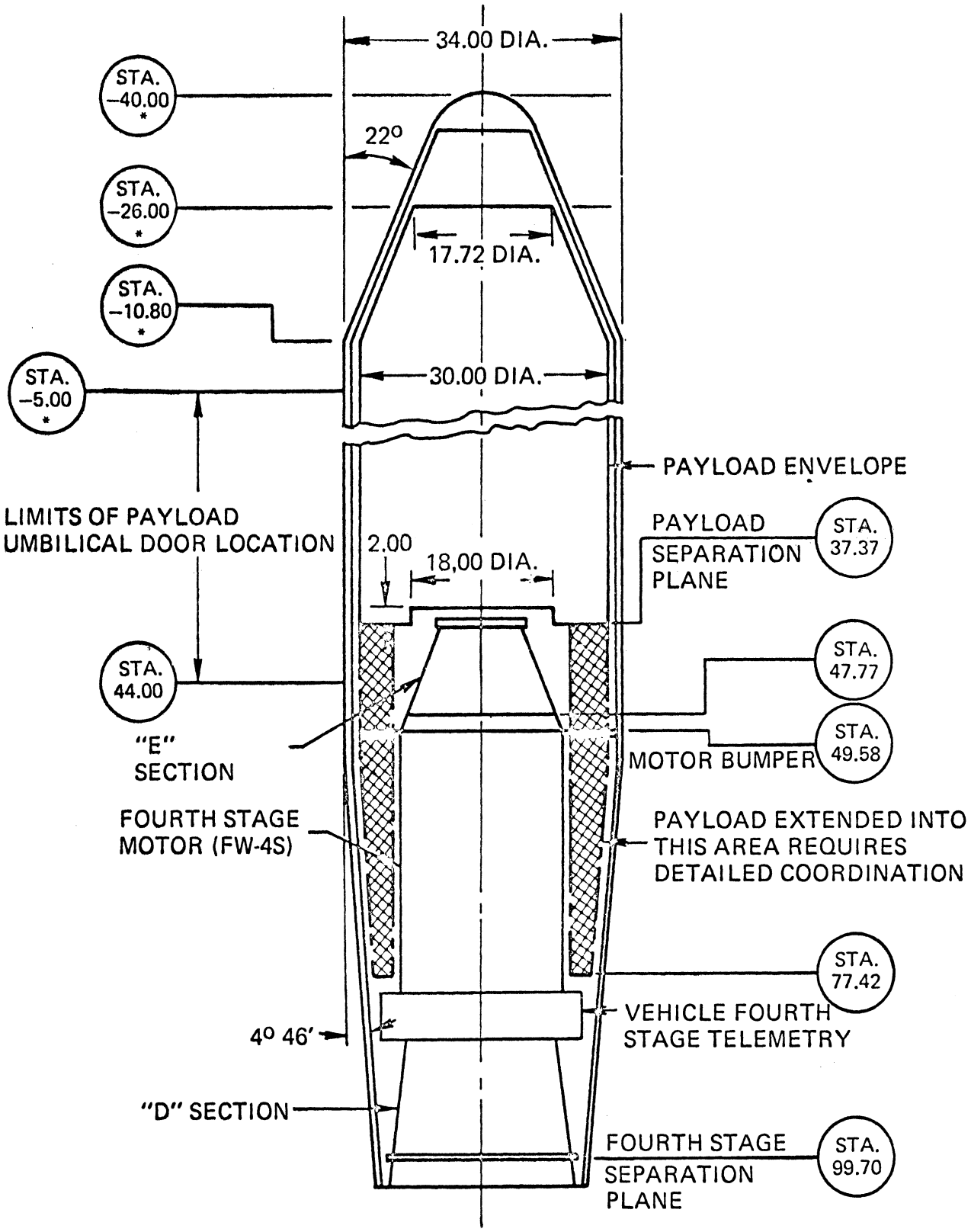

SCOUT PAYLOAD ENVELOPE – 34 INCH DIAMETER HEATSHIELD

Figure 5.1

5.6.1 Separation System

The basic "E" payload separation system chosen for SCOPE consists of three basic parts. The basic "E" section adapter and separation system is the first part, and it consists of a conical magnesium structure with springs and a spring retainer ring, to supply the force for separation. The second part is the payload support ring which has threaded holes for mating to the bottom of the payload. The third part is the payload separation clamp which consists of steel bands with v-blocks which hold the "E" adapter section and the payload support ring together. The "E" section is part of the fourth st structure and therefore the clamp holds the payload to the launch vehicle. For separation, pyrotechnic units attached to the bands are activated to release the bands and allow the energy of the previously restrained springs to push apart the payload and fourth stage with enough separation velocity to avoid collision with each other. A cross-section of this separation system is shown in Figure 5.2.

Included in the separation system is a fourth stage diagnostic telemetry system. The total weight of the "E" section, springs, separation clamp, telemetry system, and payload support ring is 33.1 pounds and this weight is added to the orbiting payload weight of 190.9 pounds as part of the Scout D capability of 320 pounds for the mission. The payload support ring stays with the payload after separation and its weight of one pound is thus added to the SCOPE weight of 190.9 pounds as the total weight in orbit.

5.6.2 Payload Interface Connector Package

SCOPE uses the option of the Scout package of three extra telemetry channels which are unused by the "E" section. SCOPE plans to use these three channels to provide the signals for activiation of despin, solar paddle and antenna deployment, and for initiation of our communications. Once separation from the fourth stage has occurred, SCOPE can no longer use these channels, therefore they will be used for activating operations occurring prior to separation. The weight of using this option is 0.75 pounds.

5.6.3 Spin-up

For spin-up, there are six available combinations of three different spin motors to choose from to obtain the desired spin rate of between 110 and 120 revolutions per minute. For the SCOPE calculated value of payload roll inertia of 2.40 slug-ft^2, and the total Scout measured inertia of 8.81 slug-ft^2 for the fourth stage and all the other hardware that is spun-up (Reference 6), the corresponding combination of spin motors to use would be two 0.6 KS 40 and two 1.0 KS 40 motors to get a predicted spin rate of

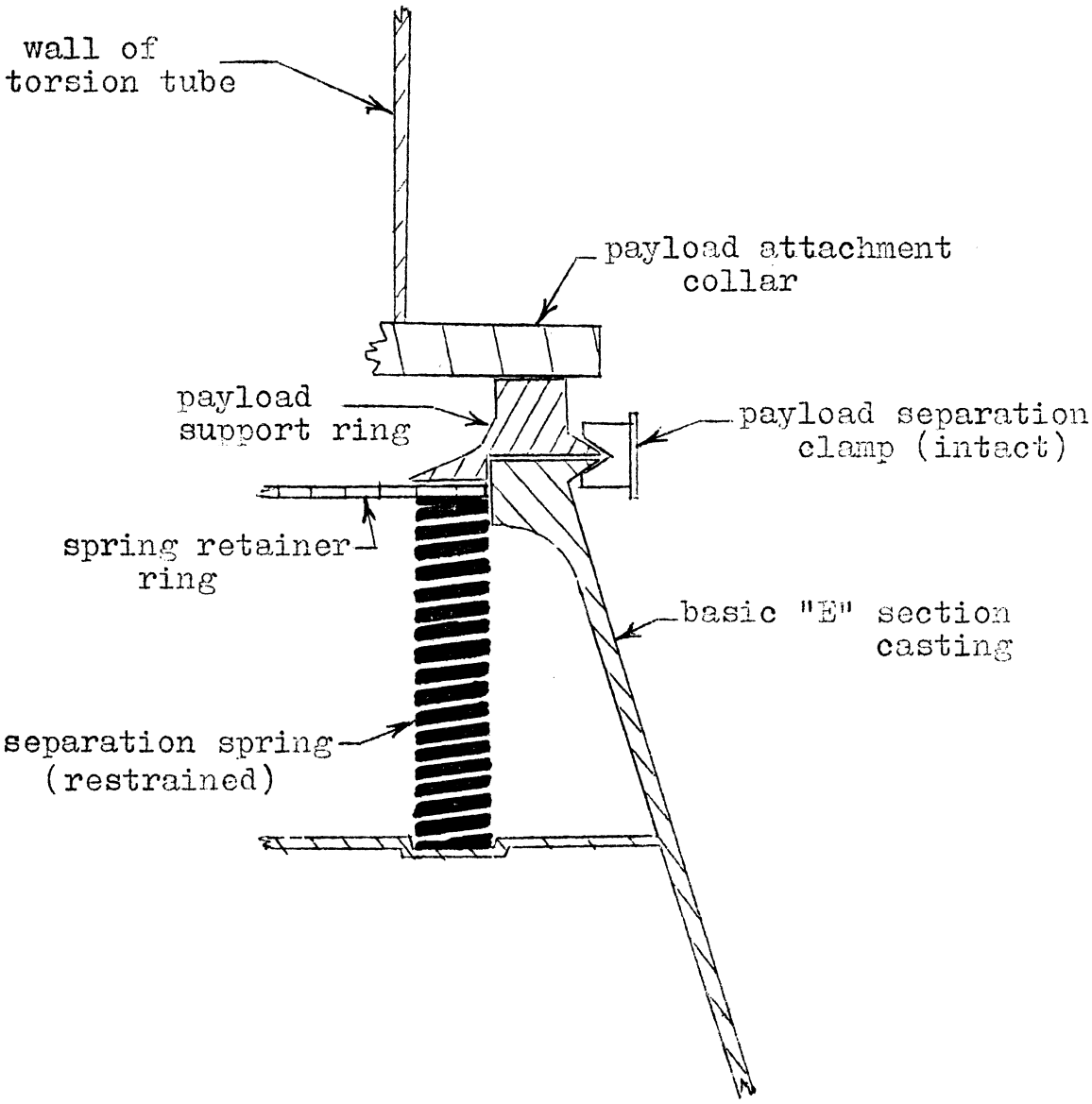

Figure 5.2 Cross-Section of Separation System

Figure 5.3

ORBIT MISSIONS

STAGE IMPACT AREAS

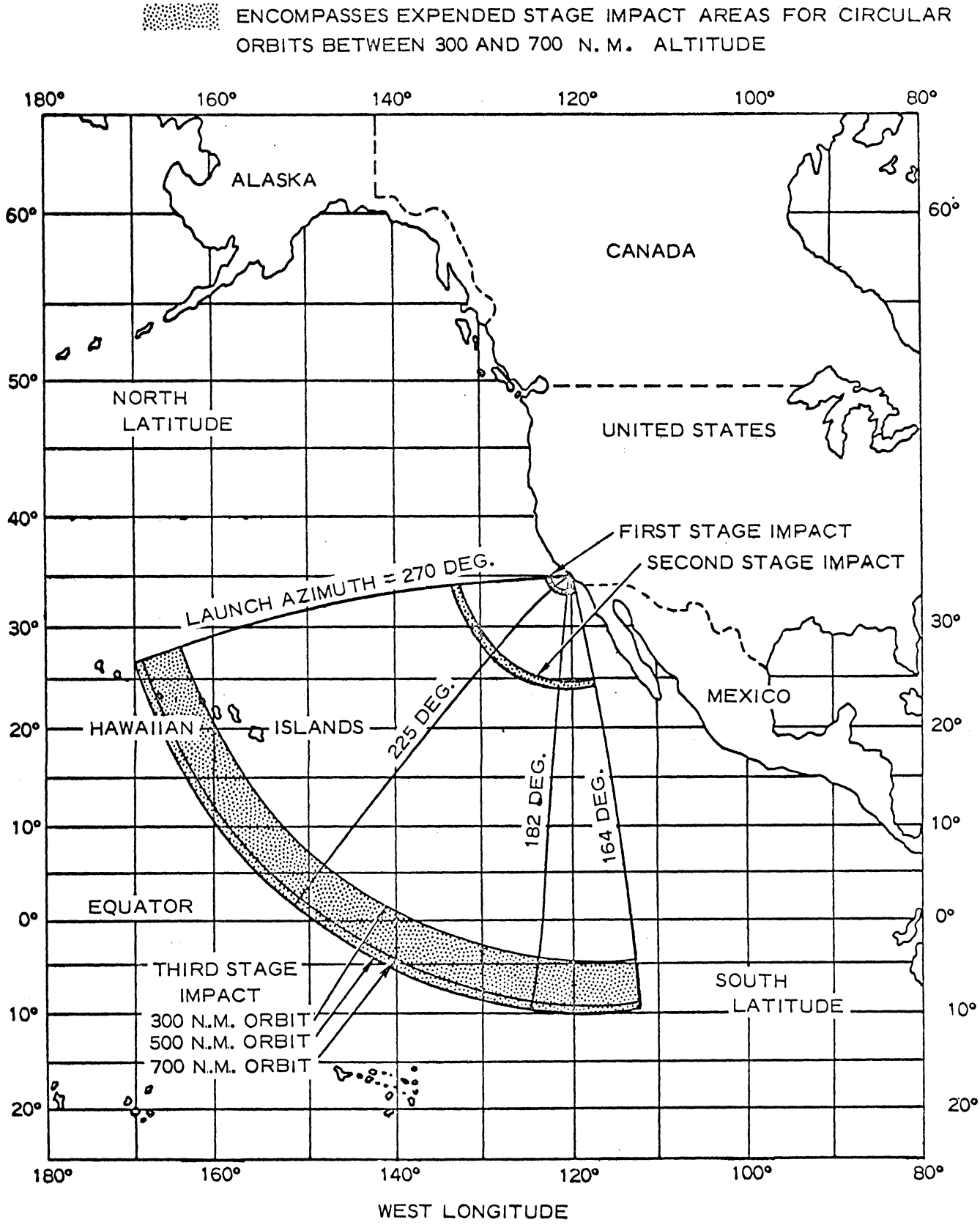

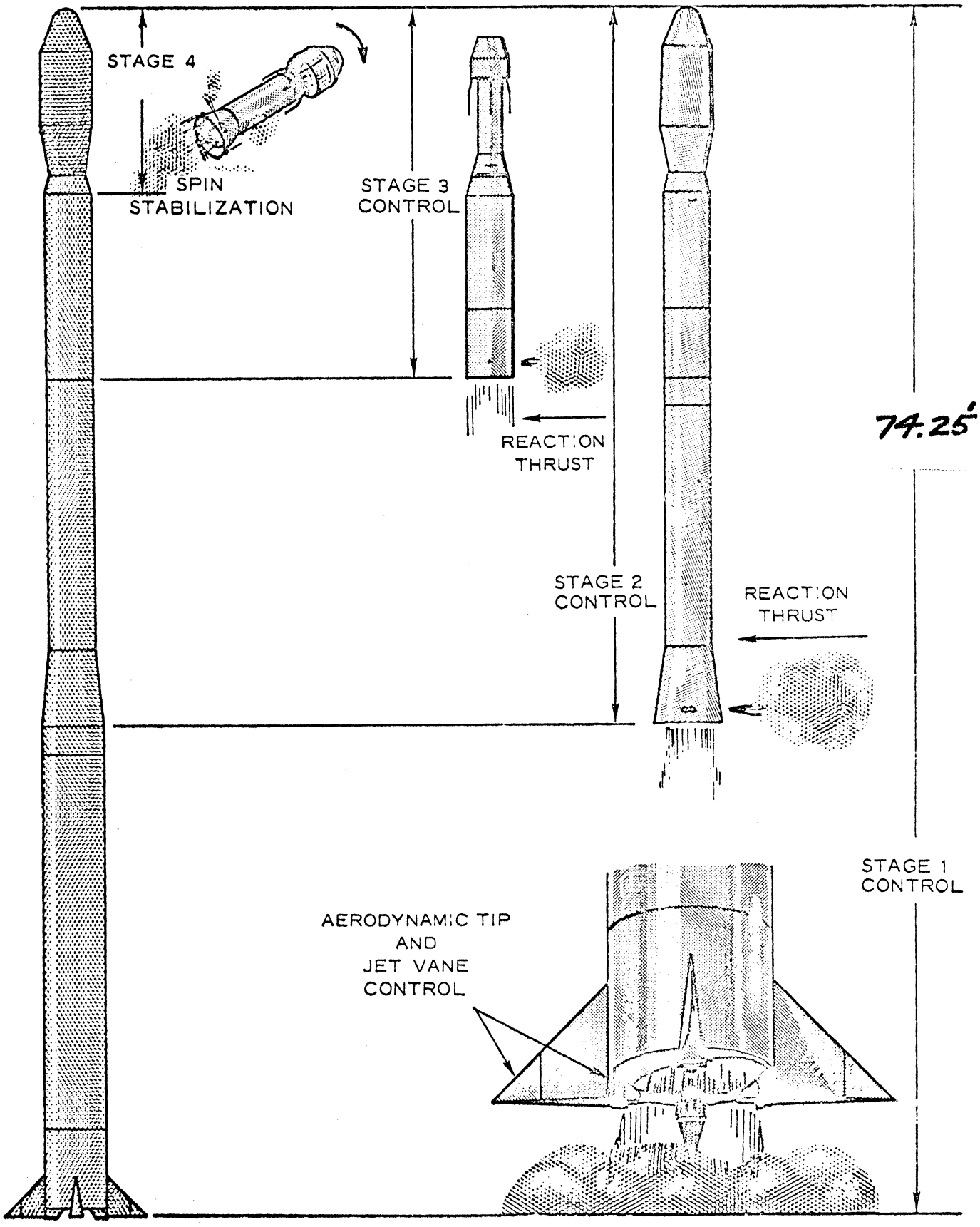

FIGURE 5.4. STAGE CONTROL SYSTEMS

Time (seconds)	Event
0	Stage 1 ignition, start timer
78	Stage 1 burnout
82	Stage 2 ignition, Stage 1 separation
120	Stage 2 burnout
123	Heatshield ejection
125	Stage 3 ignition, Stage 2 separation
155	Stage 3 burnout
603	Spin-up ignition
605	Stage 3 separation
609	Stage 4 ignition
642	Stage 4 burnout
*	Despin signal
*	Separation of Stage 4 and Payload

*These times are at ground command discretion

Figure 5.5 Launch Sequence

117 revolutions per minute (Reference 7). This spin rate is large enough to safely stabilize the spacecraft without causing substantial additional stress to the payload systems.

5.7 LAUNCH VEHICLE RANGE AND BOOSTER SPLASHDOWN

Stages one through three of the Scout D launch vehicle will re-enter the earth's atmosphere and fall into the Pacific Ocean. The range and stage splashdowns are presented in Figure 5.3 (Reference 8). The Scout launch vehicle itself is shown in Figure 5.4.

5.8 REFERENCES

1. Scout Launch Vehicle, Vought Missiles and Aerospace Company, LTV Aerospace Corporation, p. 11.

2. Scout Planning Guide, Vought Missiles and Aerospace Company, LTV Aerospace Corporation, May 1971, 1. 59.

3. Scout Planning Guide, p. 1.

4. Scout User's Manual, Vought Missiles and Aerospace Company, p. 3-42 and p. 3-64.

5. Scout Planning Guide, p. 28.

6. Personal Communication with John Pacey, LTV, Dallas, and Scout User's Manual, tables 3-2, 3-3, and 3-8.

7. Scout User's Manual, Figure 3-41.

8. Scout User's Manual, Figure 5-25.

6
STRUCTURES

6.1 INTRODUCTION

The primary concern in SCOPE has been the creation of a simple, lightweight structural housing which will provide more than adequate space for the experiment package and required supportive systems, at the same time providing optimum environmental capabilities. Major consideration was given, as well, to ease of manufacturing and servicing of the assembled spacecraft. It was found that the torsion tube concept best fulfilled these requirements (Reference 1).

It will be noticed in Figures 6.1 and 6.2 that this design has provided us with an abundance of usable volume. This, and the light overall weight of the present experiment package, make it possible to include one or more subsidiary experiments, provided that they do not add too great a burden to the power system.

It was found that, in general, high strength aluminum alloys provided the maximum strength to weight ratio among economically acceptable material While advanced technology materials were considered, it was concluded that they were economically unfeasible at this stage of their development (Referenc All components were designed for minimum test forces of 25 g's longitudinal acceleration, 4 g's lateral acceleration, and a rotational acceleration of 7 revolutions per second per second (Reference 3). It should be noted that in making these calculations a conservative weight of 275 lbs was assumed for the final spacecraft weight. See Appendix D for detailed calculations.

6.2 EXTERIOR DESIGN

6.2.1 Shell Design (see Figure 6.1)

Thermal considerations led to the use of 7075-T6 high strength aluminum in making the basic right octagonal cylinder. Each face of the shell is 10.35 in by 40.0 in by 0.01 in thick. The shell will be manufactured in four basic parts: the top and bottom endplates, the sides abc, and efg, which will be formed from single sheets, and sides d and h, which will be bolted to the assembly in such a way that they may be removed, thus providing ample access to the interior for assembly and servicing procedures. The endplates are likewise made out of 7075-T6 aluminum. The are octagonal in shape with a side length of 10.35 in and a thickness of 0.03 in (It should be noted that the flat endplate design makes possible the dual launch of a smaller vehicle in a piggyback mode with only slight modification.)

BASIC PAYLOAD STRUCTURE

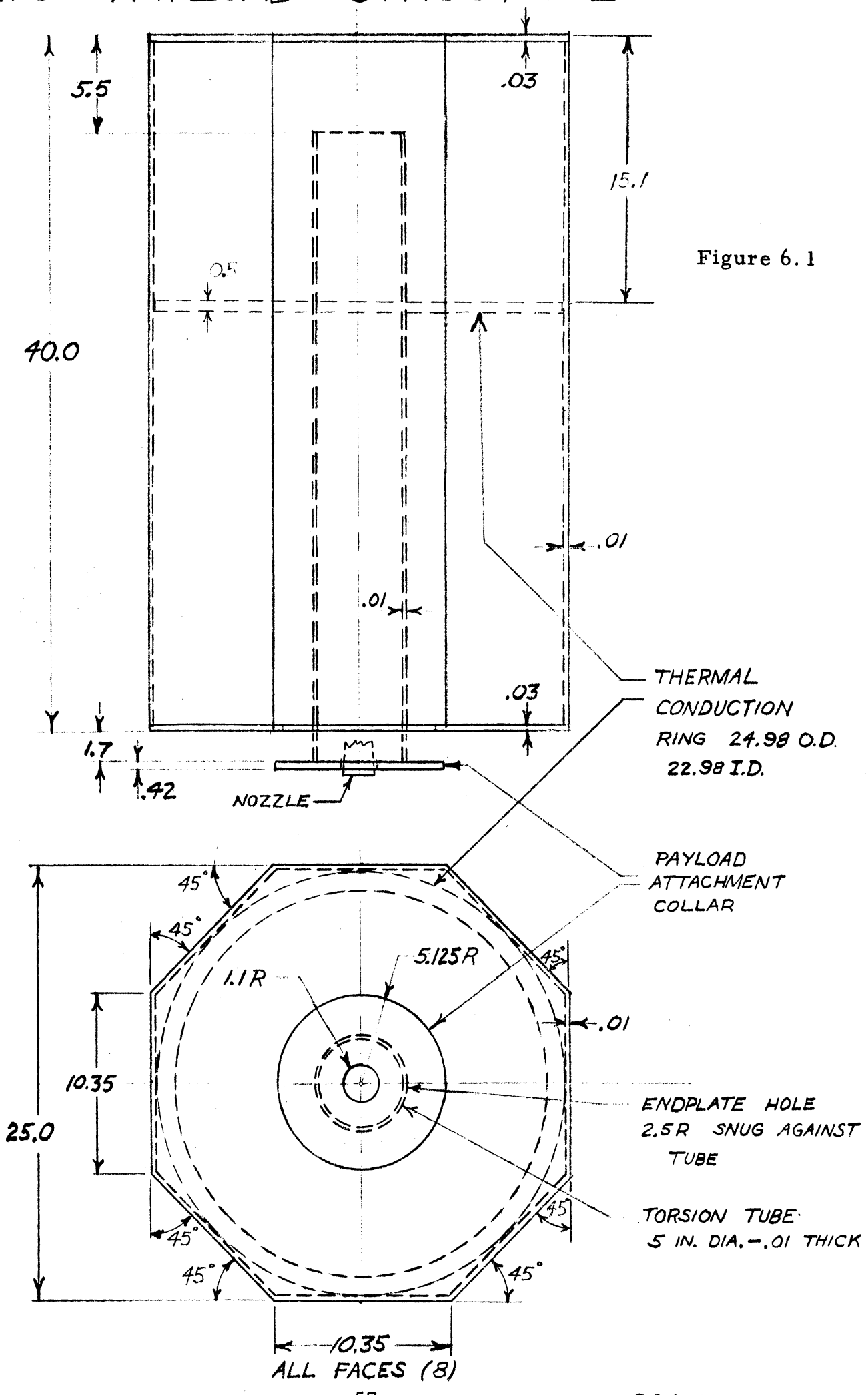

Figure 6.1

SCALE 8:1

6.2.2 Launch Configuration

At launch the vehicle is in an inverted position, with the solar panels folded down along the sides of the Scout fourth stage motor (see Figure 6.2). The turnstile antenna will also be folded along the satellite sides. Both antenna and solar panels will be held in place with a fastening band which wil be released just prior to separation from the fourth stage. In this configura the center of gravity is located on the longitudinal axis, 24.2 inches from th top (sensor) endplate. The moments of inertia in launch configuration are:

$$I_{xx} = 1000 \text{ slug-in}^2$$

$$I_{yy} = 1165 \text{ slug-in}^2$$

$$I_{zz} = 345 \text{ slug-in}^2$$

6.2.3 Operational Configuration

The configuration for nadir viewing will be as shown in Figure 6.2b. The center of gravity is still located on the longitudinal axis, though it is now only 19.2 inches from the sensor endplate. Moments of inertia in this configuration are:

$$I_{xx} = 680 \text{ slug-in}^2$$

$$I_{yy} = 1940 \text{ slug-in}^2$$

$$I_{zz} = 1460 \text{ slug-in}^2$$

6.2.4 Solar Panel Design

Design of the solar panels was guided largely by the need for a highly rigid, lightweight structure with large surface area. This lends itself to the general honeycomb sandwich type of structure (Reference 4). The panels consist of rectangular panels of 2014 aluminum honeycomb with a hexagonal cell size of 3/16 inch, and a foil thickness of 0.0007 inches. Face plates of HM21-A magnesium sheet, 0.032 inches thick areused to complete the sandwich construction.

The panels will be joined together to form the V type solar paddles as shown in Figure 6.3. Movable hinge joints are provided to allow the paddles to fold compactly around the spacecraft and fourth stage motor during launch.

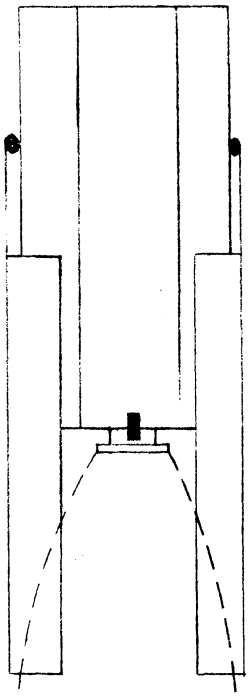

Earth

(a) Launch Configuration

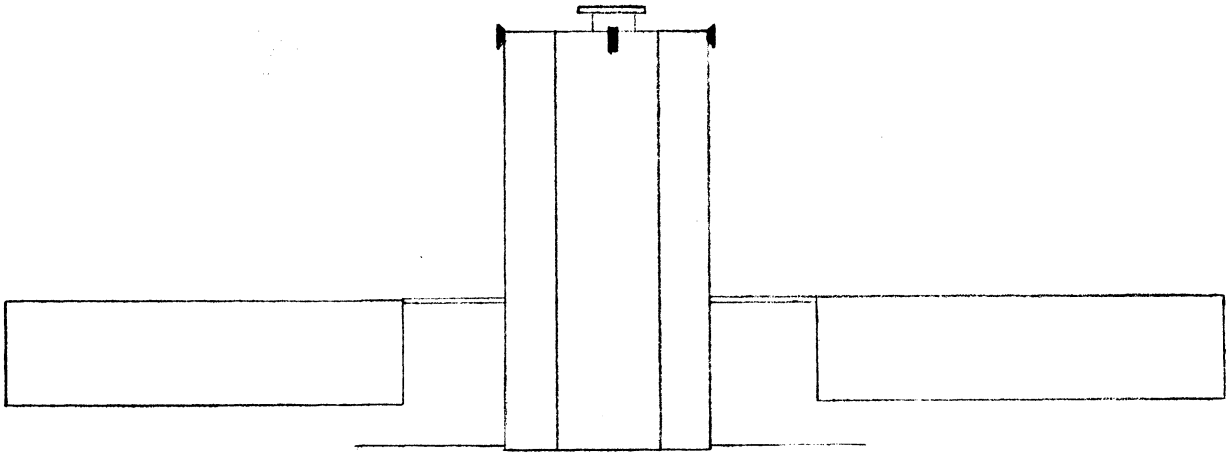

Earth

(b) Deployed Configuration

Figure 6.2 Satellite Configurations

6.3 INTERIOR SATELLITE DESIGN

6.3.1 Internal Structure (see Figure 6.1)

The torsion tube was selected over all other main support designs because of its superior strength to weight ratio (Reference 5). The tube used is a standard 7075-T6 aluminum extrusion with an outer diameter of 5.0 inches, a wall thickness of 1/16 inch, and a length of 36.2 inches. The major design consideration for this configuration was column buckling, with respect to which it has been designed to withstand a load of 2.4×10^4 pounds (see Appendix D.1).

A thermal conduction ring, also of 7075-T6 aluminum, is used for the dual purpose of thermal control and structural bracing for the solar panel booms. It is inscribed within the octagon, having an inner diameter of 24.0 inches and a thickness of 0.5 inches. It is attached to the torsion tube by seven radial strips, thus providing a strong connection between the internal and external structures.

6.3.2 Component Placement in SCOPE

Component location was determined in accord with thermal recommendations and center of gravity requirements (see Figures 6.4, 6.5, Table 6.1). The placement of components was done in such a manner as to keep the center of gravity on the longitudinal axis. The Carbon Monoxide sensor and radiometer are mounted on the torsion tube in such a manner that the thermocascade is adjacent to the "cold" wall of the spacecraft. The experimental package will be shock mounted by cantilevered flexural springs extending from the torsion tube. The interior of the torsion tube is used as a low temperature fluctuation compartment in which the NiCd batteries and other highly temperature sensative components are positioned. Momentum wheels and gyros are placed on the rotational axes. A coordinate system has been set up using these axes. The exact location of each component can be found using Table 6.1 and Figures 6.4 and 6.5.

6.3.3 The Attachment Ring

The payload support collar is designed to provide the interface between SCOPE and the fourth stage of the Scout launch vehicle (see Figure 6.6). It is a flat circular ring manufactured from 7075-T6 aluminum with an outer diameter of 9.50 in, and an inner diameter of 2.20 in to accommodate the Delta V motor nozzle, and a thickness of 0.42 in. For a detailed analysis see Appendix D.2.

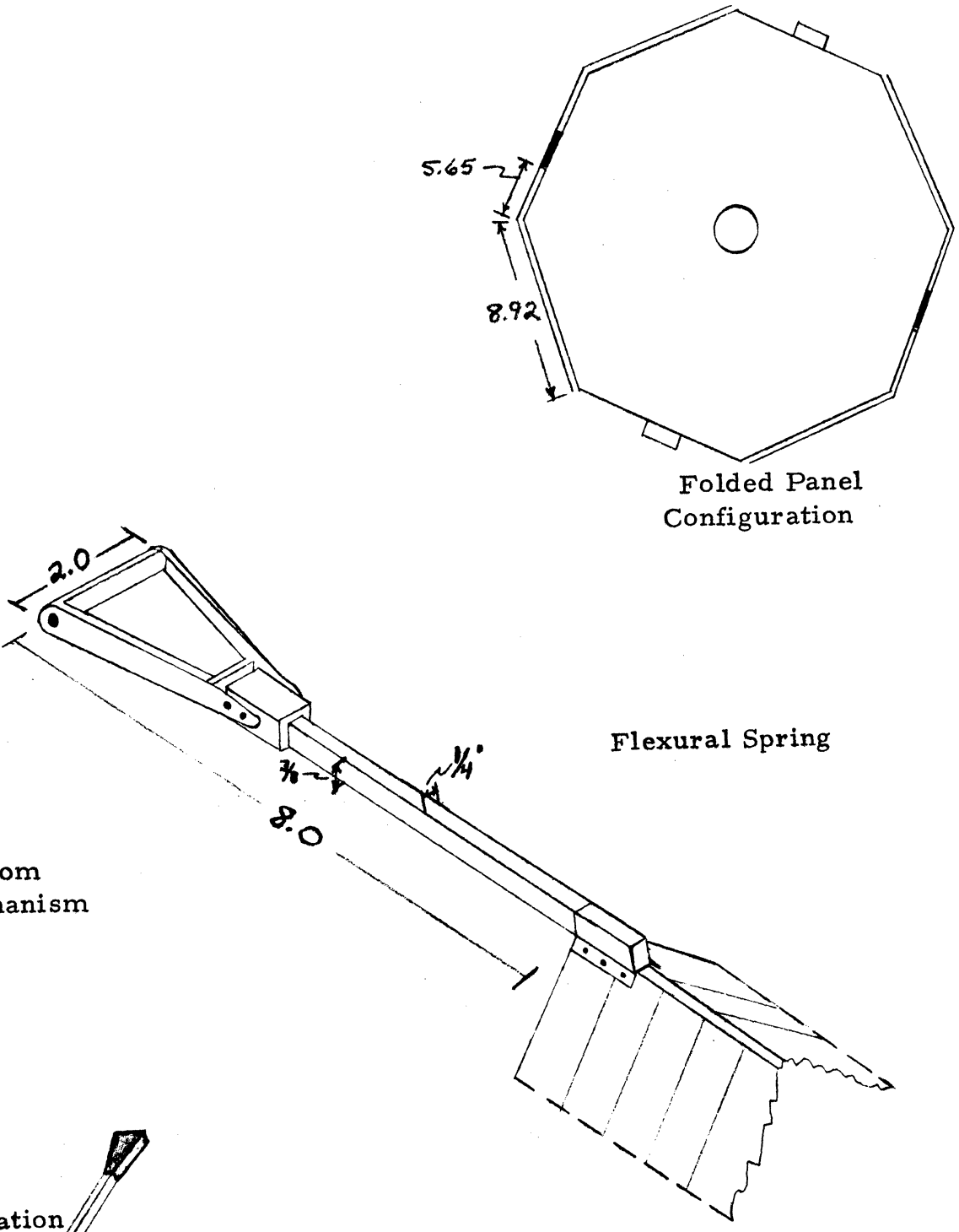

Figure 6.3 Paddle Boom Mechanism

Figure 6.4 Layout-Side View

Scale 1:6

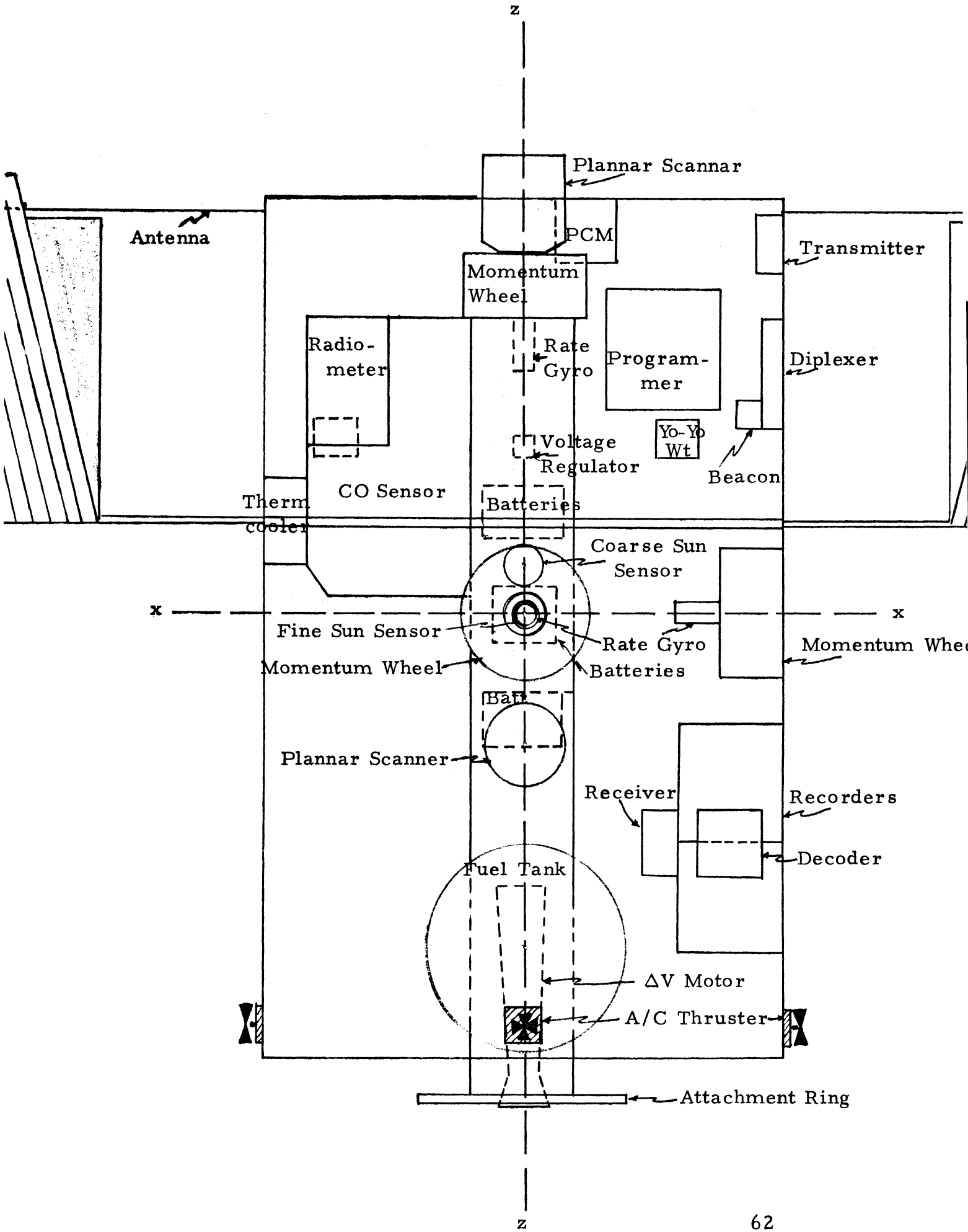

Figure 6.5 Layout- Top View

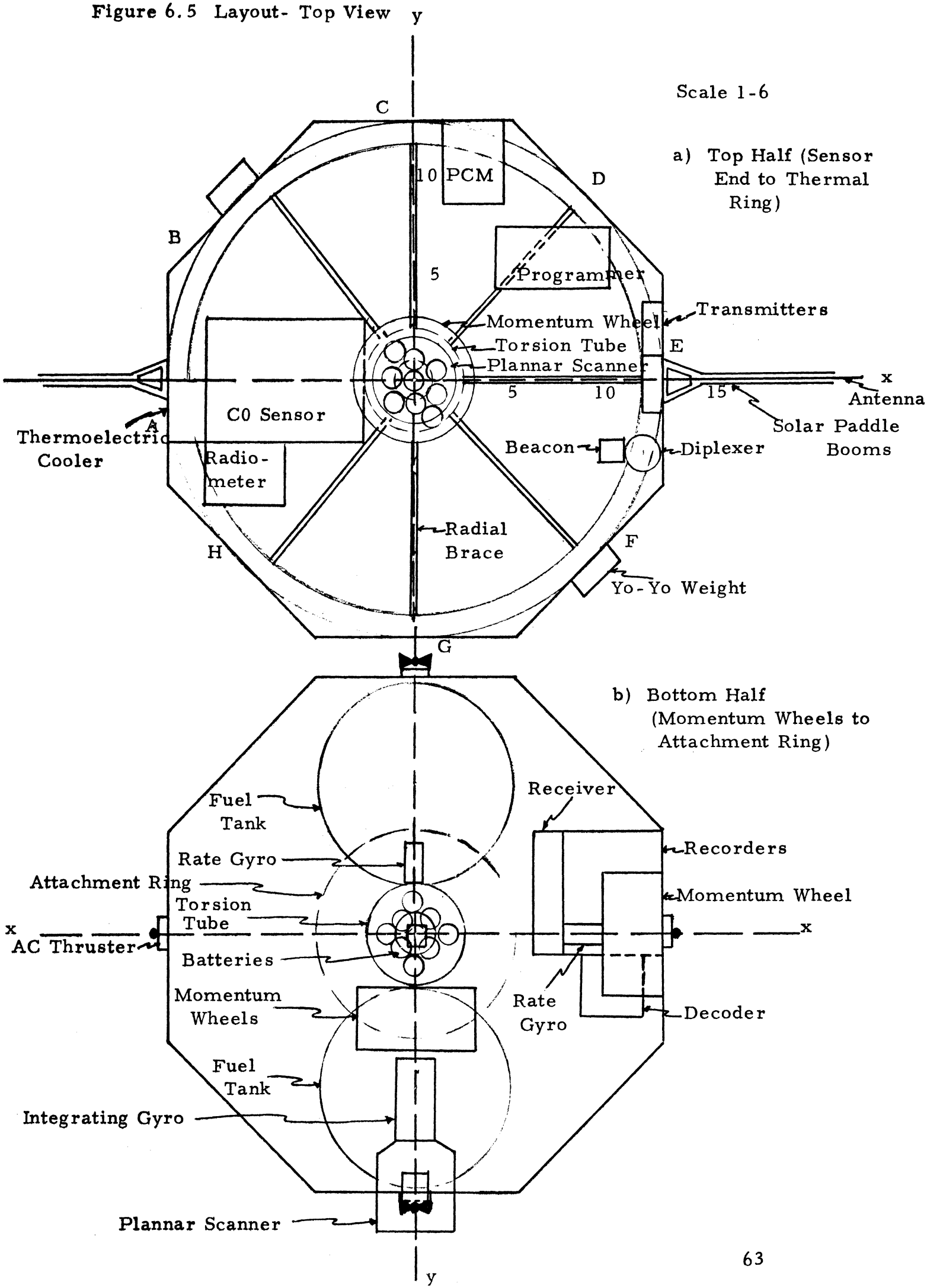

PAYLOAD ATTACHMENT COLLAR

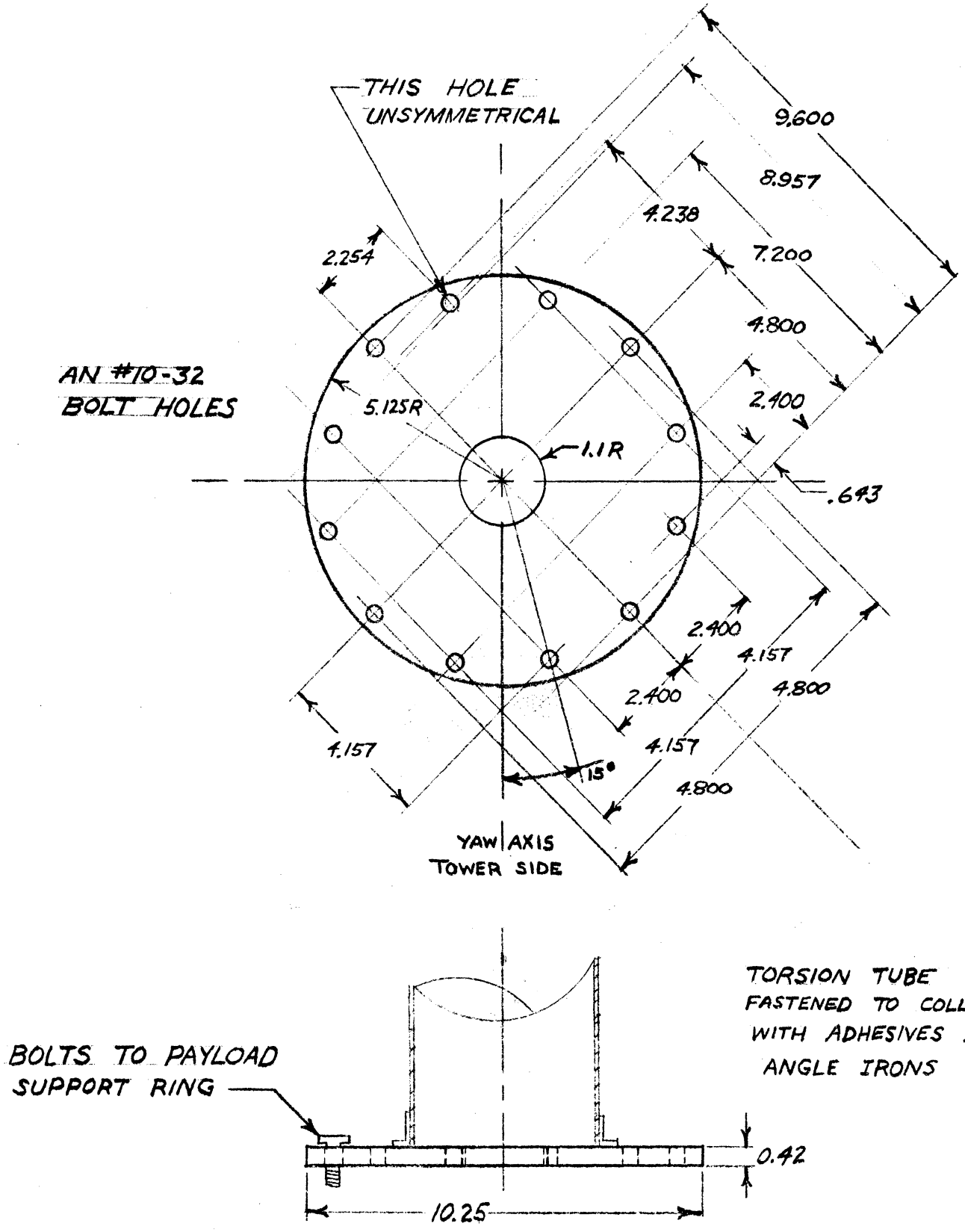

MATERIAL: 7075 T-6
WEIGHT: 3.33 LBS.

Figure 6.6

SCALE 4:1

6.4 WEIGHT BUDGET

Structures	29.26 lbs
Thermal	10.00 lbs
Sensor	37.30 lbs
Power	33.45 lbs
Launch and Orbital	29.00 lbs
Attitude and Control	25.80 lbs
Communications	26.11 lbs
Sub Total	190.92 lbs
Contingency	25.0 lbs
Total	215.92 lbs

Individual component weights for each subsystem are in Table 6.1.

6.5 REFERENCES

1. Sibila, A. I., Curfman, Jr., H. J., "The Role of Small Satellites in Space Applications Missions", British Interplanetary Society, Vol. 24, January, 1971, pp. 451-474.

2. Rauch, Sutton, & McCreight, Ceramic Fibers and Fibrous Composite Materials, New York: Academic Press, 1968.

3. Scout Planning Manual, Vought Missiles Company, LTV, Aerospace Corporation, May 1971, pp 33-35.

4. Osgood, Spacecraft Structures, New Jersey: Prentice Hall, 1966.

5. Mangurian, Aircraft Structural Analysis, New York: Prentice Hall, 1947.

Table 6.1

Component Coordinates
Operational Configuration

Group	Item	Mass (lbm)	Origin at S/C Center of Gravity: Component Center of Gravity x	y	z
Structures	Oct. Shell	3.22	0	0	-0
	Torsion Tube	3.52	0	0	-4
	Sensor End Plate	1.50	0	0	19
	Motor End Plate	1.50	0	0	-20
	Separation Ring	3.32	0	0	-22.
	Solar Panels	16.20	0	0	10.
Thermal	Thermal Ring	4.00	0	0	4
	Thermal Insulation	3.00	0	0	-20
	Coatings	2.00	0	0	0
	Thermal Grease	1.00	0	0	4
Sensor	G. E. Sensor	33.50	-6.5	0	7
	Therm. Cascade	.50	-11.5	-1.5	2
	Radiometer	1.00	-7.5	-4.5	10
	Mirror	.80	-5.8	-2.0	19
	Servos	1.50	-6.0	-2.0	18
Power	Solar Cells	20.51	0	0	10
	Batteries	8.94	0	0	0
	Voltage Regulator	4.00	0	0	-9
Launch & Orbital	Telemetry Package	33.10	Not Applicable		
	Delta V thruster	.87	0	0	-17
	Fuel Tanks & Fuel	20.45	0	0	-15
	Valves, etc	7.54	0	0	-12
Attitude & Control	Fine Sun Sensor	.13	0	12.5	0
	Coarse Sun Sensor	.48	0	0	0
	End Plannar Scannar	3.00	0	-12.4	19
	Side Plannar Scannar	3.00	0	-12.4	-6
	Despin Mechanism	1.49	0	0	-7
	Integrating Gyro	1.00	0	-8.0	-2
	Momentum Wheel 1	4.60	0	0	15
	Momentum Wheel 2	4.60	0	-4.0	0
	Momentum Wheel 3	4.60	11.0	0	0
	Rate Gyro 1	.24	0	0	13
	Rate Gyro 2	.24	0	3.6	0
	Rate Gyro 3	.24	9.9	0	0

Table 6.1 (cont'd)

Group	Item	Mass (lb)	Center of Gravity x	y	z
Communications	Transmitters	1.00	11.8	1.2	17.5
	Receiver	1.25	6.8	2.4	-10.3
	Beacon	.16	11.5	-3.4	13.1
	Programmer	3.00	7.1	5.9	12.2
	Diplexer	.30	12.0	2.6	11.2
	PCM	2.00	3.0	11.0	17.2
	Turnstile Antenna	3.00	0	0	18.7
	Recorders	11.40	10.0	2.4	-10.3
	Wire - Misc	3.00	0	0	12.7
	Decoder	1.00	10.0	-1.6	-10.3

7
COMMUNICATION SYSTEM

7.1 INTRODUCTION

In determining the communication system to be used on board Project SCOPE, certain parameters had to be met: the system had to be of high reliability since the entire mission would be aborted if a failure occurred; weight had to be kept low so that the low cost Scout D rocket could be used for insertion into orbit; and most important of all, the system had to be compatible with both the experiment package and with a ground tracking and communication system.

The VHF (Very-High Frequency) band was chosen to satisfy the requirements for the communication system. Equipment designed for this band has reached state of the art performance. They are extremely reliable (greater than 95%), light weight (through extensive use of integrated circuits), and low in cost. The VHF band is presently designated for small scientific satellites of which SCOPE is a member. The frequency is therefor compatible with a world wide ground station network, STADAN, which incorporates a very reliable tracking network at the VHF band.

Magnetic tape-tape recorders were chosen to store sensor data on board SCOPE due mainly to the weight restriction. Core memory was considered due to its greater reliability but had to be rejected because of its far greater weight and power requirements. The recorders have a life expectancy of one year with 70% use which is satisfactory for SCOPE's planned mission. An extra recorder has been included to guarantee mission success. To avoid the problem of speed accuracy and wow and flutter of the recorders, pulse code modulation was used in the communication system.

7.2 GROUND SYSTEM

7.2.1 STADAN Network

SCOPE has chosen the STADAN (Space Tracking and Data Acquisition Network) and its sites to handle the functions of command, data acquisition, and telemetry. STADAN is part of NASA's NASCOM Communications network which is the primary network employed by earth orbital scientific satellites.

The STADAN network is composed of a total of 15 ground stations which contain a variety of parabolic dish antenna sizes and a variety of tracki systems. SCOPE will employ only the following 9 ground stations because these sites all contain either 40 foot (12.2 meters) or 85 foot (25.9 meters) parabolic dish antennas and all are equipped with the MINITRACK tracking system.

Ground Stations	Antenna Size
Barstow, California	40 ft
Gilmore Creek, Alaska	85
Greenbelt, Maryland	40
Johannesburg, South Africa	40
Kauai, Hawaii	40
Orroval Valley, Austraila	85
Quito, Equador	40
Santiago, Chile	40
Tananarive, Madagascar	40

The strategic locations of these 9 stations will provide adequate satellite coverage.

7.2.2 Tracking

The STADAN network has incorporated within its sites four different tracking systems.

MINITRACK-Radio Inferometer Tracking System
MOTS-Minitrack Optical Tracking System
SATAN-Satellite Automatic Tracking System
R&RR-Range and Range Rate Tracking System

SCOPE will employ the facilities of the MINITRACK Radio Inferometer Tracking System because it is the most tested and reliable system, it meets requirements for accuracy, and its facilities are available at all of the 9 ground stations that will be communicating with SCOPE.

MINITRACK requires only that SCOPE carry a light weight beacon which sends out a signal with a frequency of 136 MHz.

An inferometer will measure the location of the satellite by determining the phase difference between the radio waves measured at different points. MINITRACK guarantees a tracking accuracy of $\pm$ 20 seconds of arc, which for a 320 (515 km) mile orbit equals 185 feet (56.4 meters).

7.2.3 Data Compilation

SCOPE will be dumping recorded data at all 9 ground stations during different orbits. The recorded data will all be directly forwarded to STADAN's processing center located at the Goddard Space Flight Center (GSFC) in Greenbelt, Maryland via landline cable, submarine cable, wideband microwave, high-frequency radio, and communications satellites.

GSFC will be involved with the processing of the scientific data from the satellite's experiment package.

7.2.4 Coverage Capabilities

The coverage capabilities of all ground stations can be considered to be approximately equal. The tracking geometry is shown in Figure 7.1. All calculations have taken a line 5 degrees above the horizon as a maximum range even though coverage of the satellite is possible below the horizon due to the refraction of the atmosphere in bending the transmission beam. However, there is a possibility of error when the satellite is below the horizon and even when the satellite is at the horizon. By adding the safety margin of 5 degrees above the horizon, most errors can be eliminated. This results in a coverage distance of 1178 nm (2190 km) at the surface of the earth, a total maximum coverage time per station of 10.5 minutes, and a maximum look distance of 1270 nm (2350 km).

7.2.5 Ground Stations Timeline

The following list is an approximate schedule of ground station coverage for the first 8 orbits. Note that at least one ground station is passed over every orbit. This trend continues throughout the entire flight. Since SCOPE's recorders are capable of recording 2 complete orbits, there is never a chance of loosing data by exceeding storage capabilities maximum data dump time is 93.9 seconds (Section 7.3.2).

Location	Orbit	Station Acquisition Time
Madagascar	.5	10.5 minutes
Alaska	.75	8.5
Hawaii	1.0	3.0
South Africa	1.5	10.0
Hawaii	2.0	5.0
Alaska	2.75	3.0
Australia	3.25	3.0
Australia	4.25	3.0
Chile	4.75	2.0
Maryland	5.0	2.0
Chile	5.75	8.5
Equador	5.75+	10.5
Maryland	6.0	10.5
California	7.0	3.0
California	8.0	8.5
Alaska	8.25	5.0

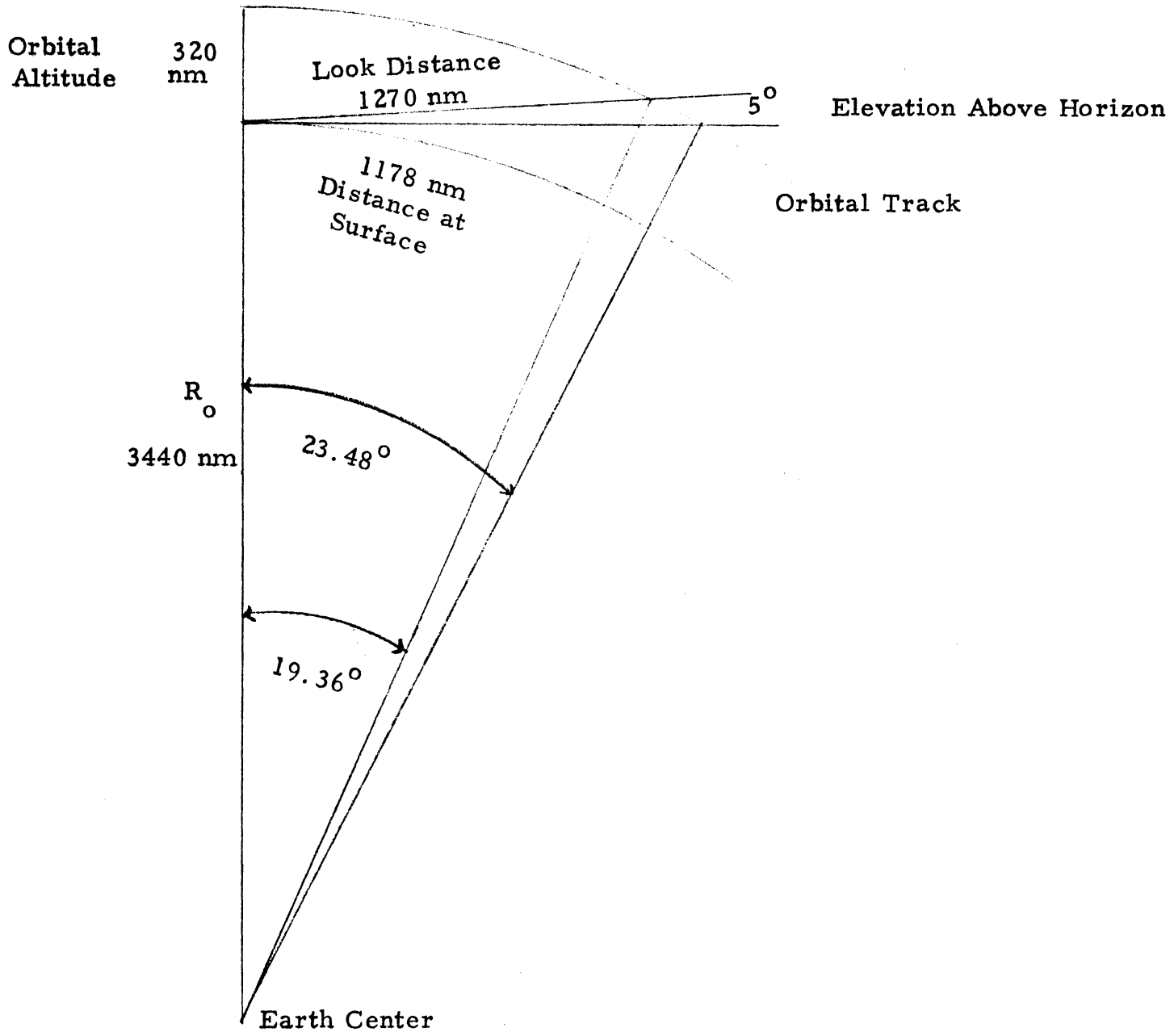

Figure 7.1 Satellite Tracking and Transmitting Geometry

7.3 ONBOARD COMMUNICATION SYSTEM

7.3.0 Overall System Description

The communication system on Project SCOPE is composed of a PCM system module, two data storage magnetic tape-tape recorders, two transmitters, a tracking beacon, an antenna and diplexer, two receivers with a command decoder and the command programmer and distribution unit. This equipment represents an extremely reliable, light weight telemetry system.

Pulse Code Modulation (PCM) is used in the SCOPE communication system for data processing. This modulation will accommodate the digital output from the satellite's experiment package and provide low error quantization of the analog information from the satellite housekeeping sensors PCM is also the best system available when magnetic tape-tape recorders are used for data storage since PCM signals are relatively unaffected by wow, flutter, small amplitude variations and other instability problems associated with tape recorded data storage.

The PCM signal is frequency modulated at the transmitter for transmission to earth. Thus the communication system is a PCM/FM system. A step by step description of the block diagram layout, Figure 7.2 of the on board communication system follows.

7.3.1 PCM System Module

The input signals from the satellite's various sensors are sampled by the time division multiplexer of the PCM system module. Time division multiplexing samples all input channels (one data frame) sequentially during each second. The analog signals from the satellite housekeeping sensors are quantized by the module in an analog-to-digital converter. The multiplexi functions are controlled by an internal clock synchronizer which also provides outputs for word (channel) and end of frame reference synchronizatio The multiplexed inputs are then combined in a serial pulse train. This serial pulse train is referred to as the output format of the communication system as this format is received by the ground stations.

The output format is a pulse train composed of the digital output data from the experiment package, the quantized analog information from the satellite housekeeping sensors and the end of frame reference synchronization The basic format is a 70 channel, non-return to zero pulse train of which 64 channels are the experiment package data outputs, four channels are for satellite housekeeping and two channels are for end of frame reference synchronization.

The first 64 channels of the output format are composed of the experiment package data. Each channel is 15 bits long. The experiment package also has ten housekeeping outputs, each 15 bits long. These

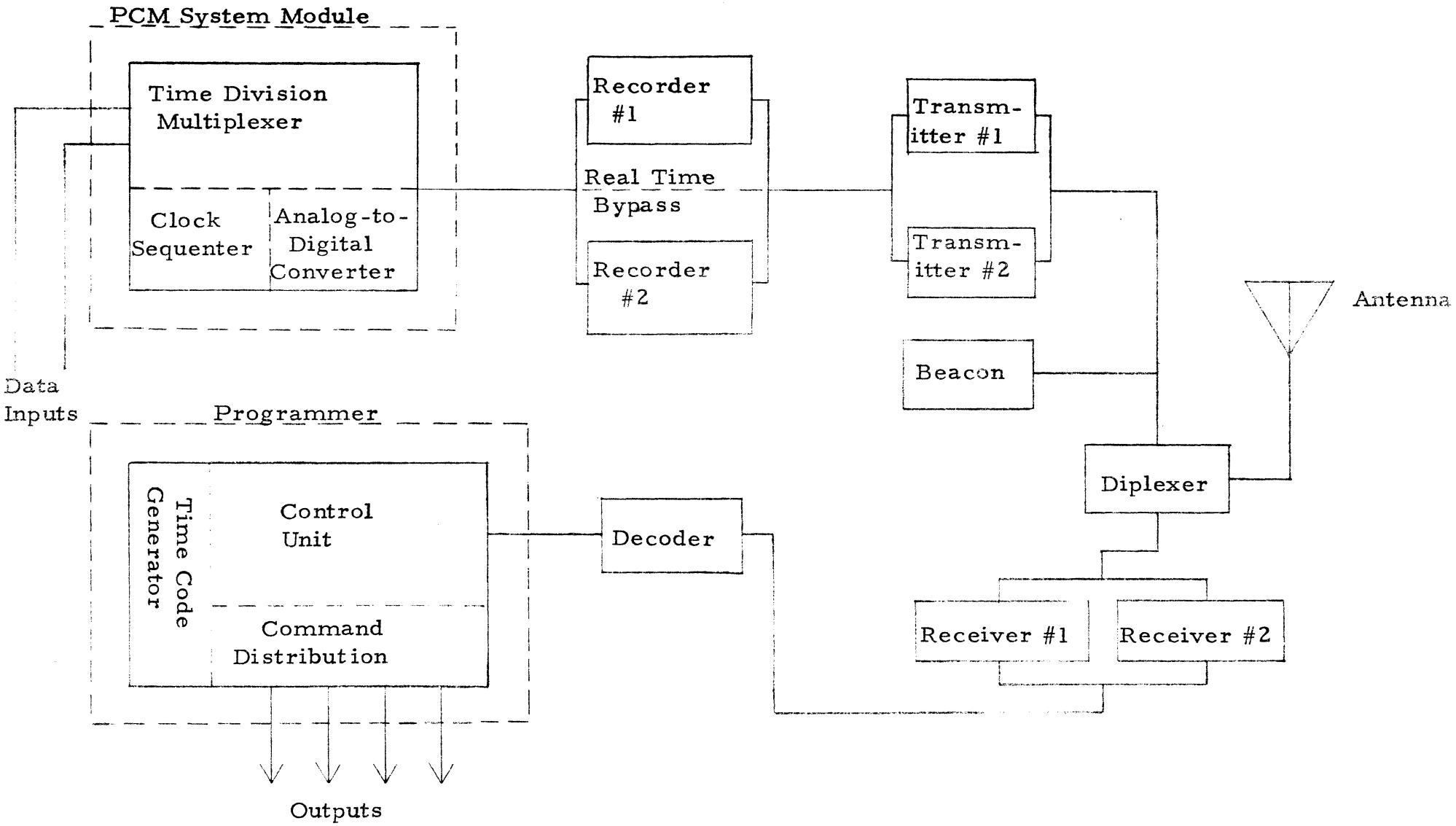

Figure 7.2 Communication System Block Diagram

housekeeping outputs are sampled once during a 30 second cycle creating two forms of output format. This is described more fully below.

The analog satellite housekeeping signals are quantized into a non-return to zero pulse train consisting of ten-bit words (channels) each of which commence with a word synchronization pulse followed by eight bits representin the sampled information and ending with an odd parity bit to provide for error detection. Each pulse is 5 $\pm$ .5 volts and a no pulse is 0 $\pm$ .5 volts. Upon completion of the full sequence of data channels a two word end of frame reference synchronization is inserted into the pulse train. This frame synchronization is composed of ten-bit words of Barker Code and its complement. The output from the satellite housekeeping sensors are inserted on the pulse train after the experiment package data.

The pulse train format from the PCM system module has two forms. Both forms are present in each cycle of output where one cycle is repeated every 30 seconds.

The first form is present in the first ten seconds of each cycle with each second completing one data frame. Each frame of this form is composed of the 64 experiment package channels followed by one channel for the experiment package housekeeping functions, followed by two channels for satellite housekeeping information and finally, two channels for end of frame reference synchronization. Thus each frame will have a total of 69 channels and 1015 data bits. Each second, or frame of this output form samples a different experiment package housekeeping output thus sampling all ten outputs in the first ten seconds of each cycle.

The second form is present in the last twenty seconds of each 30 second cycle. Each second, or frame of output starts with the 64 experiment package data channels followed by four channels for satellite housekeeping data and ending with two channels for end of frame reference synchronization. This second form of output format thus has 70 channels and 1020 data bits for each frame.

The pattern of 30 frames is repeated for each cycle. A graphical display of one cycle of output format is shown in Figure 7.3. The output format from the PCM system module is sent to the data storage tape recorders before being transmitted to the ground stations.

7.3.2 Magnetic Tape-Tape Recorders

The two magnetic tape-tape recorders are each capable of storing the data for a complete orbit. They operate in tandem fashion so that during data transmission to a ground station, one recorder is playing back the previous orbit's stored data while the second recorder begins recording present sensor and housekeeping data (shown in Diagram below):

(Recorder #1) record playback off

(Recorder #2 on record

data transmission
(2 minutes)

Should one of the recorders fail, only 2 minutes of data time per orbit will be lost. Should both of the recorders fail, SCOPE will still be able to operate in a real-time mode.

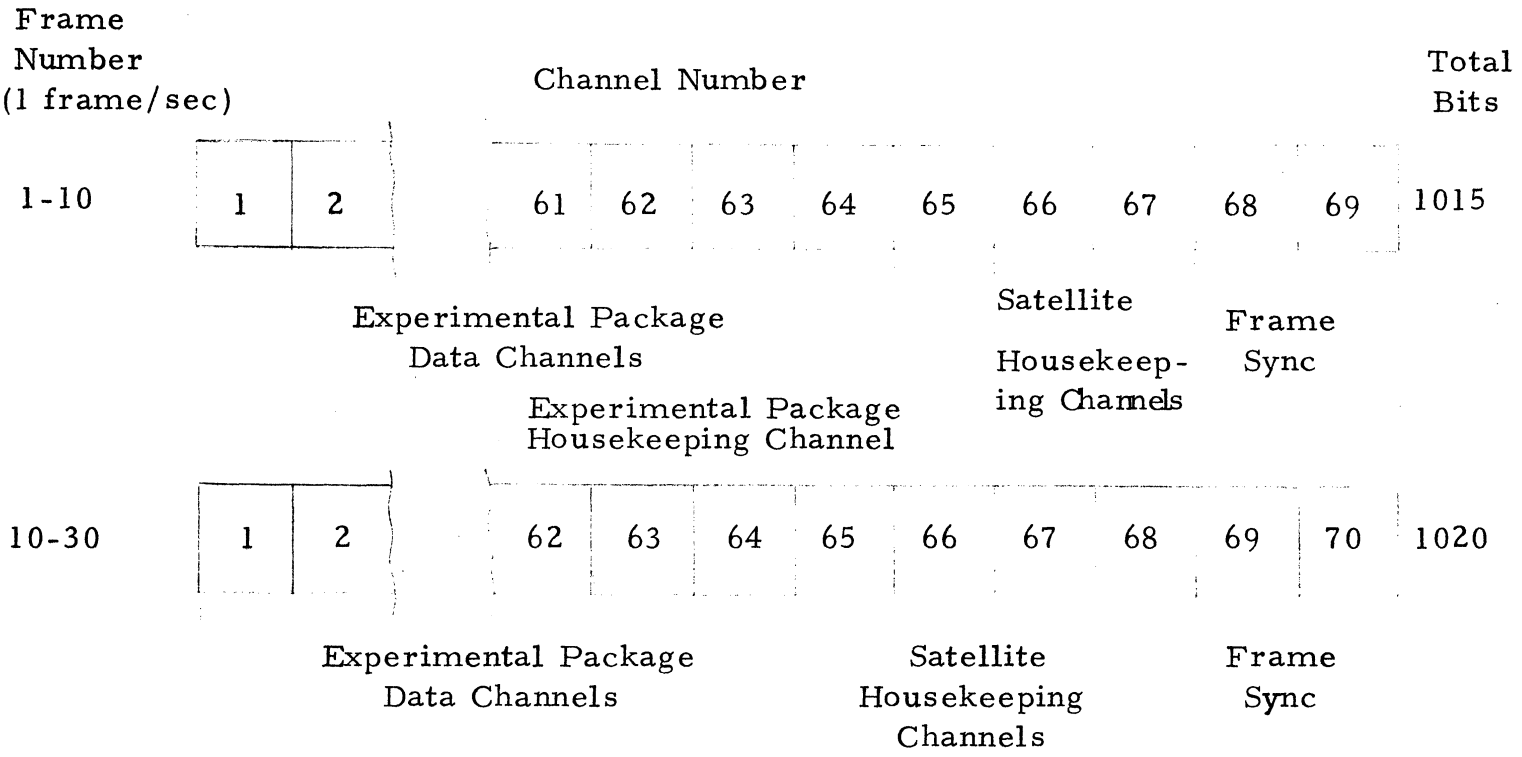

Figure 7.3 One Cycle of Output Format

1.	Transmitter #1	On-Off
2.	Transmitter #2	On-Off
3.	Tape Recorder #1	On-Off (Record)
		On-Off (Playback)
4.	Tape Recorder #2	On-Off (Record)
		On-Off (Playback)
5.	Beacon	On-Off
6.	Receiver #1	On-Off
7.	Receiver #2	On-Off
8.	Experiment Package	On-Off-Standby
9.	Mirror	Control
10.	Delta V Rocket Motor Valves	Control
11.	Momentum Wheels	Control
12.	Reaction Jets	Control
13.	Rate Gyros	On-Off
14.	Sun Sensors (Wide Angle)	On-Off
	(Fine Sensor)	On-Off
15.	Planar Scannars	On-Off
16.	Rate Integrating Gyro	On-Off

An internal time code generator is included for delayed and timed commands. Ground stations may activate any program through real time or by delayed action.

7.3.2 Equipment Specifications

The following is a summary of the equipment to be used in the communications system. A complete table of specifications is also included.

The pulse code modulation system is a microcircuit module, Type 710, manufactured by Teledyne Telemetry Company, Los Angeles, California. This design was chosen for its versatility, reliability, and compactness. It is composed of a time division multiplexer and an analog-to-digital converter with internal clock synchronization and sequencing. The module will mix the digital output of the experiment package and the digitized analog housekeeping data from the satellite into a non-return to zero pulse train. The module has a capability of 500,000 bits per second data handling rate and a 96 channel capacity.

The two magnetic tape-tape recorders, model C.J., are manufactured by Kinelogic Corporation, Pasadena, California. They are ultra-reliable, digital one-track recorders using one inch width tape with a maximum length of 480 feet. For recording, the tape will be run at 1 ips. 313 feet of recording tape is required for one orbit's data with a playback time of 93.9 seconds. The maximum recorded data rate is 1020 bps.

Item & Manufacturer	Quan.	Total Wt. (lbs)	Dimensions (in)	Power (watts)	Voltage	Thermal (^{o}C)	Max. Accel. 3-axis	Additional Comments
PCM Module (Teledyne)	1	2.0	3.75 x 3 x 2.75	11.2	28 ± 3	-55 +110	100 g	Custom built to specifications
Recorder (Kinelogic)	2	11.4	6 x 7.75 x 4.75	4.0 playback 2.0 record at 28 ± 7		-40 +85	100 g	Digital, Endless loop
Transmitter (Microcom)	2	1.0	2.375 x 1.25 x 2.415	15.4	28 ± 4	-20 +85	100 g	
Beacon (Microcom)	1	0.156	1.75 diam x 1.130	2.8	28 ± 4	-30 +85	750 g	
Turnstile Antenna	1	3.0	19.7 long	0.0	----	----	----	
Diplexer (Ball Bros.)	1	0.3	5 x 1.5 x 1	0.0	----	-10 +30	100 g	
Receiver (HAC)	2	1.25	6 x 4 x 1	0.5	28 ± 4	-20 +80	100 g	
Decoder (Conic)	1	1.0	2.35 x 4 x 3	0.0	----	-40 +70	100 g	
Programmer (Adcole)	1	3.0	5.5 x 5.5 x 3	1.5	28 ± 3	-20 +80	100 g	Custom designed
Misc. (wire, etc.)		3.0						

Total Weight is 26.11 lbs

Power: Night 4.8 watts Day 18.0 watts

The transmitters, due to state of the art electronics are extremely low in weight and power requirements. They are manufactured by Microcom Corporation (Model T-11), Horsham, Pennsylvania, and will operate at 138 MHz for approximately two minutes per orbit. Nominal output is 3.5 watts with a 2 watt minimum under worst conditions of high temperature and low line voltage.

The beacon, operating continuously at 136 MHz, guarantees tracking of SCOPE through MINITRACK of the STADAN network. It is manufactured by Microcom Corporation (Model XB-10) and is crystal controlled for accuracy. Its output is 0.5 watts which is sufficient for tracking.

The turnstile antenna is symmetrically mounted on the octagonal deck facing the earth. Each individual monopole has an input impedance of 50 ohms and a length of 19.7 inches. The separate monopoles are hinged at their bases so that during the launch phase, they can be stored within the shroud. Once in orbit, the monopoles will be extended outward through the use of four springs contained in the hinges.

The diplexer, manufactured by Ball Brothers Research Company, Boulder, Colorado, enables the use of only one antenna for both transmitting and receiving. This helps reduce the weight and simplifies the design of SCOPE.

The receivers are also low in weight and power requirements due to the extensive use of integrated circuits. They are manufactured by Hughes Aircraft Company, Newport Beach, California, and will operate at 150 MHz continously. An automatic switching control in the programmer will sense a power failure in the receiver and automatically turn the backup receiver on.

The decoder, manufactured by Conic Corporation, San Diego, California, takes the signal from the receiver and decodes it into language the programmer can understand.

The programmer is custom built by Adcole Corporation, Waltham, Massachusetts. It will be similar to the programmer used on the OFO satellite in August of 1970 which performed similar operations to those required by SCOPE.

7.3.3 Up-Down Link Considerations

The up-down link calculations are necessary to determine satellite on board transmitting power needed. This transmitting power is dependent upon the ground system used, the data rate transmitted, the range of the satellite and atmospheric and space attenuation of the radio signal.

The up link is the communication link between the ground station transmitter and the satellite receivers. This link is not usually crucial since sensitive spaceborne receivers exist and the ground stations have enough transmitting power for earth orbital missions.

The down link is the communication link between the ground station receiving antenna and the transmitter on the satellite. This link defines the spaceborne transmitting power needed for a certain signal-to-noise ratio at the input to the ground station receiver. This crucial calculation and the results are presented in summary below. The actual calculations are in Appendix F.

System Parameters

Nominal orbital altitude	320	nm
Maximum satellite range	1270	nm
Minimum receiving antenna diameter	40	ft
Receiving antenna gain	22.2	db
Receiver signal-to-noise ratio	17	db
Transmitting frequency of satellite	138	MHz
Bandwidth transmitted	100	kHz
System noise temperature	2900	^{o}K
System noise power	193.9	dbw
Free space attenuation	142.0	db
System losses	10	db
Transmitting antenna gain	0.6	db
Satellite transmitting power required	1.66	watts

The STADAN receiving network is used for Project SCOPE. It has a minimum 40 foot parabolic dish receiving antenna. The network operates with a 100 kHz bandwidth in the VHF frequency range. This bandwidth will allow a data rate of transmission of approximately 45 kbps (kilobits per second) allowing for doppler shift and frequency instability in the PCM system.

The calculated power requirement for the on board transmitter is well within reach of modern spaceborne transmitters. To provide a safety margin a transmitter with an effective RF transmitting power of 3.5 watts nominal and 2.0 watts minimum was chosen.

7.4 SUMMARY

The proposed communication system is lightweight, reliable, efficient and within the budget requriements of Project SCOPE. Ultra-reliabl

components were used whenever possible and backup units were provided for least reliable and crucial equipment. To comply with the STADAN ground system the satellite operates in the VHF range, transmitting at 139 MHz and receiving at 150 MHz. A PCM/FM system was used for data processing to obtain accurate data transmission with an error probability of 1 bit per 10^7 These conditions allowed the use of "off the shelf" components which were readily available and flight proven.

7.5 REFERENCES

1. Stiltz, H. L., Aerospace Telemetry, Volume I and II, Englewood Cliffs, New Jersey, Prentice-Hall, 1966.

2. Electronic Engineers Master, Garden City, New York, United Technical Writing, 1969, pp 2036-2037.

3. Gruenberg, E. L., Handbook of Telemetry and Remote Control, New York McGraw-Hill, 1967.

4. Krassner, G. N. and Michaels, J. V., Introduction to Space Communication Systems, New York, McGraw-Hill, 1964.

5. Nichols, M. H. and Rauch, L. L., Radio Telemetry, Ann Arbor, Michigan, University of Michigan, 1959

6. Ehling, E. H., Range Instrumentation, Englewood Cliffs, New Jersey, Prentice-Hall, 1967.

7. Balakrishnan, A. V., editor, Space Communications, New York, McGraw-Hill, 1963.

8. Filipowsky, R. F. and Muehldorf, E. I., Space Communication Techniques, Englewood Cliffs, New Jersey, Prentice-Hall, 1965.

9. Foster, L. E., Telemetry Systems, New York, J. Wiley and Sons, Inc, 1965.

10. Corliss, W. R., Scientific Satellites, NASA/GSFC, Report SP-133, 1967.

11. Corliss, W. R., The Evolution of the Satellite Tracking and Data Acquisition Network, STADAN, NASA/GSFC, Report N67-17637, January 1967.

12. NASA Facts, Spacecraft Tracking and Communications, NASA, Report N67-40513, June 1967.

13. Cliff, R. A., Application of the Stored-Program Computer to Small Scientific Satellites, NASA/GSFC, Report TN D-3988, June 1967.

14. Townsend, M. R., A Medium-Data-Rate Digital Telemetry System, NASA, Report TN D-2315, June 1964.

15. Habib, E. J., Keipert, F. A. and Lee, R. C., Telemetry Processing for NASA Scientific Satellites, NASA/GSFC, Report TN D-3411, August 1

16. M. I. T., Aerospace Electronic Systems Technology, NASA, Report SP - 154, May 1967.

17. Athey, S. W., Magnetic Tape Recording, NASA, Report SP-5038, January 1966.

18. Small Applications Technology Satellite, NASA/GSFC, 1970, pp. C-14.

19. Klass, P. J., "NASA Considers Satellite Network," Aviation Week and Space Technology, October 13, 1969, pp. 58-70.

20. Edited, "Communication System for ISIS-A," Proceedings of IEEE, June 1969, pp 923-932.

21. Cooley, Peter and Curona, L. J., Some Considerations for the Problem of Space Communications, University of Michigan, September 1966.

22. General Electric, Philco and Martin, Telemetry, Tracking and Command Subsystem for Solar Probe Mission, NASA/AMES Release, Working Paper #122, January 1967.

23. Kendrick, J. B., Space Data, TRW Space Technology Laboratories, 1965

8
POWER

8.1 INTRODUCTION

The required electrical power for SCOPE is provided by a system of solar cells and nickel-cadmium batteries. The paddle mounted solar cells will be used in daylight to power the satellite subsystems and to charge the batteries which will be used for night operation.

Two other types of power systems were considered. The first type, a radioisotope thermoelectric generator (RTG), was rejected because of its high weight, expense, and high heat dissapation. The second type, fuel cells, has a high volume and is inapplicable to long missions, so it too was rejected.

The solar cell and nickel-cadmium battery system meets the mission requirements and has proven reliable in many missions to date. It was therefore selected for SCOPE.

8.2 MISSION REQUIREMENTS

Electrical power is needed for three of SCOPE's subsystems, communications, attitude and control, and the carbon monoxide sensor, for a nominal period of one year. Thermal control, being a passive system, requires no power.

SCOPE's power requirements can be divided into three modes: nadir viewing (day), limb viewing (day), and night operation. The different components operating in these modes are listed with the power required in Table 8.1. For attitude and control and communications the required power is the same for nadir and limb, with additional power needed for short periods for orbital trim, the 90^{o} flip (only on the initial orbit), and data dump. The carbon monoxide sensor requires less power for the limb mode, as it is operating for a shorter period of time. Also, a small amount of power is needed for the launch vehicle to release latch valves.

The two power profiles (plots of power required vs time of orbit) for nadir and limb are given in Figures 8.1 and 8.2 respectively. The data dump occurs only once per orbit, either on the day or night side, so the system is designed for the worst case, a night dump. Also, since the nadir operation requires the most power, the system is designed for this case.

Table 8.1
Power Requirements

Attitude and Control	Power (watts) Orbital Trim	Nadir Limb	90° Flip
Momentum Wheels	13.8	13.8	13.8
Rate Gyros	10.5	10.5	10.5
Integrating Gyros	3.0	--	3.0
Planar Scanner 1	3.5	--	3.5
Planar Scanner 2	--	3.5	3.5
Coarse Sun Sensor	--	--	--
Fine Sun Sensor	--	--	--
Total Night		27.8	
Day		27.8	
Communications			
VHF Transmitter		15.4	
VHF Receiver		0.5	
Beacon		2.8	
Programmer with Memory		1.5	
Recorder-Playback		4.0	
Record		2.0	
Diplexer		0.0	
PCM System		11.2	
Decoder		0.0	
Total Night		4.8	
Night with data dump		24.2	
Day		18.0	
Day with data dump		37.4	
C0 Sensor			
Operating		15.0	
Standby		5.0	
Launch Vehicle			
Release Valves		54.0 (for 30 millisecs)	

All systems will operate at 28 volts with the exception of the rate gyros and the integrating gyros which will operate at 26 volts.

Figure 8.1 SCOPE Power Requirements. Nadir Mode of Operation for one Complete Orbit (Beginning and Ending at Sun Acquisition)

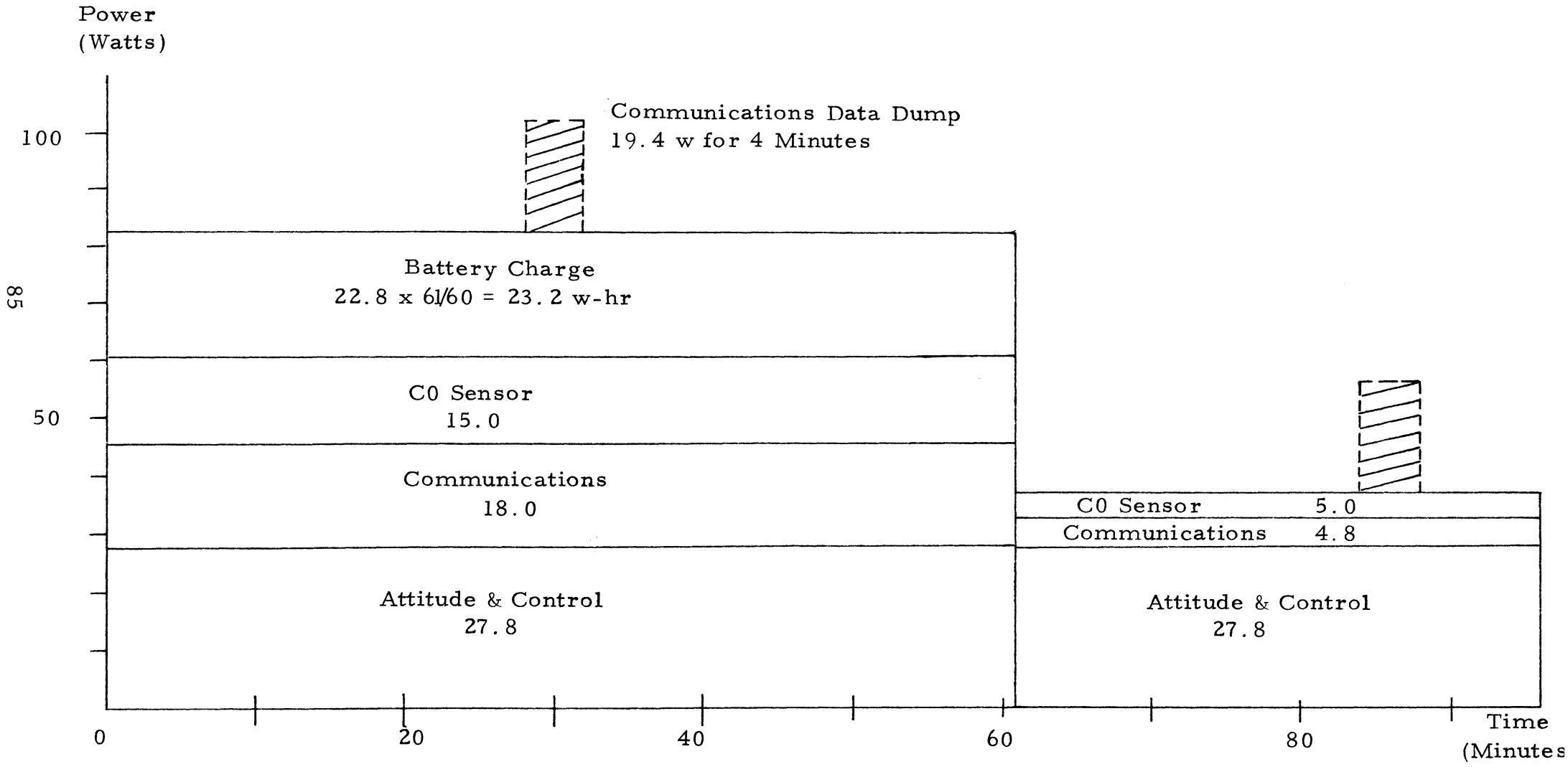

Figure 8.2 SCOPE Power Requirements. Limb Mode of Operation for one Complete Orbit (Beginning and Ending at Sun Acquisition)

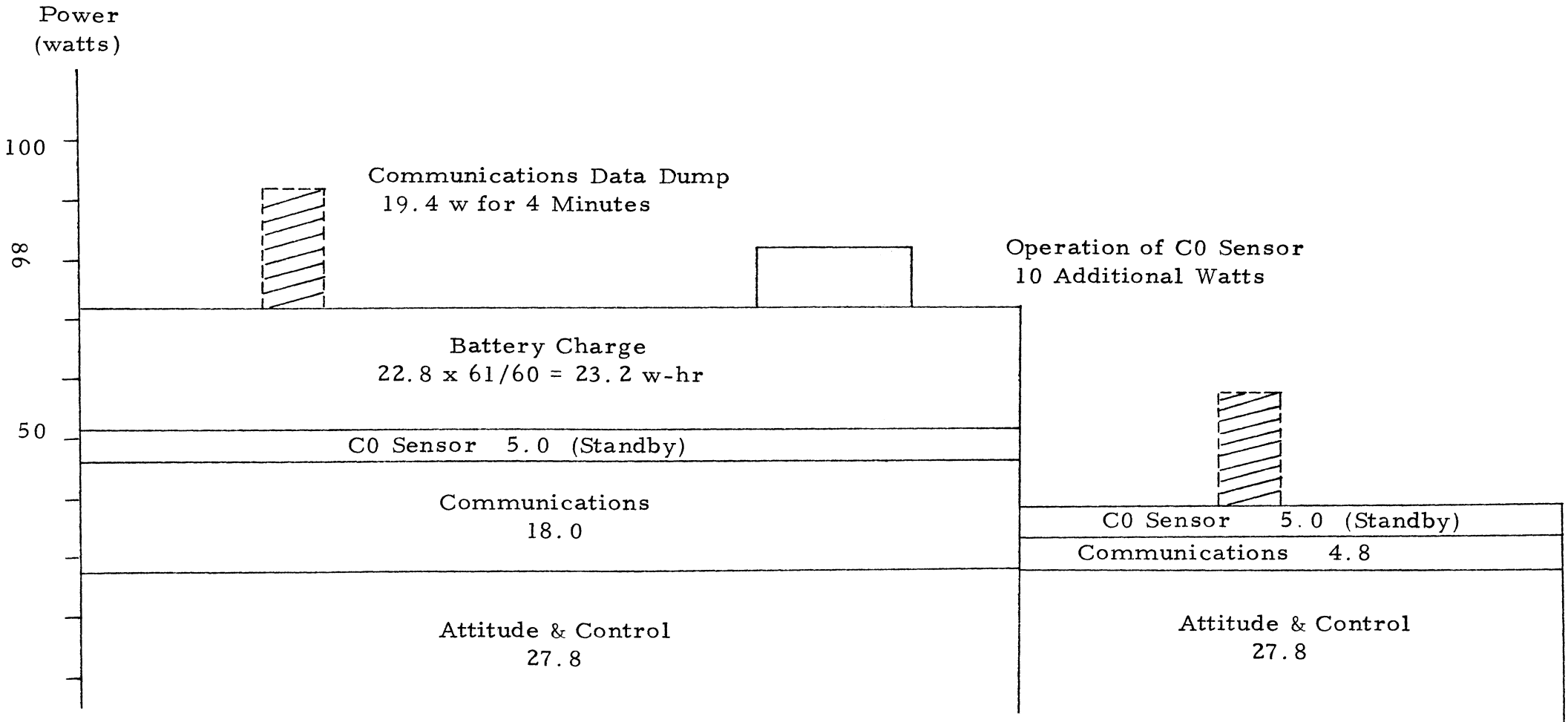

8.3 SOLAR CELLS

The solar cells could be mounted in three ways: rigid paddles, rotating paddles, and body mounted panels. Because of the small area available , body mounted cells were rejected. Rotating paddles that could be oriented to constantly face the sun would allow a minimum number of solar cells, but the possibility exists of orientation failure causing the entire mission to fail. Therefore, rigid paddles were selected.

Each of the two paddles consists of two sections connected by a common edge, separated by an angle of 60^{o}. Because the rigid paddle experiences a changing sun angle, changing temperatures, and is in the sunlight for greater than 50% of the orbit, an angle of 60^{o} was found to produce a more constant power output and a minimum paddle area (see Appendix F. 1).

The solar cells used are 2 cm x 2 cm N/P silicon cells. The 0. 014 inch thick cells have a 0. 006 inch thick blue-red cover glass with an antireflective coating. The cover glass provides protection from unwanted solar radiation and extends the life of the cell.

At the worst operating temperature the cell supplies 0. 125 amps at 0. 4 volts. Therefore, 73 cells are connected in series strings to provide the necessary 28 volts. Seventy-two of these strings provide the required power, resulting in a total of 5256 solar cells (see Appendix F. 2).

For reliability, each one half section of solar paddle is divided into sets of 5, 6, and 7 strings placed in parallel, (see Figure 8. 3). A diode is placed in series with the paddles to prevent current reversal when the cells are not producing power.

During launch the paddles are folded around the satellite and held in place by a metal band. Upon reaching orbit the band is removed by a pyrotechnic device and the paddles deploy by spring mechanisms, locking into place. In the event the spring mechanisms fail, the satellite can be spun to force the paddles out until they lock.

8.4 BATTERIES

Three major types of batteries are available for satellite use: silver-zinc, silver-cadmium, and nickel-cadmium. SCOPE's batteries must be able to be recharged once every orbit for a period of one year, that is, 5500 times; this factor determined the batteries to be used. Silver zinc batteries cannot be recharged more than a few hundred times, and silver cadmium not more than two to three thousand. Therefore, nickel-cadmium batteries, capable of 6,500-7,000 cycles when discharged 35%, were

Figure 8.3 Solar Paddle Folds Along Both Lines Designated BB' for Launch. The paddle folds along AA' to form a 60° angle for deployment.

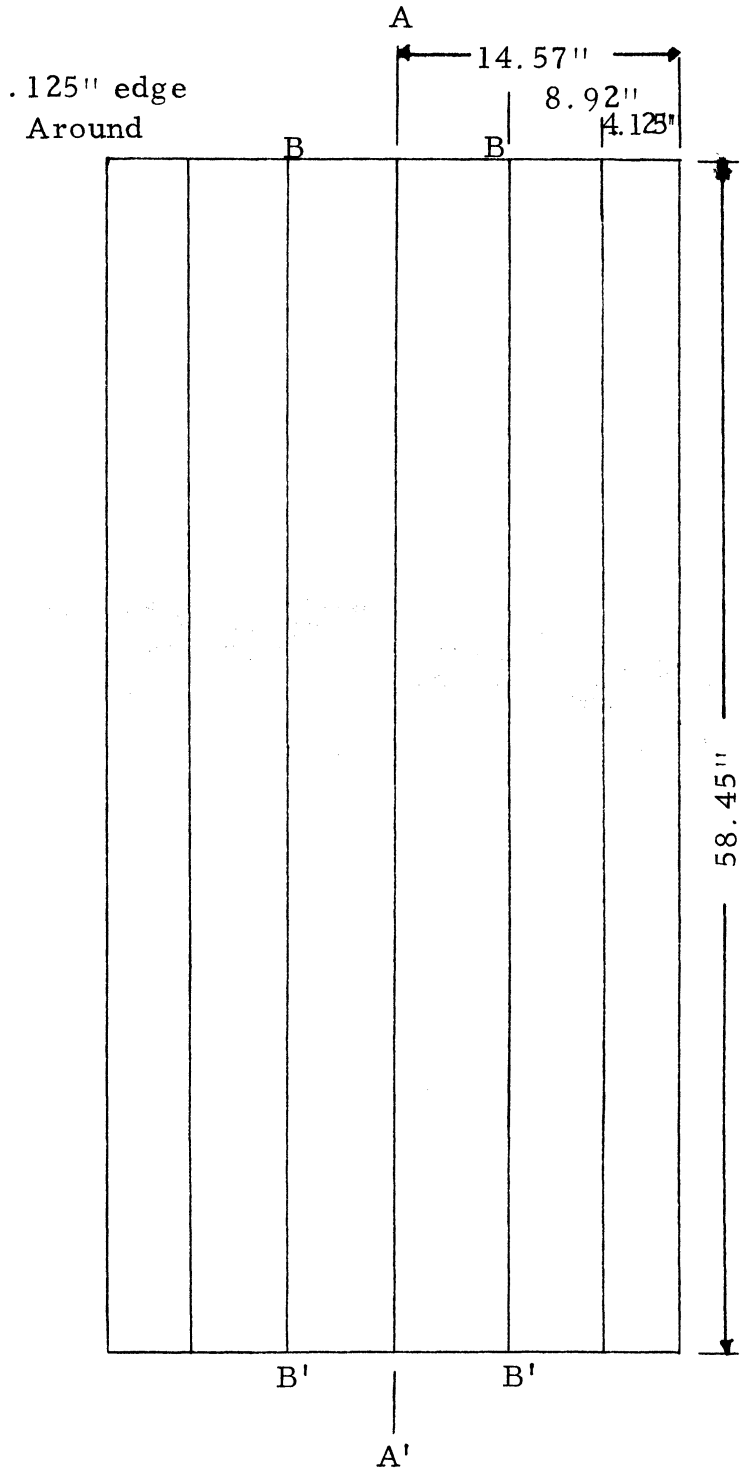

From the centerline, AA', out, each division is 7, 6, and 5 solar cells wide respectively.

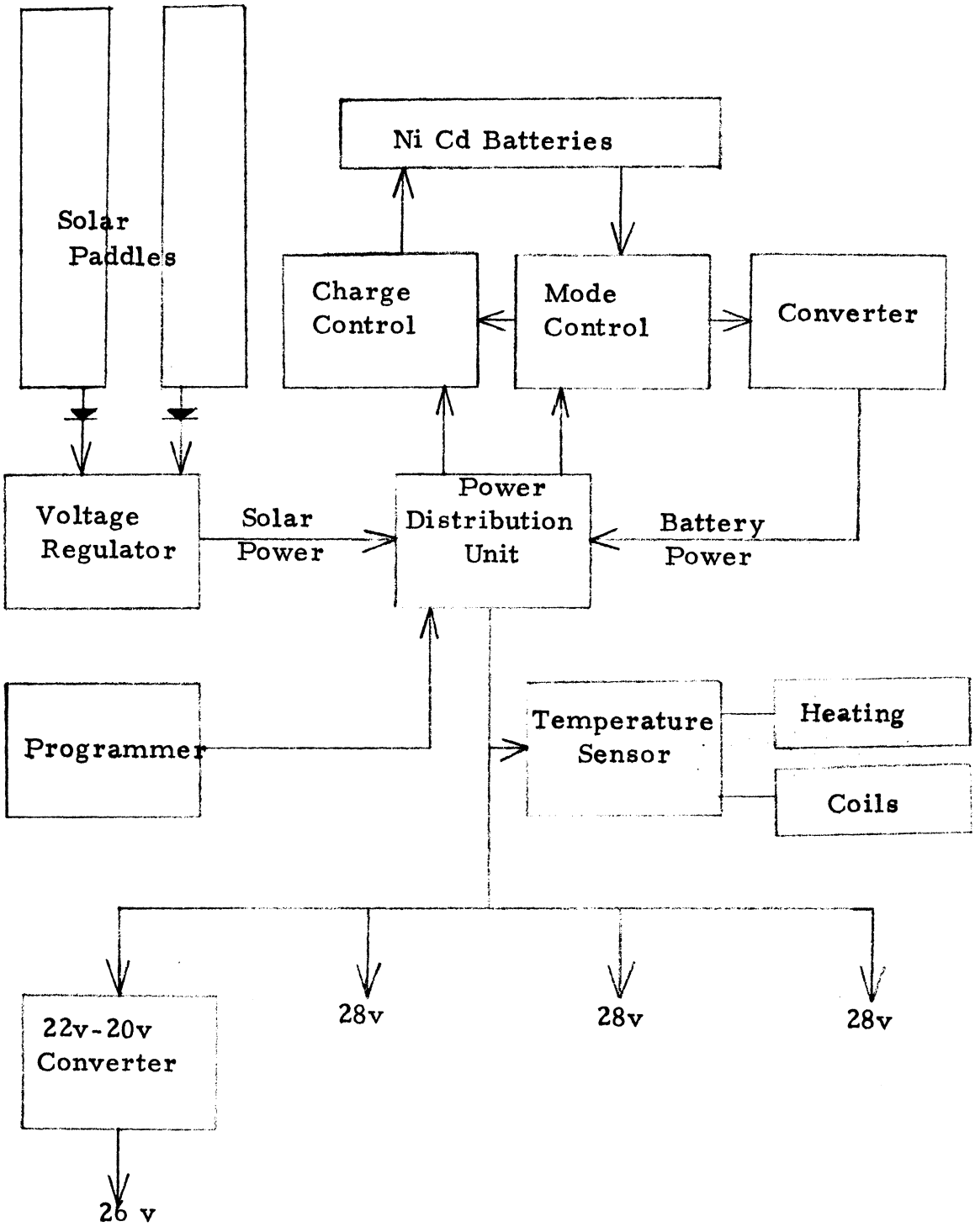

Figure 8.4 Power System Block Diagram

selected. Since the batteries must supply 28 volts, twenty-six 2.4 amp-hr batteries will be used.

When the satellite is in the sunlight the excess power from the solar cells will be used to charge the batteries (see Appendix F.3).

8.5 COMPLETE SYSTEM

Power from the solar cells and batteries is coordinated by a mode controlling device (see Figure 8.4). Whenever the power from the paddles is sensed to be less than that required by SCOPE's subsystems, the mode control permits power to be drawn from the batteries. When more power is available from the solar paddles than is necessary to run the subsystems, excess power is then diverted through a charge control into the batteries.

When it is desired that a certain subsystem be in operation, the programmer sends a signal to the power distribution unit which then routes power from either the paddles or the batteries to that system. The distribution unit contains two relays for each separate subsystem, one operating relay, and one redundant relay.

The power from the paddles and the batteries is regulated to 28 volts DC, except power diverted to the attitude gyros which is converted to 26 volts DC.

In the event the passive thermal control cannot maintain a high enough temperature in the satellite, a sensor will divert power to heating coils.

8.6 REFERENCES

1. Gibson, R., "Design Data for Space Power Systems," The Bendix Corp., Aerospace Systems Division, February 16, 1970.
2. Francis, H., "Space Batteries," NASA Report SP-5004, 1964.
3. Pro, S., "Power Conditioning for Satellite Systems," Air Force Report SAMSO-TR-67-10, March 1967.
4. "Space Power Systems, Part II," North Atlantic Treat Organization AGARDograph 123, November 1969.
5. Belove, L., and McCarthy, R., "The Sealed Nickel-Cadmium Battery Cell," Sonotone Corporation, BA-112, 1963.

9
THERMAL CONTROL

9.1 INTRODUCTION

In order to insure an optimum operating environment for all of SCOPE's subsystems it will be necessary to control the thermal environment. This is necessary since virtually all of SCOPE's components, especially the experiment package, are temperature sensitive. Keeping in mind both mission and equipment requirements, it was concluded that the best means of temperature control would be a passive system. The passive temperature control system makes use of thermal coatings, insulation, and conduction materials to protect against the environment that will be encountered. All the thermal requirements of SCOPE will be met, both reliably and economically, without system dependance upon mechanical or electrical devices. As a precautionary measure, an auxillary thermal control system will be incorporated into SCOPE. This system will activate in the event of the satellite encountering an unusually large temperature fluctuation, and will remain activated until the desired internal temperature range is regained.

9.2 THERMAL ANALYSIS

During SCOPE's lifetime, two distinct periods require thermal consideration. These are the launch and orbital insertion period and the orbital period. The great difference in conditions surrounding SCOPE at these times makes it necessary to consider these period individually. In addition, the solar cell array of SCOPE must be considered independently from the main body of the satellite due to differences in the thermal environment.

9.2.1 Launch and Orbital Insertion Thermal Analysis

During the launch and orbital insertion phase the thermal requirements are determined by the environment inside the heat shield and by the delta V motor during orbital corrections. The environment inside the heat shield is the result of two factors: aerodynamic heating due to skin friction and heat conduction from the launch vehicle's engines. The combined effect of these factors will increase the temperature inside the heat shield to a maximum of 150°F according to the Scout User's Manual. This temperature does not exceed the subsystem requirements. After launch the heat shield is jettisoned and the satellite is put through orbital correction maneuvers by means of a delta V rocket motor attached to the base of the satellite. The firing of the engine will create temperatures near SCOPE which could be harmful. The heat conducted into the satellite from the motor must be taken into account. To reduce this heat conduction to a negligible value, multilayer insulation must be wrapped around the motor. Twenty-five layers of Al-Mylar, glass fiber, or a similar composite will be sufficient to insulate SCOPE's subsystems from damage (see Appendix G).

9.2.2 Orbital Thermal Analysis

After SCOPE has been placed in its proper orbit and has attained operating status the criteria for thermal control becomes more stringent. A study of SCOPE's subsystem temperature requirements revealed that the ideal temperature range for SCOPE will be:

$$80 > T > 40\ ^{o}F.$$

This was based upon the "Temperature Budget" shown in chart (9.1). To realize this range, internal heat and the sources of radiation in space travel must be taken into account. The three types of radiation that would effect SCOPE in the orbit chosen about the earth are, solar, reflected solar, and planetary. The solar radiation or solar energy flux varies as the inverse square of the distance from the sun. This value can be assumed to be constant since Earth's orbit varies only by 3% during the year. The reflected solar radiation is dependent upon the reflective power of the Earth, (Albedo), the solar flux constant, and the altitude of the satellite. Since the altitude of SCOPE is nearly constant and the values of the solar flux and the albedo are constant this value can be assumed to be constant. The third type of radiation, the planetary radiation, is a result of energy emitted by the Earth. The value of this radiation can be considered constant since it is only dependent upon altitude. The sun's radiation contributes most of the energy absorbed by the satellite, while the solar reflected and planetary radiation contribute lesser but appreciable amounts (see Appendix G Figure 9.1 shows where in the orbit the various types of radiation affect the satellite, (Reference 11).

By controlling the amount of energy absorbed and emitted by SCOPE the operational temperature range will be maintained. The amount of energy absorbed or emitted by SCOPE can be controlled by utilizing a specific combination of thermal coatings on the exterior of the satellite. To maintain the required temperature range a combination of paints which result in an absorptivity to emissivity ratio of .10/.154 will be used (Appendix G). This ratio was the result of an iterative study of the desired maximum and minimun skin temperatures and the desired average skin temperature of SCOPE. Using this absorptivity to emissivity ratio the average skin temperature of SCOPE is $63^{o}F$ (Appendix G). The thermal time constant, which is the rate at which the satellite's temperature rises on the sunside of the orbit and drops on the darkside, was found to be $4.1^{o}F/hr$ (Appendix G). To find the actual temperature of SCOPE throughout the orbit an iterative process involving the thermal time constant and the average temperature must be employed. By this process the maximum skin temperature was found to be $66^{o}F$ at the point where the satellite enter Earth's shadow (Chart G.2). The minimum

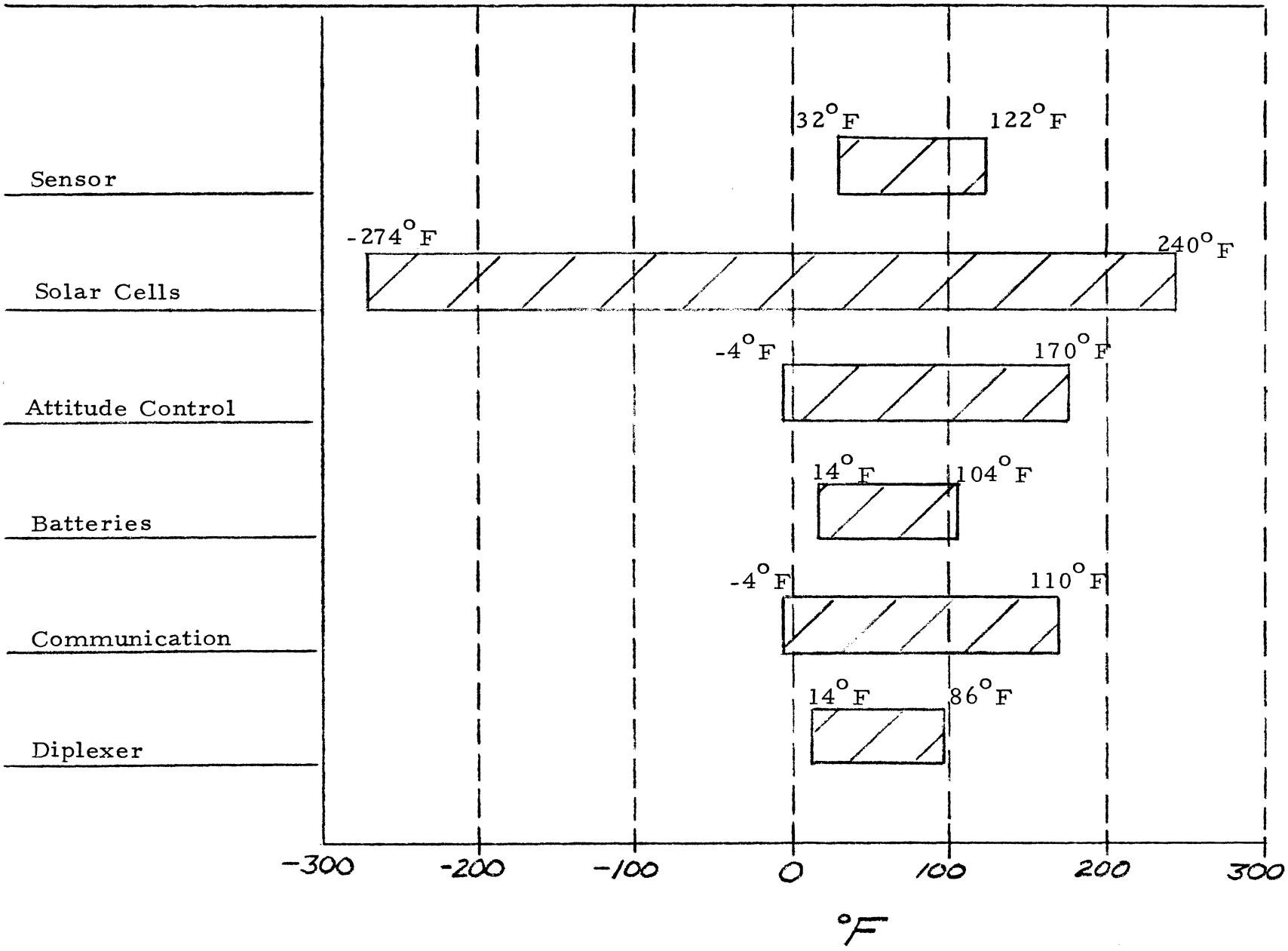

Chart 9.1

Temperature Budget

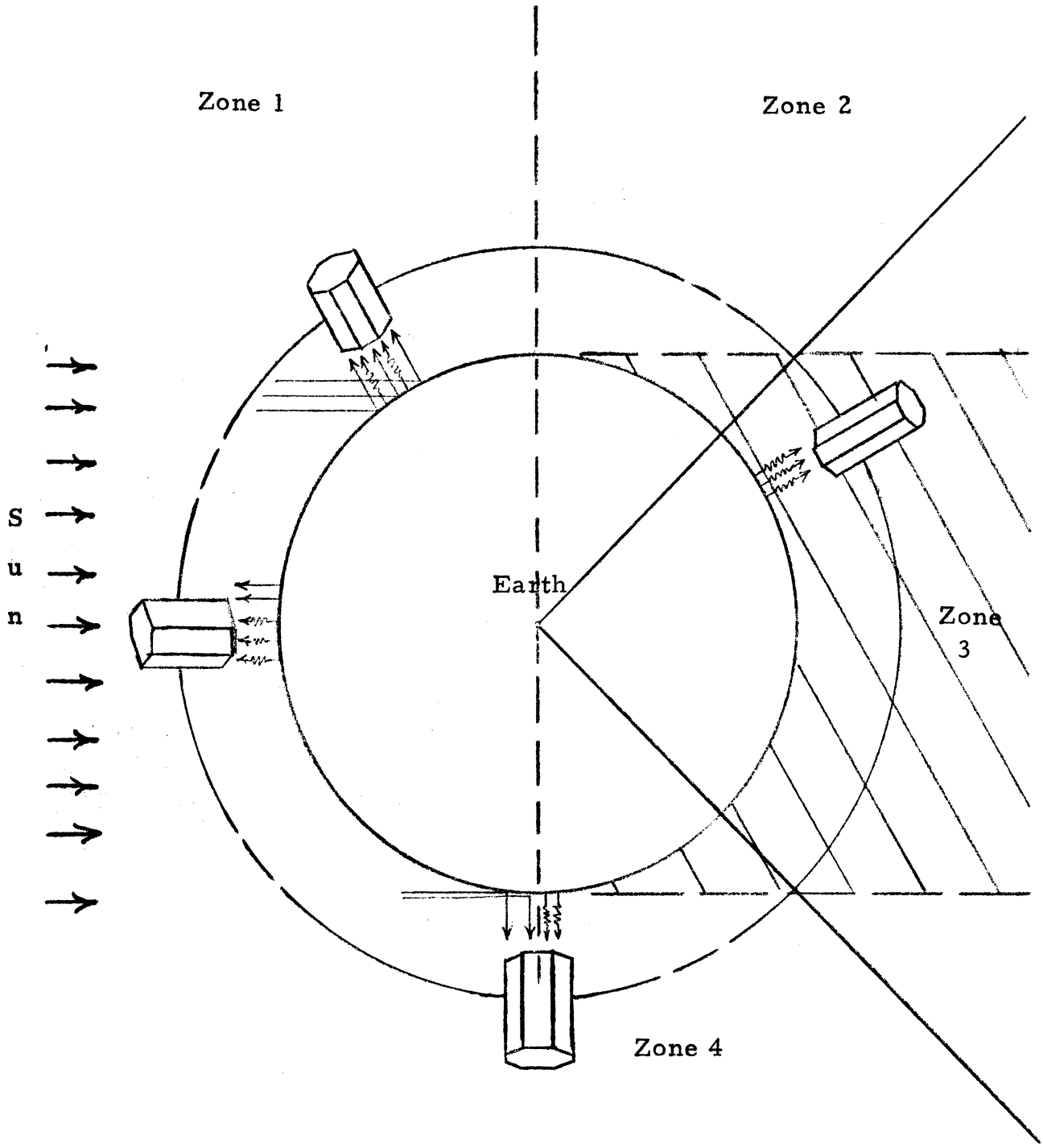

Zone 1: Solar, Albedo, and Planetary Radiation

Zone 2: Solar, and Planetary Radiation

Zone 3: Planetary Radiation

Figure 9.1
Radiation Zones

temperature for SCOPE is 63°F at the point where the satellite leaves Earth's shadow (Chart G. 2). (A computer program was used to calculate these values and values at other points in the orbit. See Appendix G for a listing of the computer program and the data output.)

9.2.3 Solar Panels

The source of power for SCOPE's systems is supplied by the sun through the use of solar cells. The efficiency of the cells is dependent on the temperature. The efficiency of the solar cells continually decreases with increasing temperature; therefore, the maximum temperature attained must be within the cells operating range (see Figure 9.1. The solar cells that were selected for SCOPE were silicon solar cells. The surfaces facing the sun have an absorptivity of .7 and an emissivity of .84 (11). Since the panels are exposed to the same types of radiation as the satellite, it is necessary to provide a way for the panels to dissipate heat so an excessive temperature will not be attained. This is achieved by coating the back side of the solar panels with a white (reflective) paint. Calculations shown in Appendix G give the temperature the cells will be at in the worst case. This is when the panels are exposed to direct solar radiation. In this case the maximum temperature the cells reach is 150°F. A graph of the temperature variation with orbit can be found in Figure 9.2. These values were obtained as shown in Appendix G. The solar panels are at a distance of 8 inches from the satellite. This allows the panels to dissipate heat without heating up the sides of the satellite (10).

9.3 PASSIVE THERMAL COMPONENTS

Five (5) types of passive thermal control systems are employed: thermal paints, multilayer insulation, a thermal conduction ring, thermal greases, and selective positioning of components.

The primary means of thermal control on SCOPE is the painting of the exterior surfaces. The thermal paints used on SCOPE will need to have an abso absorptivity to emissivity ratio of .10/.154, as has been previously mentioned. A combination of S-13G, white and CAT-A-LAC, black paint have been specified for this purpose. These paints where chosen because they will result in the desired absorbance to emittance ratio, they are easy to apply, and they will not deteriorate when subjected to the space environment (11).

To protect the internal components of SCOPE from temperature fluctuations in orbit and excessive local temperatures during the firing of the delta V motor, the use of multilayer insulation will be required (Appendix G). The insulation that will be used on SCOPE is of the composite type (i. e., Al Mylar, glass fiber, or silk netting, etc). This type of insulation was chosen

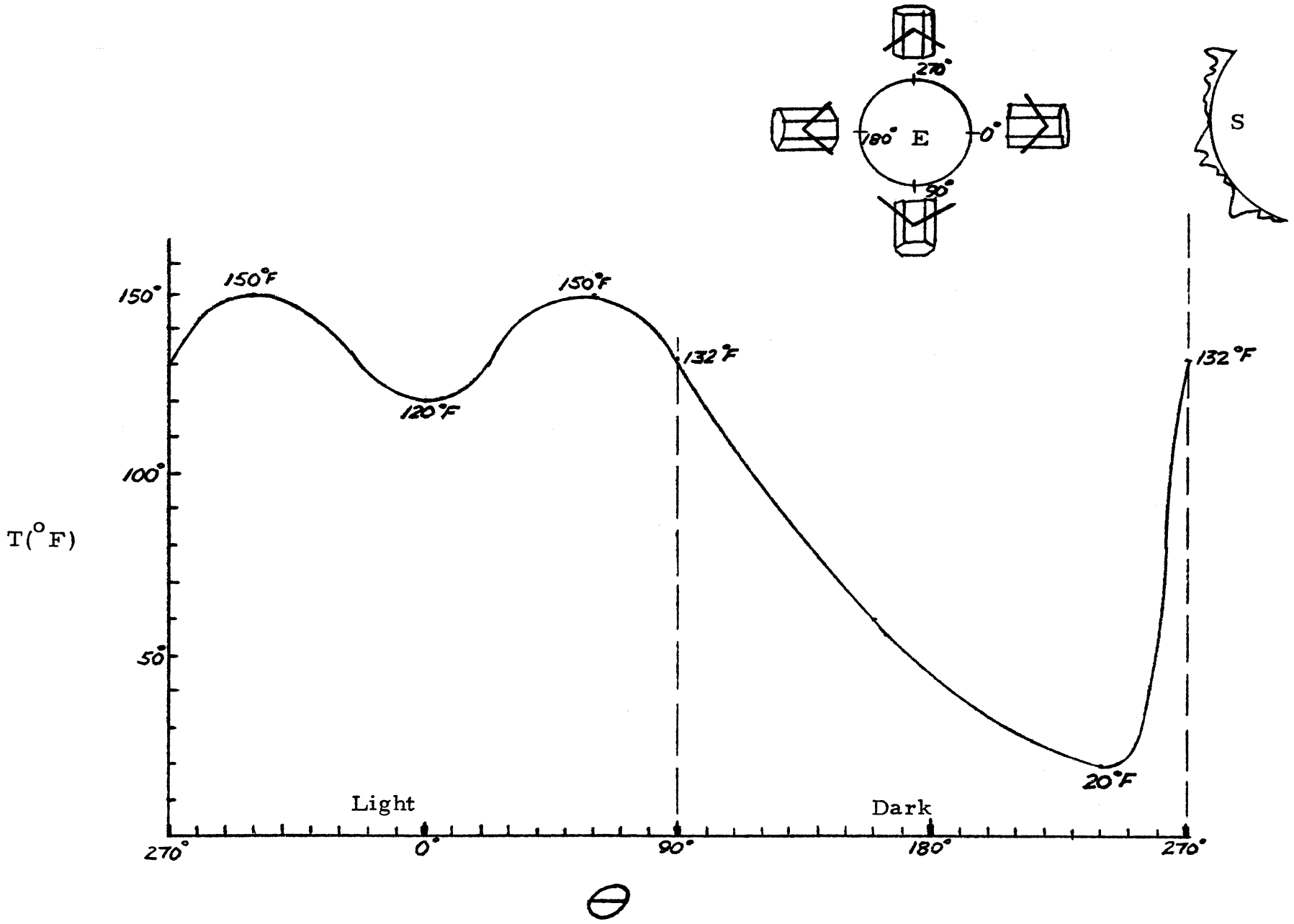
270°
180° E
0°
90°
S
150°
100°
50°
T(°F)
150°F
150°F
132°F
120°F
132°F
20°F
Light
Dark
270°
0°
90°
180°
270°
θ

after considering SCOPE's needs and the qualities the composite insulations possess, such as the low weight and conductivity values. Specifically, the insulation used on SCOPE will have a conductivity of 2.0×10^{-4} BTU/hr/ft^{o}F, a density of 5 lbs/ft, and will be 2/3 of an inch thick (40 layers/in) (Appendix G).

Due to the orientation of SCOPE in its orbit the amount of energy absorbed by each panel of the spacecraft will vary. This follows from the fact that at any one time (except on the dark side) some portion of the satellite is subjected to direct solar radiation while other portions are receiving little or no radiation whatsoever. Thus, the temperature of SCOPE will not be stable. To exemplify this problem the energy flux on each of SCOPE's panels was calculated at important points in the orbit. These values can be found in Chart (G. 2) in Appendix G and are pictorially represented in Figure G. 2 (Appendix G). This problem can be alleviated by transferring energy from high energy areas to low energy areas. On SCOPE this problem is met by allowing the energy to be transferred through the skin of the satellite and through an aluminum conduction ring. The amount of heat which can be transferred through the walls of SCOPE is limited by the thermal conductivity and the dimensions of each panel. To further induce the transfer of energy from panel to panel, the inside walls of each panel will be coated with thermal grease. By using thermal grease the conductivity of energy from panel to panel will be increased from 400 BTU/hr/ft -^{o}F for a dry panel to 1350 BTU/hr/ft -^{o}F for a greased panel (11).
An aluminum conduction ring was also incorporated into the satellite (see Figure 6. 1). This conduction ring, which is 1/2 inch by 1 inch in cross section, will encircle the interior of the satellite. This ring will provide a path for transferring large amounts of energy around the satellite (Appendix G). The ring has also been used to help increase the structural rigidity of SCOPE (see Section 6).

Although each of the internal components that will be placed on board SCOPE have individual temperature ranges, it is desirable to group certain components together in selective positions. On SCOPE three such positions are specified: the sensor area, the communications area, and the fuel-battery area. The sensor area is composed of the experimental package. The communications area is made up of the majority of the communications equipment. The fuel-battery area contains the fuel tanks at the base of the satellite and the batteries within the center support tube (see Section 6).

9.4 AUXILIARY THERMAL CONTROL SYSTEM

In order to protect the satellite from some unforeseen temperature fluctuation which may result in satellite temperatures above or below SCOPE's operating range, an auxilary thermal control system has been incorporated into the satellite's power system. The idea behind this system

is relatively simple. In each of the areas mentioned in the previous section a thermal switch and a power shunt has been placed. In the event of a large temperature rise in the communications area, for example, the thermal swit will shut off all power to that area. This will cause a sharp drop in the internal energy in that area and subsequently lower the temperature. Once the temperature returns to normal the thermal switch opens again and the equipment in that area will resume operation. In case of a large temperature drop in the fuel-battery area, for example, the thermal switch will divert the power flowing through it into the power shunt in that area. As the current flows through the shunt heat will be given off and thus cause the temperature to rise. After the temperature has risen within the desired limit the thermal switch will shut off the current flow to the shunt and the components in that area can return to normal operational modes. This syste will be sufficient protection against extreme environmental fluctuations for all of SCOPE's systems.

9.5 REFERENCES

1. Gaumer, R. E. Material Science and Technology for Advanced Application Englewood Cliffs, N. J., Prentice Hall, Inc. 1963, pp 199-214.

2. Glaser, P. E., Black, I. A., Lindstrom, R. S., Ruccia, F. E., and Wechsler, A. E., Thermal Insulation Systems, NASA, Report SP-5027, 1

3. Hemmerdinger, L. H. and Hembach, R. J., Handbook of Military Infrared Technology, Washington, D. C., Office of Naval Research, Department o Navy, 1965, pp 783-824.

4. Howell, J. R., and Siegel, R., Thermal Radiation Heat Transfer, NASA Report SP-164, 1969.

5. Introduction to the Derivation of Mission Requirements Profiles for Syste Elements, NASA, Report SP-6503, 1967.

6. Kreith, F., Radiation Heat Transfer for Spacecraft and Solar Power Plan Design, Scranton, Pennsylvania, International Textbook Company, 1962.

7. Nagy, J., Eoff, J., and Pass, J., Project OBSERVER, Ann Arbor, Michigan, University of Michigan, 1968, pp 94-104- & pp 137-147.

8. Panian, T., Von Renner, L., Cotterill, H., Anderson, T., Wahtera, K. Dixon, R., May, D., Goodwin, C., and Eftekhar, K., Project MISSAC Ann Arbor, Michigan, University of Michigan, 1968, pp 48-51 & pp 93-97

9. Sibert, M. E., Space Materials Handbook, Wright-Patterson Air Force Base, Ohio, Air Force Materials Laboratory, Air Force Systems Command, 1968, pp 77-172.

10. Van Vliet, R. M., Passive Temperature Control in the Space Environment, New York, New York, MacMillan Company, 1965.

11. Simms, R. J., Notes on Thermal Control, Ann Arbor, Michigan, Bendix Corp., 1972.

10
PROGRAM AND COST ANALYSIS

10.1 INTRODUCTION

A feasibility analysis of the developmental program and the project cost is included in this section. These two considerations are important to the determination of the project feasibility.

10.2 PROGRAM DEVELOPMENT PLAN

It is desirable to have the satellite operational by May 1975. It is expected that this date will allow scanning of the earth in all four seasons from a sun-synchronous orbit.

The program development plan was designed assuming that NASA is coordinating activity. Good coordination among each of the subcontractors should insure that the development time line outlined in Chart 10.1 will occur on schedule.

10.2.1 PHASE A - FEASIBILITY STUDIES

Phase A of the project is the conceptual feasibility studies of the project. Recommendations, cost estimates and scheduling are included in these studies.

10.2.2 PHASE B - MODEL DESIGN AND FABRICATION

Phase B of the project includes preliminary design of the satellite system by selected contractors. Following NASA approval of the system, models are fabricated and tested as the final designs of the flight model are produced.

10.2.3 PHASE C - FINAL MODEL FABRICATION AND TEST

The final models to be used for flight are produced and tested in Phase C. Flight models are delivered to the launch site and undergo final checkout. The satellite will be launched approximately 24 months after contract award.

10.2.4 PHASE D - OPERATION

The satellite will remain operational for about one year. Experimenta data is collected and satellite systems are closely monitored.

10.3 COST ANALYSIS

The cost analysis assumes that a central agency will coordinate the overall development of the project. The cost breakdown of the system is illustrated in Chart 10. 2. The total estimated cost is approximately $5.4 million for two satellites.

10.4 COMMUNICATION NETWORK

The STADAN network must be rented for data acquisition during the mission if NASA is not the sponsoring agency. The cost of rental of this network is approximately $2 million. Other costs such as data processing and analysis are assumed to be paid by the sponsoring agency and are not included.

10.5 CONTRACT FOR SATELLITE

The analysis uses a cost plus fixed fee (CPFF) contract in the estimate. This type of contract is in wide use and is expected to be used in Project SCOPE. Also assumed was a burden rate of 100% and a General and Administrative (G&A) rate of 20%. A fixed fee of 10% is also included.

10.6 CONTRACT FOR LAUNCH VEHICLE

LTV is the launch vehicle contractor. The contractor will provide the launch vehicle, launch site support as well as the actual launching operations. The cost is approximately $2. 2 million.

10.7 REFERENCE

1. Project STRATUM, Department of Aerospace Engineering, University of Michigan, December 1967.

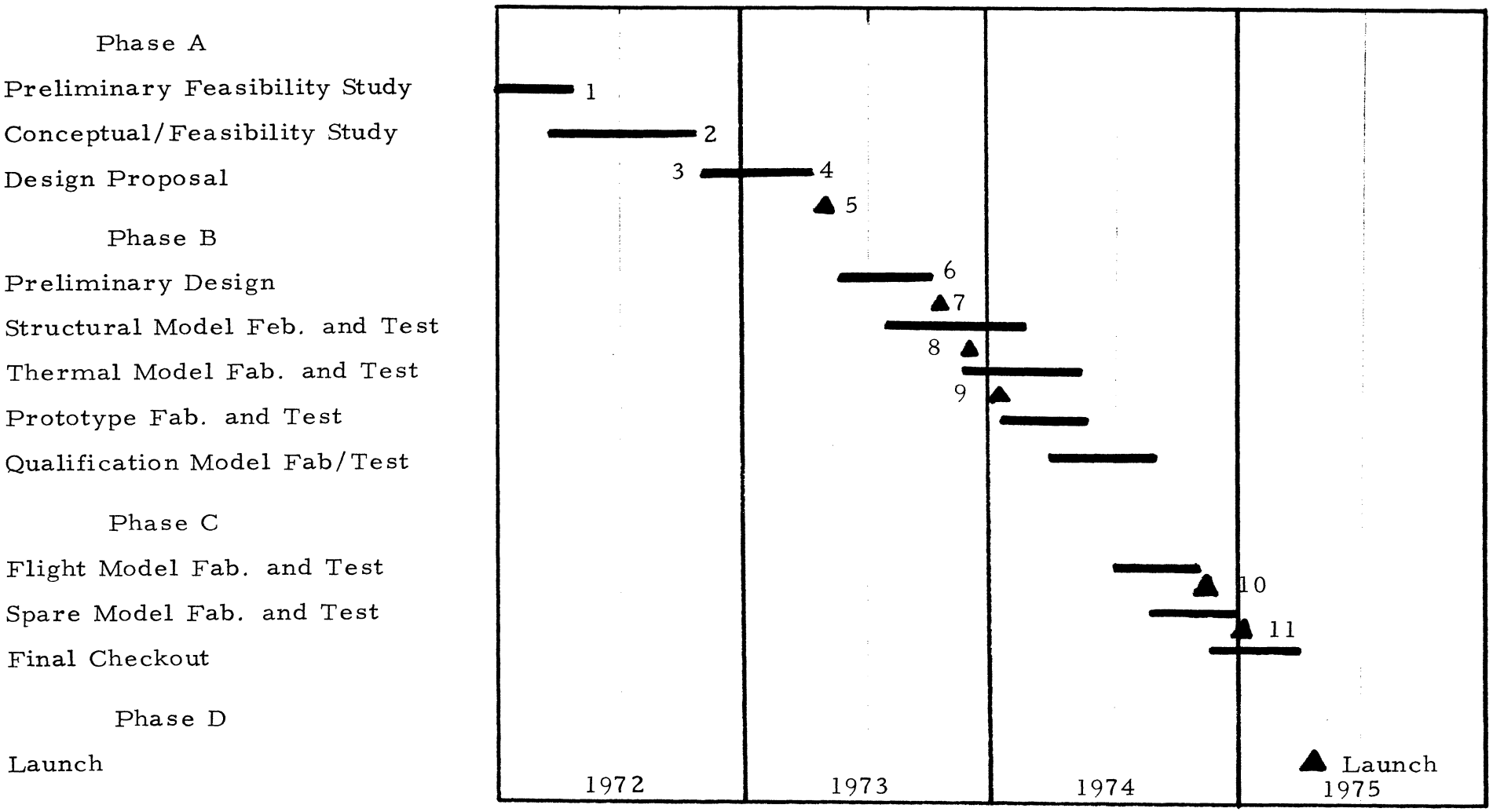

1 Submission of prel. feasibility study

2 Submission of feasibility study

3 Request for proposal

4 Submit design proposal

5 Contract awarded

6 Submit preliminary design

7 NASA approval

8 Sensor experiment delivery

9 Subsystem deliveries

10 Flight model delivery

11 Spare model delivery

Chart 10.1 SCOPE Development Schedule

SCOPE Cost Estimate
Cost Plus Fixed Fee Contract

Item	Cost
Sensor experiment	$ 120,000
Communications	106,000
Thermal	2,000
Attitude Control	80,000
Structures	2,000
Power	140,000
Propulsion System	20,000
Launch Vehicle	2,200,000
	2,670,000
Direct Labor	
Engineering and prototype Models	150,000
Thermal Model	120,000
Qualification Model	150,000
Flight model and one spare	300,000
	$ 3,390,000
Labor Burden at 100%	720,000
	$ 4,110,000
General and Administrative Costs at 20%	822,000
	$ 4,932,000
Fixed Fee of 10%	493,200
Total	$ 5,425,200

Chart 10.2

11
MISSION SEQUENCE

11.1 INTRODUCTION

The sequence of events in the mission of SCOPE is detailed in this section.

11.2 MISSION SEQUENCE

Date	Event
May 1, 1975	Launch from VAFB at approximately 12:00 noon VAFB time
	Vehicle Despin
	Stage 4 separation from payload
	Power up earth scanner No. 1 and tank pressure transducers
	Track 1 - 1 1/2 revolutions
	Open latch valves 1 through 7
	Pitch 180^{o} if needed for orbit trim
	Fire engine
	Track 1 - 1 1/2 revolutions
	Pitch down 180^{o} if needed for orbit trim
	Fire engine
	Pitch down 90^{o} to orientate sensor to earth's surface
	One month's time allotted for vehicle outgassing commences
June 1, 1975	Nadir viewing measurements begin and continue for six months
Nov 23	Limb viewing measurements begin and continue for two days
Nov 25	Nadir measurements continued
Feb 21	Return to limb mode of operation
Feb 23	Return to nadir mode
Mar 23	Return to limb
Mar 25	Return to nadir
May 1, 1976	Expected end of mission

APPENDIX A
Determination of Limb Acquisition and Measurement Times

Using the radius of the earth as 3430 nautical miles, and a nominal 320 nautical mile satellite altitude, the total time in limb viewing mode and the limb data taking time per orbit may be derived. In Figure A. 1, ϕ represents the total angle during which limb attitude control is necessary. This is calculated as follows:

$$\cos \phi = (3430 \text{ nautical miles})/(3750 \text{ nautical miles}) = 0.915$$

therefore, $\phi = 23.8^{\circ}$

The time during which limb attitude control is desired is found using the nominal orbital velocity of 96.44 minutes per orbit. Then,

$$\left(\frac{23.8^{\circ}}{360^{\circ}/\text{orbit}}\right)\left(\frac{96.44 \text{ min}}{\text{orbit}}\right) = 6.47 \text{ minutes}$$

Actual limb measurements will be made up to an altitude of 43.1 nm (80 km Using α to designate the angle between the beginning of data taking, Figure A. 1 is used again. Then:

$$\cos \alpha = \frac{3473 \text{ nm}}{3750 \text{ nm}} = 0.926$$

therefore, $\alpha = 22^{\circ}$

Hence the measurements will be made through the angle

$$\beta = \phi - \alpha = 23.8^{\circ} - 22.0^{\circ}$$

therefore, $\beta = 1.8^{\circ}$

And the time to perform the measurements is

$$\left(\frac{1.8^{\circ}}{360^{\circ}/\text{orbit}}\right)\left(\frac{96.44 \text{ min}}{\text{orbit}}\right) = 0.483 \text{ minutes} = 28.9 \text{ seconds}$$

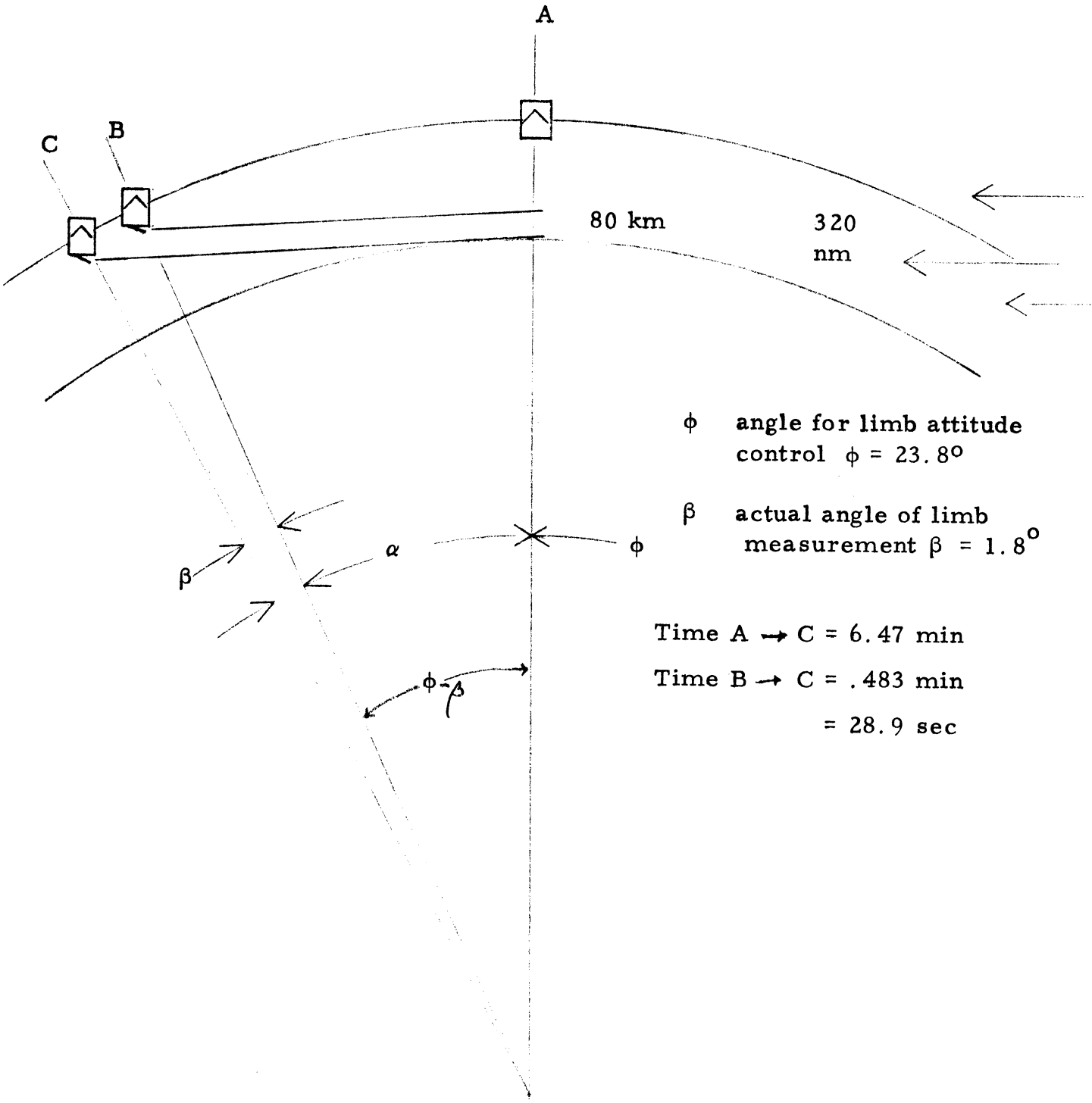

ϕ angle for limb attitude control ϕ = 23.8°

β actual angle of limb measurement β = 1.8°

Time A → C = 6.47 min

Time B → C = .483 min

= 28.9 sec

Figure A.1

APPENDIX B
ATTITUDE CONTROL

B.1 CALCULATION OF AERODYNAMIC TORQUES

B.1.1 Calculation of the Center of Pressure

The satellite is symmetric about the z-axis, so the center of pressure will be located somewhere along it. Choosing the sensor end as a reference

	Area (in^2)	Dist. from reference (in)	Area x distance (in^3)
Body	1000	20	20×10^3
Panels	1456	8.85	12.9×10^3
	$2456\ in^2$		$32.9 \times 10^3\ in^3$

Therefore the distance from the reference point to the center of pressure is

$$C.\ P. = \frac{32.9 \times 10^3\ in^3}{24.56 \times 10^2\ in^2} = 13.4\ in$$

Thus C. P. - C. M. offset = 13.4 - 19.2 = -5.8 in. (C. M. found in Section 6.2.3)

B.1.2 Calculation of Aerodynamic Pressure Torque

$$\tau = (A)\ (M)\ (P)$$

where τ = torque due to aerodynamic pressure
A = area of satellite subject to pressure = 17 ft^2
M = C. P. - C. M. offset = -5.8 in
P = pressure due to aerodynamic forces

At 320 nm and at 23,500 ft/sec

$$P = P_o + \frac{1}{2}\rho V^2 = 2.22 \times 10^{-7}\ lb/ft^2 \qquad \text{(Reference 8)}$$

Therefore,

$$\tau = -1.82 \times 10^{-6}\ ft\text{-}lb$$

This is a constant torque acting about the pitch axis.

B.2 CALCULATION OF SOLAR PRESSURE TORQUES

$$\tau = (A)\ (M)\ (P)$$

where

τ = torque due to solar pressure

A = maximum area exposed to pressure = 17 ft^2

M = maximum C.P. - C.M. offset = .483 ft

P = pressure due to solar forces acting upon a totally reflective surface = 1.805×10^{-6} lb/ft^2 (Reference 9)

Therefore

$$= 1.48 \times 10^{-6} \text{ ft-lb}$$

This torque is cyclic over the period in which the satellite is exposed to the sun (approx. 63 min) with a zero torque at local noon. Assuming that we have a maximum torque for 1/2 of the period (i.e. assuming a square wave, thus overestimating the torque)

$$M_{max} = \tau \times \Delta t$$

where

Δt = 31.5 min

$$M_{max} = 2.80 \times 10^{-3} \text{ ft-lb-sec}$$

The torque will be reversed for the next 1/2 period.

B.3 THRUSTER MISALIGNMENT

Assuming a misalignment of the 5 lb burner of 0.1°.

$$\tau = \text{thrust x misalignment}$$

$$= (5 \text{ lb}) \frac{(20.8 \text{ ft})}{12} \quad (\sin 0.1^{\circ})$$

$$= 1.84 \times 10^{-2} \text{ ft-lb-sec}$$

$$M = \tau \times \Delta t$$

where

Δt = time of longest burn = 384.3 sec

$$M = 7.145 \text{ ft-lb-sec}$$

B.4 UNLOADING OF MOMENTUM WHEELS

$$= F \times (\Delta x)$$

where

F = thrust = 0.11 lb

Δx = distance from thruster to axis

Roll Δx = 1.04 ft

Pitch Δx = 1.04 ft

Yaw Δx = 1.04 ft

Therefore,

τ = .115 ft-lb for roll thrusters

τ = .115 ft-lb for pitch thrusters

τ = .115 ft-lb for yaw thrusters

Δt = time of thruster firing

$= M/\tau$

where

M = momentum load of Bendix wheel No. 1778600 = 0.4 ft-lb-sec

Δt = 3.492 sec for roll thruster burn time

= 3.492 sec for pitch thruster burn time

= 3.492 sec for yaw thruster burn time

M_F = weight of fuel required for unloading

$= \frac{F\,\Delta t}{I_{sp}}$ where I_{sp} = specific impulse = 207 sec

$M_F = 1.893 \times 10^{-3}$ lb for roll

$= 1.893 \times 10^{-3}$ lb for pitch

$= 1.893 \times 10^{-3}$ lb for yaw

B.5 FUEL REQUIREMENTS

The time for the aerodynamic torque to cause the wheels to saturate is

$$t = \frac{.4 \text{ ft-lb-sec}}{1.82 \times 10^{-6} \text{ ft-lb}} = 2.2 \times 10^{5} \text{ sec} = 2.54 \text{ days}$$

Therefore the pitch wheel will unload every 2.54 days. The amount of fuel used in one year will be

$$W = 365.25 \frac{\text{days}}{\text{yr}} \times \frac{1}{2.54} \frac{\text{unloading}}{\text{days}} \times \frac{1.893}{1} \times 10^{-3} \frac{\text{lbs of fuel}}{\text{unloading}}$$

$$= 0.272 \text{ lb/yr.}$$

Thr thrusters will also be used to correct the misalignment torque. The torque available to correct misalignment is

$$\tau = 0.115 \text{ ft-lb}$$

The amount of fuel needed is

$$W = \frac{F \times M}{\tau \times I_{sp}}$$

$$= .033 \text{ lb}$$

Fuel is also needed to perform rotations. The time required to rotate the satellite by an amount θ_t is given by

$$\Delta t = \frac{2 I_{axis} \theta_t}{\tau}$$

For a 180^o rotation about the x-axis

$$\theta_t = \pi \text{ radians}$$
$$I_{xx} = 4.72 \text{ slug-ft}^2$$

Thus $\Delta t = 16.1$ sec

For a 90^o rotation about the y-axis

$$\theta_t = \pi/2 \text{ radians}$$
$$I_{yy} = 13.5 \text{ slug-ft}^2$$

$$\Delta t = 19.2 \text{ sec}$$

The total fuel weight required for two reaction jets working in conjunction to effect a rotation of θ_t is given by

$$W = \frac{4 I_{axis} \theta_t}{I_{sp} L \Delta t}$$

where L = separation distance between thrusters

Thus, $W_{180^o} = 8.55 \times 10^{-3}$ lb

$W_{90^o} = 10.3 \times 10^{-3}$ lb

B.6 YO-YO DESPIN CALCULATIONS

The equation relating the cable length with the mass of the end weight is:

$$\frac{I}{(L + a)^2 - a^2} = M \qquad \text{(Reference 5)}$$

where

L is the length of the cable in inches
a is the radius of the satellite in inches
I is the moment of inertia of the satellite plus fourth stage in slug-in^2
M is the total mass of end weights in slugs

For the cable to wrap 1 1/2 times around the satellite:

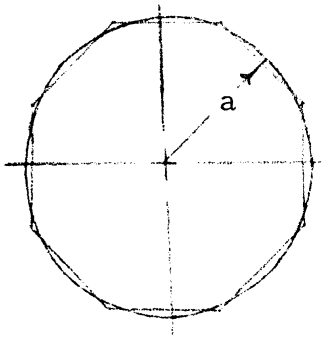

L = 1 1/2 x 8 sides x 10.04 in/side - 2.5 in
(2.5 = length of end weight + distance from centerline to hook)
L = 118 in

c = 8 sides x 10.04 in/side

I = 345 slug in^2 + 19.4 slug in^2
= 364.4 slug in^2

To find an average value of radius a set

$$c = 2\pi a$$

which gives

$$a = 12.78 \text{ in} = 1.064 \text{ ft}$$

I has been calculated as 364.4 slugs-in^2 (see Section 6.2.2)

$$M = \frac{364.4}{(118 + 12.78)^2 - 12.78^2} = .0215 \text{ slugs}$$

Taking acceleration due to gravity as 32.2 ft/sec^2

$$\text{weight of each end weight} = \frac{.0215\ (32.2)}{2} = .344 \text{ lb}$$

Time to despin is given by

$$t = \frac{(L/a + \arctan L/a)}{\theta_o}$$

where θ_o is initial spin rate

$$\theta_o = 120 \text{ rpm} \times 2/60 = 12.56 \text{ rad/sec}$$

$$t = \frac{(118/12.78 + \arctan 118/12.78)}{12.56} = .853 \text{ sec}$$

The maximum tension in the cables is given by

$$\text{Tmax} \frac{nat^2}{I} = 14.0$$

where n is the number of cables and 14.0 is a constant for our spacecraft, taken from Reference 3.4 (NASA TN D-1012 Figure 15)

$$\text{Tmax} = \frac{14.0\ (364.4)}{2(12.78)(.853)^2}$$

$$\text{Tmax} = 22.8 \text{ lb.}$$

To assure the safety of the cable against failure, we need to know the miaximu amount of tension the cable can take. For this we use a cable of low tensile strength for calculation to assure safety (taken from Reference 3.3).

Tensile strength of mild steel hot rolled (1020 HR)

$$\text{T.S.} = \frac{\text{Fmax}}{A}$$

$$\text{Fmax} = \text{T.S.}\ (A) = (61,000)\ (.00305)$$

$$\text{Fmax} = 186 \text{ lb}$$

$$\therefore \quad \text{Fmax} > \text{Tmax}$$

a is the maximum deceleration and is found for our spacecraft to be 25 rad/sec^2 (taken from Reference 3.4 NASA TN D-1012 Figure 13).

APPENDIX C

C.1 DEFINITIONS

Unless otherwise stated in the individual sections, the following definitions pertain to Appendix C.

A = cross-sectional area of SCOPE vehicle normal to flight-path direction
a = altitude
β = the inverse of the scale height. For the earth, $1/\beta$ = 23,500 ft
C_D = coefficient of drag
D = vehicle drag-weight parameter, = $C_D A/W_o$
e = orbital eccentricity
F = thrust
g_o = acceleration of gravity at the earth's surface
I_{sp} = specific impulse
i = inclination of the orbital plane to the equator
$J = 1.632 \times 10^{-3}$, a constant
l = latus rectum
m = mass of satellite
R_A = apogee radius
R_o = earth radius
r_1 = present radius
Δr_{fs} = change in radius 1/2 revolution away from burn of thruster
ρ_k = density of the atmosphere at altitude k
ΔT = time change
τ = torque
θ = angle from perigee to any point on the orbital ellipse
ΔV = velocity change
V_{lc} = local circular velocity
W_o = earth surface satellite weight
$\dot{w}$ = weight flow

C.2 LIFETIME

For a circular orbit about a perfectly spherical earth, it can be shown that the time necessary for the orbit to decay from altitude 1 to altitude 2 is

$$t_{1-2} = \frac{1}{D\, g_o \sqrt{g_o R_o (\beta R_o)}} \left[\frac{1}{\rho_1} - \frac{1}{\rho_2} \right] \text{ sec}$$

For the earth, this equation reduces to

$$T = (1.386 \times 10^{-11}) \quad \frac{1}{\mathcal{W} \beta R_o} \quad \left[\frac{1}{\rho_1} - \frac{1}{\rho_2} \right] \quad \text{days}$$

The equation, with point 2 as the earth's surface, has been plotted (see Figure C.1) (Reference 4.1, p 2-477). For lifetime calculations we assumed that $C_D = 1$, $W_o = 190.0$ lb + 15 lb contingency, and $A = 8$ ft^2. Then $\mathcal{W} = C_D A / W_o = 0.0388$ ft^2/lb. For a desired lifetime of 10 years or 3650 days, $T\mathcal{W} = (3650 \text{ days})(0.0388 \text{ ft}^2/\text{lb}) = 142$ days ft^2/lb.

The graph indicates that the altitude of a 10-year circular orbit falls somewhere between 310 and 340 nm. 320 nm was chosen in the initial phases of the project in order to determine the values for such important parameters as orbital period and ground track, with the realization that some small loss in lifetime might arise if the weight of the vehicle were to be decreased during project development.

The lifetime equation is dependent on a knowledge of atmospheric densities from ground to orbit, but an exact density profile is unfortunately difficult to determine. Local density depends on local temperature, and the atmosphere's temperature profile varies appreciably. Due to these variables it was decided in calculating orbit altitude to allow for a lifetime error of one full order of magnitude, in order to be sure that SCOPE will have at least its minimum acceptable lifetime of one year.

C.3 SUN SYNCHRONIZATION

The oblateness of the earth has an effect on orbits about the earth: orbital planes are caused to precess about the polar axis. The rate of precession is a function of the orbital inclination, and the sense is to the west for posigrade orbits, to the east for retrograde.

The governing equation is

$$\Delta\Omega = \text{precession rate to the west} = \frac{2\pi J (\cos i) R_o^2}{a^2 (1 - e^2)^2} \text{ rad/revolution}$$

The plane of an orbit about a spherical earth will remain inertially fixe throughout the earth's revolution about the sun.

Since the earth revolves to the east, the orbital plane will rotate 360° to the west each year with respect to the earth-sun line. A sun-synchronous orbit will be obtained if the inclination is set so as to generate a precession rate which exactly cancels this change in orientation between the orbital plane the earth-sun line. Thus $\Delta\Omega$ must = 360°/year to the east, or = -360°/year to the west.

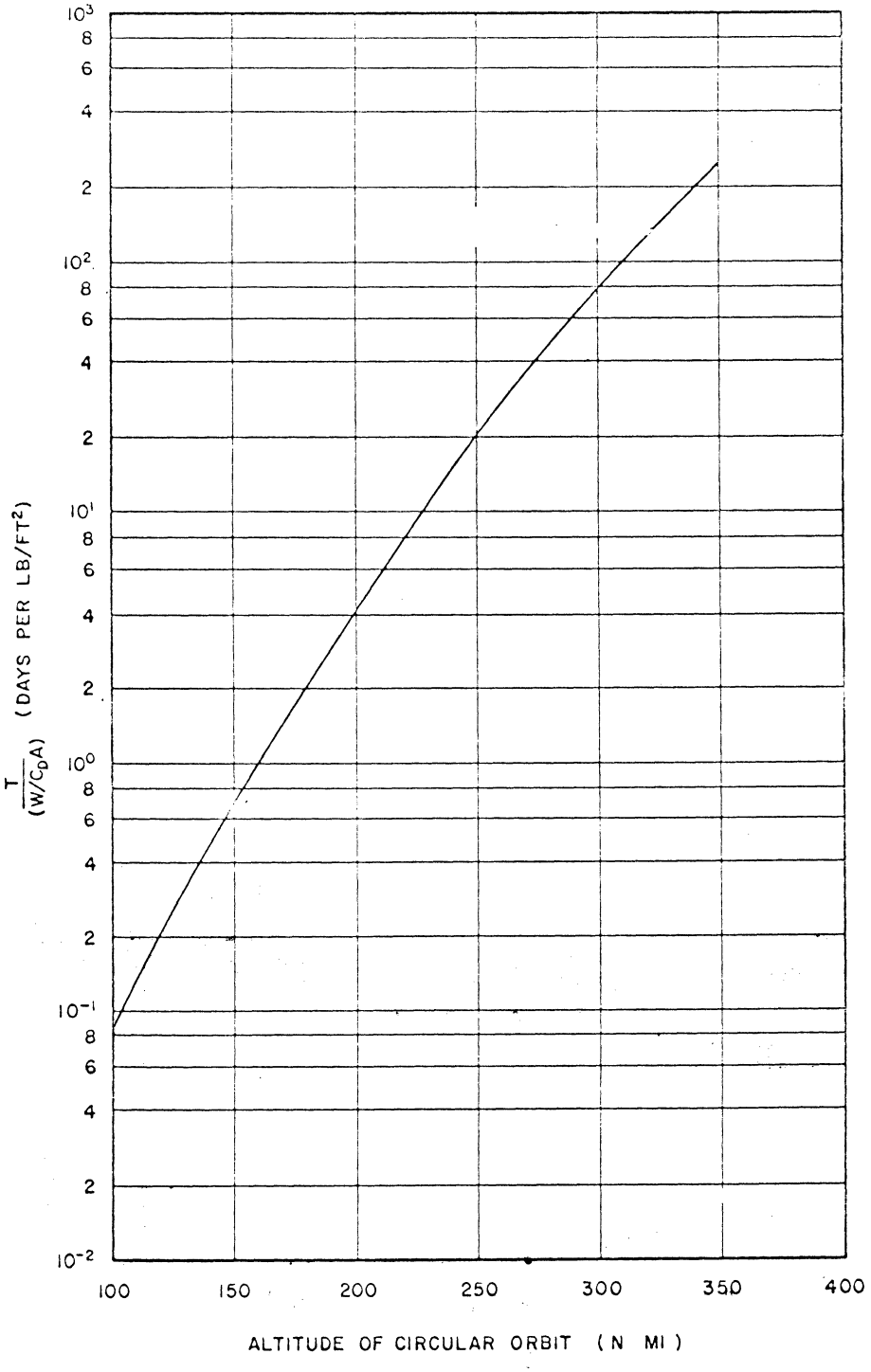

Figure C. 1 Graph of T $\frac{W}{C_D A}$ vs Altitude (Ref 2, p 2-477, Sec. 4)

$$\frac{-2\pi \text{ radians}}{\text{year}} \times \frac{1 \text{ year}}{365 \text{ days}} \times \frac{1 \text{ day}}{14.9 \text{ revs}} = -0.00115 \text{ rad/rev}$$

$$-0.00115 \text{ rad/rev} = \frac{2\pi J (\cos i) R_o^2}{a^2 (1 - e^2)^2}$$

with R_o = 3440 nm, a = 320 nm, e = 0, and since $-\cos i = \cos (180^o - i)$, then $i \cong 82.3^o$ measured from the westward direction of the equator, or 97.7^o measured from the eastward.

Errors in inclination of the orbital plane due to launch inaccuracies can be substituted into the above equations to yield the precession rates above (or below) the rate required for sun-synchronization, and thus the drift rates observed by some solar observer as the year progresses. The results for selected errors are shown in Section 4.3.3.

C.4 GROUND TRACK CALCULATION

The ground tracks were obtained analytically from the application of some theorems of solid trigonometry. In order to explain the process, the following definitions are given.

A great circle on the surface of a sphere is that traced by the intersection of the sphere and a plane passing through the sphere's center. If the earth is considered a perfect sphere, examples of great circles would include the equator and the lines of longitude.

A spherical triangle is a triangle whose sides are formed by great circles. The side lengths themselves may be stated in terms of degrees or radians, since they can be considered arcs on the sphere's surface subtended by angles radiating from the sphere's center.

For all spherical triangles (see Figure C.2), the following relations between sides and angles may be stated

$$\frac{\sin a}{\sin A} = \frac{\sin c}{\sin C} = \frac{\sin b}{\sin B} \quad (1)$$

$$\cos a = (\cos b)(\cos c) + (\sin b)(\sin c)(\cos A) \quad (2)$$

where A, B, and C are the angles of the triangle and a, b, and c are the opposite sides (Reference 4.6).

Consider the earth to be a perfect sphere, one which, for the moment, does not rotate. Consider a spherical triangle on the earth's surface where sides are the following: side b is the equator, side c is a line of longitude,

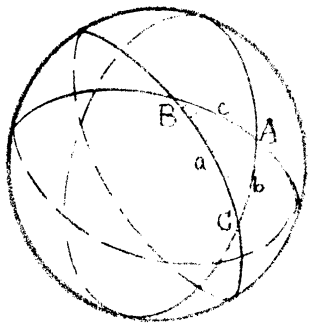

Figure C. 2 The Spherical Triangle

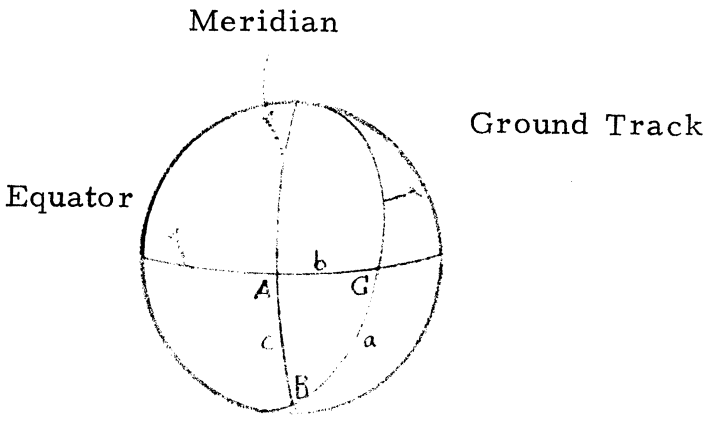

Figure C. 3 Specific Spherical Triangle for Ground Track Calculation

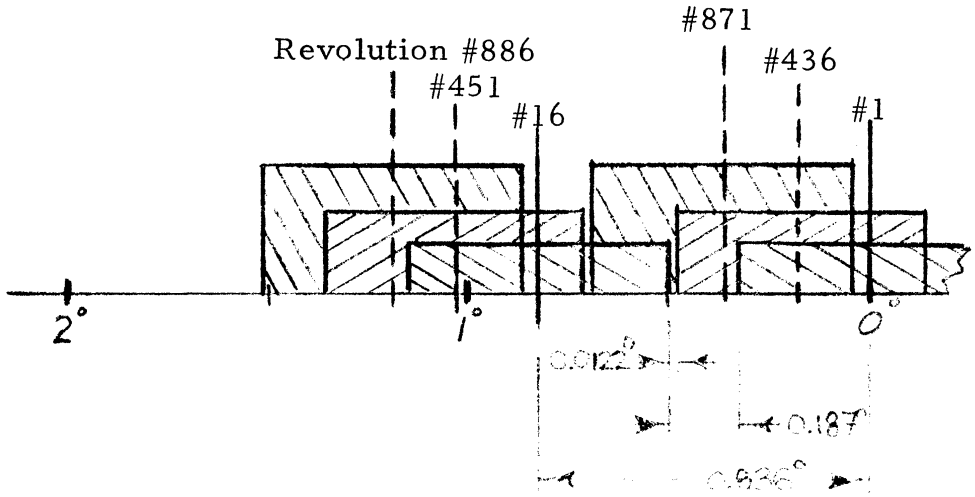

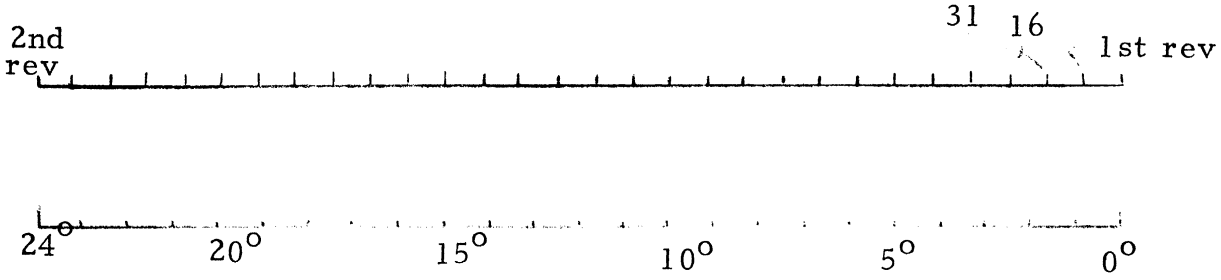

Figure C. 4 Equatorial Line with Revolutions and Scan Widths. The Top Section is a Blowup of the First Two Equatorial Degrees Shown Below.

i. e. a meridian, side "a" is the great circle traced by the intersection of the earth's sphere and the plane of motion of a body in orbit about the earth (Figure C. 3).

If point C is considered to be the point of 0^{o} longitude and 0^{o} latitude, then the following will be true:

Side c is the latitude of point B, since it is the angular distance of B along a meridian from the equator.

Angle A is 90^{o}, since the meridians are normal to the equator.

Side b is the longitude of point B, since it is the angular distance of B's meridian from point C.

Angle C is equal to the inclination of the orbital plane to the equator.

Given the orbital inclination, and assuming that the spacecraft is passing over point B, then a relationship between the spacecraft latitude and longitude can be calculated from (1) and (2).

Specifically:

$$\frac{\sin a}{\sin A} = \frac{\sin c}{\sin C} \text{ and, since } A = 90^{o}, \quad \sin a = \frac{\sin c}{\sin C} \qquad (3)$$

$$\cos a = (\cos b)(\cos c) + (\sin b)(\sin c)(\cos 90^{o}) \qquad (4)$$

$\cos 90^{o} = 0$

Given that C in SCOPE's case is 82.3^{o}, then substituting some given latitude c into equation (3) yields a value for "a", which, in turn, substituted into (4) yields a value for b, the longitude.

The effect of the earth's rotation is to add a westward longitude to the value of b derived above. Since the spacecraft is in circular orbit, it will travel at a constant angular rate. Thus the length of side "a" is proportional to elapsed time.

The earth rotates eastward at 24.06^{o}/revolution for a 320 nm circular orbit, so that the longitude adjustment for a given (a, b, c) is

$$\frac{a}{360^{o}} (24.06^{o}) = \text{longitude change due to rotating earth}$$

For an orbit whose eccentricity $\neq 0$, the length of side "a" would be a more complicated function of time.

The above process yielded the following results for the ground track of the SCOPE satellite:

Latitude, c	Longitude, b	Longitude Correction	Total Longitude
15^{o}	2.0^{o}	1.0^{o}	3.0^{o}
20	2.8	1.4	4.2
30	4.8	2.0	6.8
40	7.4	2.7	10.1
50	8.9	3.5	12.4
60	13.6	4.1	17.7
70	22.5	4.8	27.3
80	50.0	5.6	55.6
82.3	90.0	6.0	96.0

Taking into account a launch from Vandenberg Air Force Base (approximately 120.6^{o} W longitude, 34.7^{o} N latitude), point C will in fact lie at 128.4^{o} W longitude, 0^{o} latitude. Thus the resulting 1st quadrant of the ground track will be:

Latitude	Longitude
15^{o}	131.4^{o}
20	132.6
30	135.2
40	138.5
50	140.8
60	146.1
70	155.7
80	184.0 or 176^{o} E long
82.3	224.4 or 135.6^{o} E long

Note that SCOPE's orbit is nearly polar, and that this results in a great latitude change during the first few degrees of longitude.

All remaining quadrants of the orbit will be mirror images of the 1st, either with respect to a meridian, with respect to the equator, or with respect to both in succession.

C.5 MAPPING

Figure C.4 indicates the manner in which the mapping time was determined. Since repetitive ground tracks are undesirable, it is necessary that the period of the satellite's orbit <u>not</u> be an even divisor of 24 hours. If

it were, the satellite at the end of a day would begin to retrace the path traced at the beginning of the day, and each day's ground tracks would be duplicates of those of the day before. For SCOPE project: at 320 nm circular altitude, satellite orbital period is 96.4 minutes, resulting in the completion of 14.9 revolutions per day. The 15th revolution will fall short of the 1st and the 16th beyond the 1st; neither will travel the same path as the 1st.

Ground tracks and mapping times were determined for the equator, since for a highly-inclined orbit the swaths cast by the sensor's viewing angle converge as the poles are approached. The equator is thus a worst case: once points along it have been completely mapped, the converging swaths have surely completed mapping of higher latitudes--perhaps several times over.

The earth turns 24.06^{o} to the east in 96.4 minutes; thus, as each revolution passes over the equator from north to south it will trace a path 24^{o} west of the path of the last revolution. Orbital paths will pass westward in 24^{o} jumps for the remainder of the day, until, as the end of the day approaches, the 15th revolution will cross the equator 337^{o} west of the 1st--or 23^{o} short of it. The 16th orbit will then fall just 1^{o} ahead of the first, the 17th 1^{o} ahead of the 2nd, and so on, as a new day begins. It is this sort of offset which makes possible total mapping of the available area.

At the beginning of the third day, the same offset will apply again. The 31st revolution will fall just 1^{o} beyond the 16th--or 2^{o} beyond the 1st--and it can be seen that the 24^{o} interval originally laid down between the 1st and 2nd revolutions is now being filled by progressive sets of ground tracks (as are all the other 24^{o} intervals established by the first day's revolutions). Conditions would be ideal if the scan width for revolution 16 were to be laid down immediately next to that of revolution 1; we would need only to wait for the offsets of successive days to fill the 24^{o} interval, and mapping would be complete. There are, however, gaps between scan widths 1 and 16 (and 2 and 17, 3 and 18, etc.). The 7^{o} field of view of the sensor will subtend 0.649 degrees of longitude on the equator, but each day's revolution falls 0.836^{o} beyond that of the day before: a gap of 0.187^{o} of longitude is left.

At the end of 435 revolutions, or 29 days, figure C.4 shows that a second layer of offsets begins: the 24^{o} interval between the first series of ground tracks has been filled by the succeeding sets, and the interval is now being refilled by a second "layer" of ground tracks. Revolution 436 falls between revolution 1 and 16 (just as 437 falls between 2 and 17) and its scan width covers some of the gap left between scan widths 1 and 16. The gap between scans has now been reduced to 0.0122^{o} of longitude at the equator.

A third layer of offsets is sufficient to complete mapping. Revolution 871 falls between 436 and 16 (as 872 falls between 437 and 17, and 873 between 438 and 18, etc.) and this third filling of the original 24° intervals now fills them to a close enough extent that scan width touch or overlap at all points about the earth's equatorial circumference. The third filling is completed by revolution 1305--midway through the 88th day of the mission. Mapping of higher latitudes has been finished earlier as converging scan widths have begun to overlap--for example, points greater than 14° north and south latitude are completely mapped after about two months.

C.6 ACCEPTABLE ELLIPSE

In order to calculate the maximum acceptable apogee radius, two equations of elliptic geometry are needed:

$$r(\theta) = \frac{\ell}{1 + e \cos(\theta)} \qquad (1)$$

$$R_a = \frac{\ell}{1 - e} \qquad (2)$$

We know, from Section 4.3.1, that at perigee the radius is 3760 nm ($\theta=0^\circ$), and the latus rectum is 3795 nm. Solving eq. (1) at perigee;

$$r(\theta) = 3760 = \frac{3795}{1 + e}$$

or

$$e = \frac{3795}{3760} - 1 = 0.00931$$

and using this value of e in eq. (2), $R_a|_{max}$ is;

$$R_a|_{max} = \frac{3795}{1-0.00931} = 3820.56 \text{ nm}$$

or

$$R_a|_{max} = +59.44 \text{ nm from nominal}$$

C.7 BURN CALCULATIONS

In calculating the ΔV required to correct injection errors, the following equation was used;

$$\frac{\Delta r_{fs}}{3440} = 4\left[\frac{r_1}{3440}\right]^{\frac{3}{2}} \frac{\Delta V}{25,950}$$

or

$$\Delta V = 1.885\left[\frac{\Delta r_{fs}}{\left(\frac{r_1}{3440}\right)}\frac{3}{2}\right] \qquad (1)$$

This equation is valid at all times when the initial orbit is circular. However when the initial orbit is an ellipse it is only valid at apogee and perigee.

As an example calculation, consider case 1 of table 1 (Sec. 4.3.2). Th burn will be at apogee, and the object is to raise the perigee 10 nm. Therefore;

$$r_1 = 3440 + 320 + 171 = 3931 \text{ nm}$$

$$\Delta r_{fs} = 10 \text{ nm}$$

and using eq. (1);

$$\Delta V = 1.885\left[\frac{10}{\left(\frac{3931}{3440}\right)}3/2\right] = 15.8 \text{ ft/sec}$$

Burn number two will then be at perigee (now at nominal altitude), and the object is to decrease the apogee 171 nm. Thefore;

$$r_1 = 3440 + 320 = 3760 \text{ nm}$$

$$\Delta r_{fs} = 171 \text{ nm}$$

Again, using eq. (1);

$$\Delta V = 1.885\left[\frac{171}{\left(\frac{3760}{3440}\right)} 3/2\right] = 283.5 \text{ ft/sec}$$

The total ΔV required to circularize is then 283.5 + 15.8 = 299.3 ft/sec.

To calculate the fuel used and approximate time of burn, the equations for specific impulse and Newton's law were used.

$$I_{sp} = \frac{F}{\dot{w}} \qquad (2)$$

$$F = ma = m\frac{\Delta V}{\Delta t} \qquad (3)$$

Using eq. (2) the weight flow of fuel was calculated as;

$$I_{sp} = 220 = \frac{F}{\dot{w}} = \frac{5}{\dot{w}} \qquad \dot{w} = 0.02275 \text{ lb/sec}$$

Using eq. (3), and assuming a constant thrust, the time required for a specific ΔV can be calculated;

$$\Delta t = \left(\frac{m}{F}\right) \Delta V = (1.285)\, \Delta V$$

and if applied to the burn calculated for case 1, the resultant burn times are 20.3 and 364 sec (total of 384.3 sec). Hence, the fuel required for circularization is;

$$\text{fuel} = (\Delta t)\, \dot{w} = (384.3)(0.02275) = 8.74\text{-lbs.}$$

Total impulse is thrust (5-lbf) times Δt.

C.8 DOG-LEG MANEUVER

To calculate the ΔV required for the dog-leg maneuver, consider the following vector relationship at the injection point.

Here the assumption is that yaw is the only injection error (valid since the remaining errors can be erased through circularization). The magnitude of the dog-leg vector is easily found by making a small angle assumption;

$$\Delta V_{\text{dog-leg}} = V_{\ell c} \sin (0.6^{\circ})$$

$$= 24,820\ (0.01045) = 264.5 \text{ ft/sec}$$

C.9 MISALIGNMENT TORQUE

If the thruster is misaligned 0.25°, the system will appear as follows;

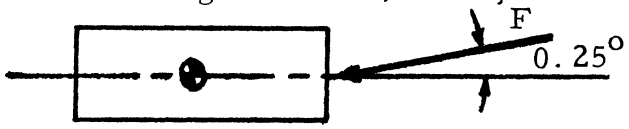

Therefore, the torque caused by this misalignment is;

$$\tau = (5\text{-lbf})\ (\frac{13}{12} \text{ ft}) \sin (0.25^{\circ})$$

$$= 0.02362 \text{ ft-lb}$$

The resulting momentum due to this torque applied over a given Δt (Δt used is for maximum ΔV);

$$\text{Momentum} = \tau \Delta t_{\text{worst case}} = (0.02362)(302)$$

$$= 7.145 \text{ ft-lb-sec}$$

This momentum must be canceled by the attitude and control jets.

C.10 FUEL TANKS

The diameter is 9.51 in, therefore;

$$\text{Total Volume} = V_t = 2\left(\frac{4}{3}\pi\left(\frac{4.76}{12}\right)^3\right) = 0.5225 \text{ ft}^3$$

Since the volume of hydrazine is one-third the total (to give a two to one nitrogen-hydrazine volume ratio);

$$V_{N_2H_4} = 0.1745 \text{ ft}^3 \quad \text{and} \quad V_{N_2 \text{ gas}} = 0.3480 \text{ ft}^3$$

Hence the weight of hydrazine is 10.95 lbs (includes two pounds for attitude and control).

To calculate the amount of nitrogen gas needed to pressurize the tanks to 300 psia at 50° F, the perfect gas law was used.

$$P = \frac{nRT}{V}$$

$$300 = \frac{\left[\left(\frac{\text{lb}_{N_2}}{28}\right)\right](1545)(506)}{(144)(0.348)}$$

$$\text{lb}_{N_2} = 0.538$$

APPENDIX D

D. 1 TORSION TUBE ANALYSIS

Analysis for Column Failure, from Mangurian (Reference 1)

Material: 7075 T-6 Aluminum, $E = 10.3 \times 10^6$ psi

density = 0.101 lb/in^3

Tube Characteristics

D = outside diameter = 5.0 in
t = wall thickness = 0.061 in
L = length = 36.2 in
c = end fixity coefficient = .25

Variables used in Analysis

ρ = radius of gyration = .707 D/2 = 1.77 in
A = area = πDt = 0.98 in^2
$L'/\rho = L/\rho \quad c = 45.2$
F_{co} = Euler column critical stress
F_{cc} = short column critical stress
P_{crit} = column critical load
P_{max} = maximum expected load

$$F_{co} = \frac{c\pi^2 E}{(L/\rho)^2} = 4.97^4 \times 10 \text{ psi}$$

Mangurian suggests using the straight-line parabola formula for short columns of Aluminum alloy. Such that

$$F_{cc} = F_{co}\left[1 - 0.385\left(\frac{L'/\rho}{\pi \quad E/F_{co}}\right)\right] = 3.05 \times 10^4 \text{ psi}$$

$$P_{crit} = F_{cc} A = 2.41 \times 10^4 \text{ lbs}$$

At a design acceleration of 25 g's (safety factor of 1.7 over expected maximum acceleration),

$$P_{max} = 182 \text{ lbs} \times 25 \text{ g's} = 4.61 \times 10^3 \text{ lbs.}$$

A comparison of P_{crit} and P_{max} for the 182 lb satellite shows that the tube will not fail as a column. According to Mangurian, if $L'/\rho > 20$, the tube is column critical. Therefore, no local crushing will occur in SCOPE.

D.2 PAYLOAD ATTACHMENT COLLAR

A payload attachment collar had to be designed to be compatible with the payload support ring as part of the payload structure. This collar is attached to our torsion tube, and the payload support ring is then bolted to the attachment collar. The payload attachment collar thus helps support the whole payload above it during the launch and had to be designed to withstand the launch forces (Reference 1).

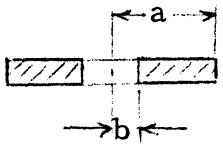

for SCOPE: $a = 4.75$ in
$b = 2.50$ in

$$\frac{a}{b} = 1.9$$

From the tables (at V = .3) which are found in the complete theory used from Timoshenko.

$$k = 1.44$$
$$k_1 = 0.64$$

$P = 182 \text{ lbs} * 15 \text{ g's} * 1.5 = 4100 \text{ lbs}$

where 15 g's * 1.5 is the maximum axial acceleration that the payload attachment collar is to be designed for. From the theory found in Timoshenko, the expression for maximum stress in the circular plate is:

$$\sigma_{max} = \frac{k P}{h^2}$$

The material used for the collar will be 7075 T-6 aluminum which has a maximum compressive yield stress of 70,000 psi. Due to the structural importance of the payload attachment collar, a safety factor of two was used. Therefore the maximum compressive stress to be tolerated is 35,000 psi. Therefore,

$$h^2 = \frac{k\,P}{\sigma_{max}} = \frac{1.44 \quad 4100\ \text{lbs}}{35{,}000\ \text{lbs/in}^2} = .1686\ \text{in}^2$$

Therefore, $h = 0.42$ inch

From Timoshenko[3], the maximum deflection at this thickness is:

$$w_{max} = \frac{k_1 \quad P \quad a^2}{E \quad h^3}$$

where

a = reaction force radius
E = Young's Modulus
k_1 = factor from Timoshenko

Therefore,

$$w_{max} = \frac{0.64 \quad 4100\ \text{lbs} \quad (4.75\ \text{in})^2}{10.4 \quad 10^6\ \text{lbs/in}^2 \quad (.42\ \text{in})^3} = 0.08\ \text{in}$$

This deflection is safely tolerable since this maximum deflection occurs at the inner radius and there is nothing to interfere with. This is as shown below in the diagram:

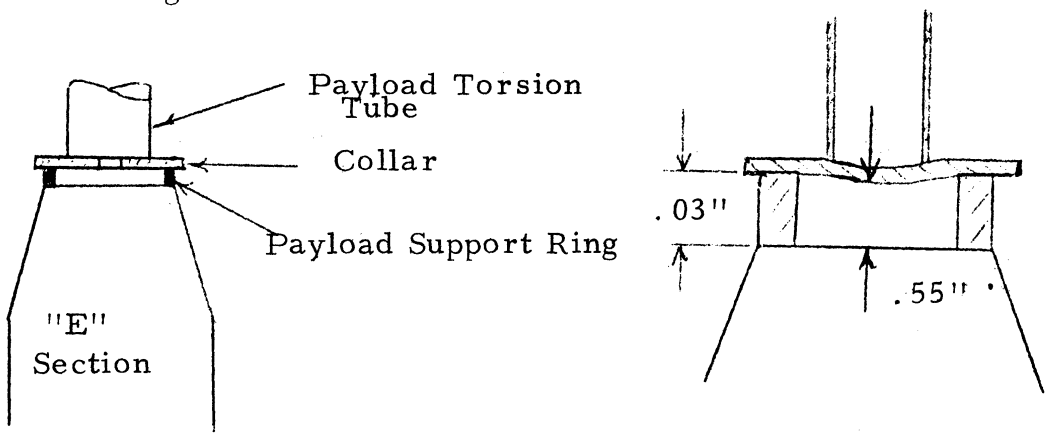

Note: This theory is slightly conservative due to the fact that there is some overlap of the payload attachment collar outward from the point of reaction force at $a = 4.75$ and also some overlap inside of the radius of payload force application $b = 2.5$ inches. The actual inside radius of the collar is 1.1 inches and the actual outside radius of the collar is 5.125 inches, and this overlap tends to stiffen the plate even more giving us an extra slight built-in safety factor.

Weight of payload attachment collar = Volume density

Therefore,

$$\text{Volume} = \pi(.42\text{ in})(5.125^2 - 1.1^2)\text{ in}^2 = 33.04\text{ in}^3$$

The density of 7075 T-6 aluminum is .101 lbs/in^3

Therefore,

$$\text{Weight} = .101\text{ lbs/in}^3 \quad 33.04\text{ in}^3 = 3.33\text{ lbs}$$

D. 3 MOMENTS OF INERTIA

The moments are calculated from these two theorems found on pp 458-450 of Seely (Reference 2).

1. $$I_a = \sum_{i=1}^{n} \tilde{I}_i + m_i d_i^2$$

where

I_a = total moment about axis A

I_i = moment of the element about its center of mass

m_i = mass of the element

d_i = distance from center of mass of the element to the axis A

2. The sum of the moments of inertia of a body with respect to two perpendicular planes is equal to the moment of inertia of the body with respect to the line of intersection of the two planes.

In this calculation components whose gross weights were less than one pound were ignored in these calculations. The axes mentioned are those for operational mode.

Sample Calculation

Torsion Tube contribution to I_{yaw}

$$I_{yaw} = mr^2 = (.11 \text{ slug})(2.5 \text{ in}) = .70 \text{ slug-in}$$

There is no contribution to mx^2 or my^2 by the tube since it is symmetric around the yaw axis. The final results of these calculations are as follows.

Moments:

undeployed solar panels (launch)

$I_{yaw} = 345$ slug-in

$I_{roll} = 1165$ slug-in

$I_{pitch} = 1000$ slug-in

deployed solar panels (operation)

$I_{yaw} = 1460$ slug-in

$I_{roll} = 1940$ slug-in

$I_{pitch} = 680$ slug-in

References Used

1. Mangurian, Aircraft Structural Analysis; New York, Prentice Hall, 1947, pp 170-178.

2. Seely, Ensign, & Jones; Analytical Mechanics for Engineers; New York John Wiley & Sons, Inc. 1958, pp 458-459.

3. Timoshenko, S. and Woinowsky-Kreiger, S., Theory of Plates and Shells, 2nd edition, McGraw-Hill, New York, 1959, pp 58-63.

ANC Committee on Aircraft Design Criteria, Strength of Materials, Report ANC-5, Dec. 1942, Amendment No. 7 October 1943.

Osgood, Spacecraft Structures, New Jersey, Prentice Hall, 1966.

APPENDIX E
COMMUNICATION LINK CALCULATIONS

Index of Variables

c	Velocity of light
D	Minimum receiving antenna diameter
F	Transmitting frequency
Δf	Transmitted bandwidth
FSL	Free Space Loss, attenuation of radio signal
G_r	Receiving antenna gain
G_t	Transmitting antenna gain
h	Orbital altitude
k	Boltzmann's Constant
L_{att}	Loss due to atmospheric and ionospheric signal attenuation
L_{cab}	Loss due to ohmic resistance in transmitting system
L_{mar}	Loss margin
L_{pol}	Loss due to polarization mismatch
L_{tot}	Total losses in communication link
P_n	Noise power of system
P_t	Transmitting power needed by satellite
R	Maximum transmitting range
$S/N)_{in}$	Signal-to-Noise power ratio at ground station receiver
T_a	Atmospheric noise temperature seen by receiving antenna
T_b	Noise temperature of planetary body seen by receiver
T_e	Effective noise temperature of communication link
T_{op}	Optimum receiving system noise temperature
T_g	Maximum galactic noise temperature
T_s	Solar temperature
V_{lc}	Local circular orbital velocity of satellite
W	Data rate transmitted in bits per second
λ	Wavelength of transmitting signal
θ	Angle between satellite local circular velocity vector and line connecting ground station and satellite.

E.1 COMMUNICATION LINKS

The Up-Down link calculations provide a method to determine the power received and transmitted at each station. Usually the ground station power is predetermined so that the up link considerations for earth orbital missions are not crucial. The down link, however, will be needed to determin the minimum satellite power required for data transmission for an acceptable signal-to-noise power ratio at the receiver input on the ground.

The results for Project SCOPE are based on the STADAN receiving network. The parameters used are the worst case values. All references in the appendix refer to Section 7, Communications.

STADAN PARAMETERS

D = 40 feet, minimum antenna diameter
F = 138 MHz, satellite transmitting frequency
Δf = 100 kHz, transmitted bandwidth
h = 359 nm, maximum allowable altitude
R = 1500 miles, maximum slant range

The basic power equation is below (Reference 1). Each term is treated separately in the following sections. For convenience, decibels are used, where a decibel is a description of a power level or power ratio;

$$\text{decibel (db)} = 10 \log_{10} (P_1/P_2)$$

or

$$\text{watt decibel (dbw)} = 10 \log_{10} (P)$$

The power equation is:

$$P_t = \frac{S/N)_{in}(kT_e)(\Delta f)(FSL)}{(G_t)(G_r)}$$

E. 2 DETERMINE $S/N)_{in}$

For a pulse code modulation (PCM) system, as on Project SCOPE, the signal-to-noise ratio is proportional to the error probability of receiving a wrong data bit. This results from Information and Sampling Theory discussed in Reference 8. The relation is summarized below:

$S/N)_{in}$ at the receiver	Error Probability
17 db	1 bit per 10^7_6
15 db	1 bit per 10^5
13 db	1 bit per 10^5

Thus for a worst case a signal-to-noise ratio of 17 db would be needed by the communication system.

E. 3 DETERMINE NOISE POWER, P_n

Noise is the random or Gaussian noise added to the signal power. It results from the radiating effect all molecules have at temperatures above absolute zero. The molecules radiate energy or power at all frequencies in a strength proportional to their temperatures. As the temperature increases the vibrational and rotational motions of the molecules increases the transmitted power. This radiating effect is purely random.

$$P_n/Hz = (kT_e)$$

$$k = 1.38 \times 10^{-23} \text{ joules}/^{o}K$$

$$T_e = T_{op} + T_a + T_s + T_g + T_b$$

Under normal operating conditions T_s and T_b will be zero since the sun or planetary body such as the moon will not be in the field of view or beamwidth of the receiving antenna. However, occasionally the satellite might be in a position where these terms are not zero and loss of signal will occur for a brief time. Operational considerations are the galactic noise temperature, the atmospheric temperature and the optimum receiver system temperature. These temperatures are a function of the transmitting frequency and are often graphed for ease of calculation (Reference 23). For a frequency of 138 MHz the following values result:

T_g	=	$2790^{o}K$	Maximum galactic noise temperature
T_a	=	$5^{o}K$	Atmospheric noise temperature
T_{op}	=	$105^{o}K$	Maximum system temperature of STADAN
T_{tot}	=	$2900^{o}K$	

Therefore:

$$P_n/Hz = (kT_e) = (1.38 \times 10^{-23})(2.9 \times 10^{3}) \text{ joules}$$

$$P_n/Hz = 4.0 \times 10^{-20} \text{ joules}$$

in decibels

$$(kT_e) = 10 \log_{10} (4.0 \times 10^{-20})$$

$$= 10 (-19.398)$$

$$(kT_e) = -193.98 \text{ dbw}$$

E.4 DETERMINE BANDWIDTH

For a PCM system the bandwidth is a function of the data rate transmitted. For the STADAN system a standard bandwidth of 100 kHz is used. This bandwidth must include doppler shift and frequency instability, thus reducing the amount of bandwidth available for data transmission. The available data bandwidth must be calculated to determine the allowable data rate. Based on IRIG standards a data bandwidth of 1.5 to 3.0 times the data rate is used in PCM (Reference 7).

$$\Delta f = 100 \text{ KHz} = f_{data} + f_{doppler} + f_{instable}$$

in decibels:

$$\Delta f = 50 \text{ db}$$

Now:

$$f_{instable} = 2(\text{(Transmitter instability + receiver instability) (frequency)})$$

$$f_{instable} = 2((10^{-5} + 10^{-12})(1.38 \times 10^{8} \text{ Hz}))$$

$$f_{instable} = 2.76 \times 10^{3} \text{ Hz}$$

And

$$f_{doppler} = 2 ((V_{lc} \cos \theta)(F/c))$$

$$f_{doppler} = 2(24,820 \text{ ft/sec})(1)(1.38 \times 10^{8} \text{ Hz}/9.69 \times 10^{9} \text{ ft/sec})$$

$$f_{doppler} = 7.06 \times 10^{3} \text{ Hz}$$

Therefore

$$f_{data} = 100 \text{ kHz} - 2.76 \text{ kHz} - 7.06 \text{ kHz}$$

$$f_{data} = 90.18 \text{ kHz}$$

Now the bit rate at data rate is betwen one third to two thirds the data bandwidth. This will define the rate at which Project SCOPE can transmit data. For tape recorded storage facilities it determines the recorder playback speed. Thus for this system the data rate is:

$$30,000 \text{ bps} < W < 60,000 \text{ bps}$$

E.5 DETERMINE FSL

The Free Space Loss is due to the spreading of the radio signal. This loss of power density will result in the receiving antenna intercepting less signal power. The Free Space Loss is based on the power transmitted from an isotropic radiator.

$$FSL = \frac{(4\pi)^2 (R)^2}{\lambda^2} = \frac{(4\pi)^2 (R)^2 (F)^2}{(c)^2}$$

or in decibels

$$FSL = 36.8 + 20 \log_{10} (R) + 20 \log_{10} (F)$$

with R in miles and F in Mhz

$$FSL = 36.8 + 20 \log_{10} (1500) + 20 \log_{10} (138)$$

$$= 36.8 + 63.4 + 42.8$$

$$FSL = 142.0 \text{ db}$$

E.6 DETERMINE ANTENNA PARAMETERS

The gain of an antenna is determined by its directivity. An isotropic antenna is a uniform radiator in all directions. A turnstile antenna such as the one on Project SCOPE is basically a circularly polarized isotropic antenna. The directivity of the ground antennas is a function of their size and the operating wavelength of the signal. Antenna theory is complex and out of scope with this discussion, for further information refer to Reference 5.

$$\text{Directivity} = \frac{(\pi D)^2}{\lambda^2}$$

Gain = n Directivity, where n is the antenna efficiency

For the STADAN parabolic receiving antennas

$$G_r \text{ db} = 20 (\log F + \log D) - 52.6$$

with F in MHz and D in feet

$$G_r = 22.2 \text{ db}$$

For the turnstile antenna

$$G_t = 0.6 \text{ db}$$

The half-power beamwidth of the parabolic antennas is

$$HP = 13.0^{o}$$

E.7 SUMMATION OF LOSSES

Losses in the system reduce the power received by the ground stations. Most losses are due to the equipment itself and is in the form of power dissipation. Other losses are due to incorrect adjustment of the antenna systems and the atmospheric scattering of the signal. Usually a margin is projected into the system to allow flexibility.

$$L_{tot} = L_{pol} + L_{att} + L_{cab} + L_{mar}$$

$L_{pol} = 0$ db since both antennas are circularly polarized and other antenna parameters are negligible such as Faraday Rotation, Luxembourg effects and chromatic aberration.

$L_{att} = 4$ db for minimum elevation angle of reception, 5^{o}

$L_{cab} = 3$ db

$L_{mar} = 3$ db

$L_{tot} = 10$ db

E.8 CALCULATION OF RF POWER NEEDED

$$P_t = \frac{S/N)_{in} (kT_e)(\Delta f)(FSL)(L_{tot})}{(G_r)(G_t)}$$

or in decibels

$$P_t \text{ (dbw)} = (S/N)_{in} + (kT_e) + (\Delta f) + (FSL) + (L_{tot}) - (G_r) - (G_t)$$

$$P_t = 17 \text{ db} + (-193.98) + 50 \text{ db} + 142.0 + 10 \text{ db} - 22.2 \text{ db} - 0.6 \text{ db}$$

$$P_t = 2.22 \text{ dbw}$$

or in watts

$$P_t = 1.66 \text{ watts}$$

E.9 LIST OF MANUFACTURERS AND ADDRESSES

Adcole Corporation
330 Bear Hill Road
Waltham, Massachusetts 02154

Ball Brothers Research Corporation
Boulder Industrial Park
Box 1062
Boulder, Colorado 80302

Hughes Aircraft Company
500 Superior Avenue
Newport Beach, California 92663

Conic Corporation
9020 Balboa Avenue
San Diego, California 92123

Kinelogic Corporation
873 South Fair Oaks Avenue
Pasadena, California 91105

Microcom Corporation
430 Caredean Drive
Horsham, Pennsylvania

Teledyne Telemetry Company
9320 Lincoln Boulevard
Los Angeles California 90045

APPENDIX F
SOLAR PANEL GEOMETRY

The desired solar paddle geometry is one which would require the minimum area to provide power for all of SCOPE systems in sunlight, and charge the batteries, which will supply the necessary power during the dark portion of the orbit. To determine the angle between the sides of the solar paddles, the positions in the orbit which yield a minimum effective paddle area must be determined.

Figure F. 1 shows the positions in the orbit where minimum effective areas might occur: A, the time of acquisition of sunlight; B, when the satellite is over the terminator; C, when one side of the paddle is parallel to the directed solar radiation; and D, when both sides of the paddle present an equal effective area. The effective surface area, S_{eff}, is a function of the true surface area, S, the angle between the two sides, 2θ, and the angle of the impinging solar radiation, γ.

$$S_{eff} = S(\theta, \gamma)$$

At the points A, B, C, and D, the following expressions hold:

A:	$= -24^{o}$,	$S_{eff} = S \cos(\theta + 24^{o})$	$= S_A$
B:	$= 0^{o}$,	$S_{eff} = S \cos(\theta)$	$= S_B$
C:	$= 90^{o} - \theta$	$S_{eff} = S \sin(2\theta)$	$= S_C$
D:	$= 90^{o}$,	$S_{eff} = 2S \sin(\theta)$	$= S_D$

The effective areas at the above points are plotted as a function of θ in Figure F. 2.

From Figure F. 2, one can see that S_A, S_B, S_C, and S_D all vary uniquely with theta; consequently, the only way to predict the power output of the paddles is to assume a value for theta and calculate the effective area at numerous points in the orbit. When S_{eff} is plotted against gamma for theta held constant, the result is a curve similar to Figure F. 3.

Noting that gamma, the solar angle varies with time, and that the effective area is a function of gamma, then

$$S_{eff} = S(\text{time}).$$

Since the power output of the paddles is directly proportional to the effective area, power is a function of time only.

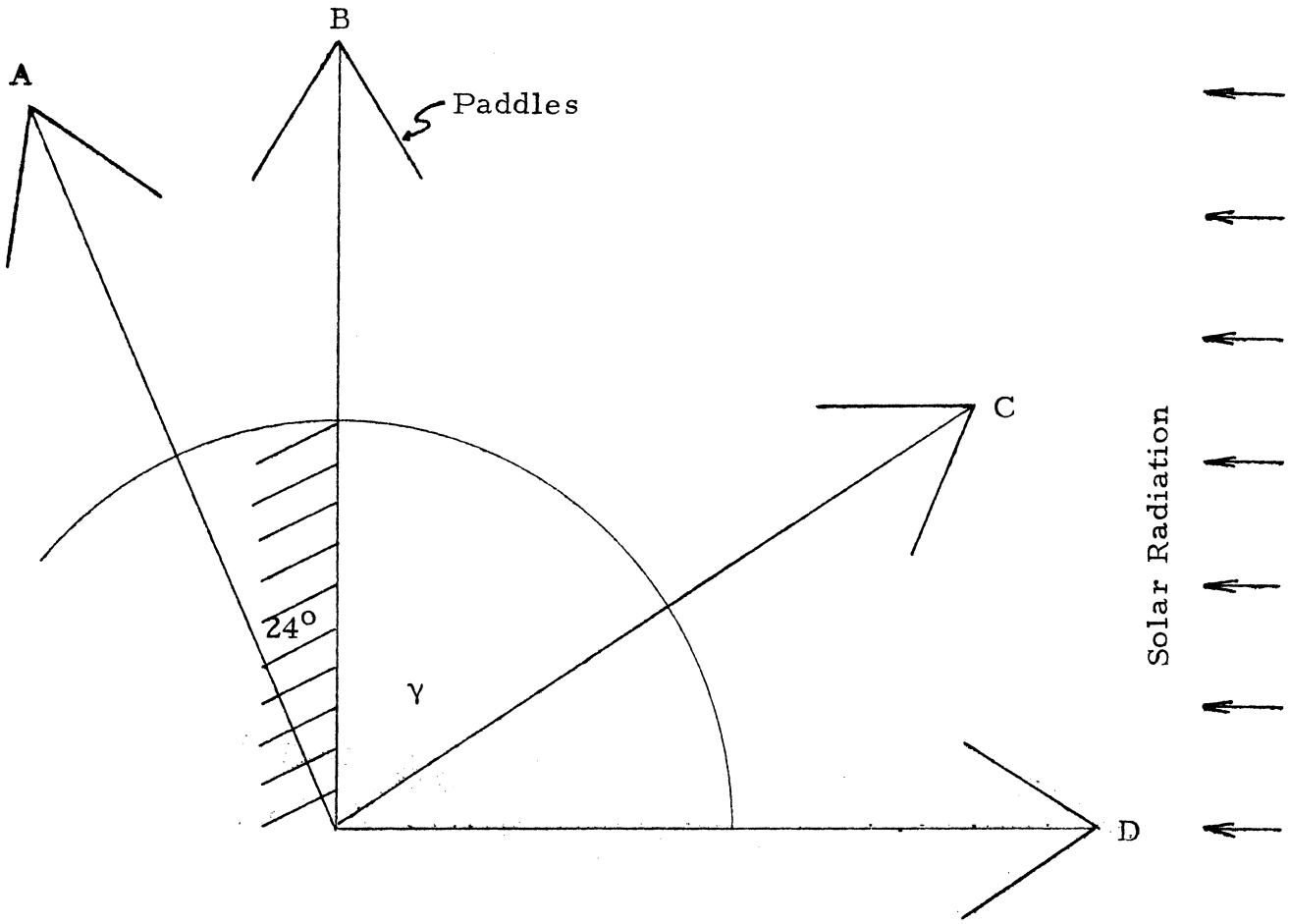

Figure F.1 Determination of Paddle Geometry

Figure F. 2 The ratio of effective solar paddle area to the true solar paddle area, S, as a function of θ, the half angle between the solar paddle sides.

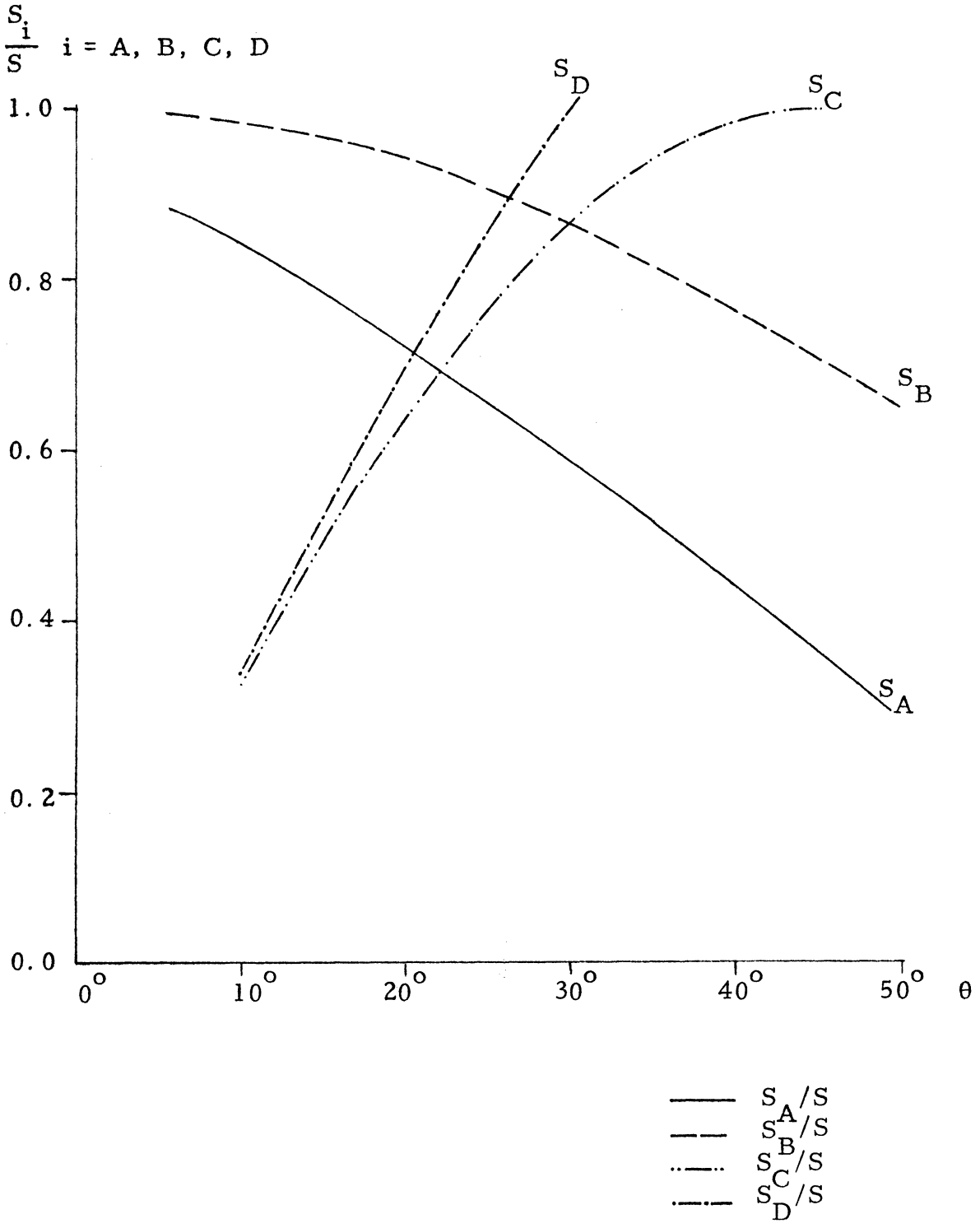

$$P = P(t)$$

If P_{req} is the power required by all of SCOPE systems excluding the power necessary to charge the batteries, P_c, then:

$$P_c = P - P_{req}$$

Letting X be the number of watt-hours necessary for night operation, P(t) is desired such that

$$\int_0^{61/60} (P(t) - P_{req}(t))\, dt = X$$

The above expression was calculated for theta equal to 10^o, 20^o, 30^o, 40^o, and 45^o. For theta equal to 30^o, the integrand equals X + 7.9 watt-hours, while all other values of theta yielded integrands less than X and hence, would require larger paddle areas. The power supplied by the paddles, P(t), is plotted in Figure F. 3 for theta equal to 30^o. All areas under the curves P(t) and P_{req} were evaluated numerically.

F. 2 CALCULATIONS

F. 2. 1 Solar Cell Efficiency

Mismatching	.93 (current loss)
Solar Constant Variations	.95 (current loss)
Diode on paddles	.96 (voltage drop)
Solar Cell Degradation	.90 (current loss)

At the predicted highest temperature each solar cell, at peak power, supplies .125 amps at .40 volts. Considering the diode loss, the available voltage is:

$$V = (.96) \times (.40) = .384 \text{ volts per cell}$$

Because of mismatching and solar constant variations, the available current is:

$$I = (.93) \times (.95) \times (.125) = .1105 \text{ amps per cell}$$

F. 2. 2 Solar Cell Requirements

The greatest daylight power demand is 60.8 watts and occurs in the nadir mode. With an expected solar cell degration of 10% and a maximum 10% loss through the panel voltage regulator, the power from the panels, P_{panel} must be:

Figure F. 3 Power Available From Solar Paddles--A function of temperature and effective area--from the time of solar acquisition, for one-half of the sunlit portion of the orbit.

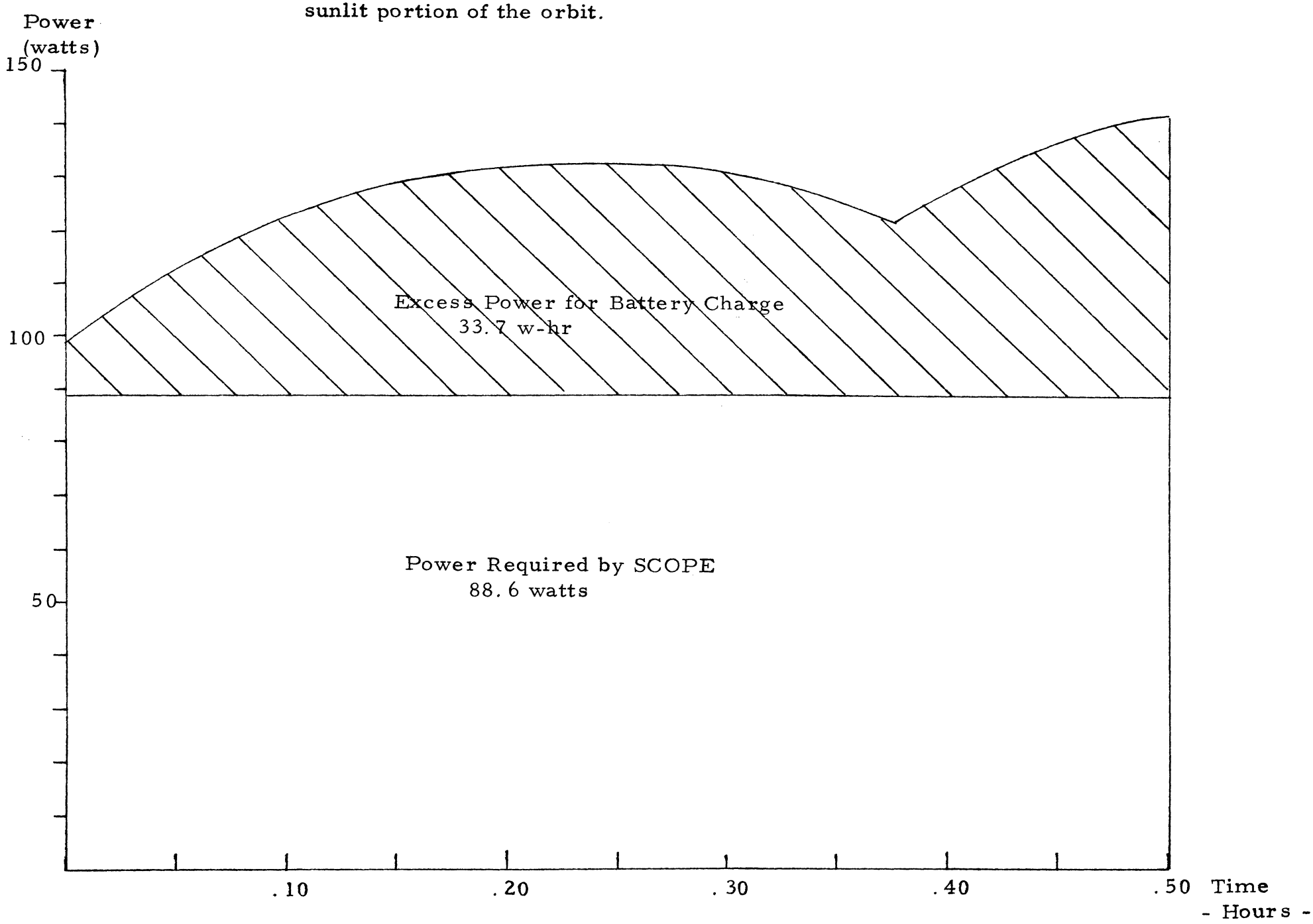

$$P_{panel} = \frac{60.8}{(.90) \times (.90)} = 75 \text{ watts}$$

The panel output current, I_{panel}, is

$$I_{panel} = \frac{75}{28} = 2.68 \text{ amps}$$

To provide 2.68 amps, there must be N_p solar cells in parallel

$$N_p = \frac{2.68 \text{ amps}}{.1105 \text{ amps/cell}} = 24.2 \text{ cells}$$

Since the solar panels must supply 2.68 amps at the worst solar angle $\gamma = -24^o$, the actual number of solar cells in parallel is N_p whence

$$N_p = \frac{24.2}{.675} = 35.8 = 36 \text{ cells}$$

The term, .675 is equal to cos (54^o) x 1.14, and takes into consideration the solar angle and the effect of temperature.

The number of solar cells in series is determined by the lowest output voltage of each cell and the voltage at which the systems will be operating. None of SCOPE systems require a voltage greater than 28 volts, thus the number of solar cells in series is

$$N_s = \frac{28}{.384} = 73 \text{ solar cells}$$

Hence, the total number of solar cells, N, is given by

$$N = 2(N_s \times N_p) = 5,256 \text{ solar cells}$$

F.2.3 Battery Requirements

From Figure 8.1, the greatest number of watt-hours necessary for night operation is

$$37.6 \times \frac{35}{60} + 19.4 \frac{4}{60} = 23.2 \text{ watt-hours}$$

With a maximum loss of 10% through the battery output power regulator, the actual demand X becomes

$$X = \frac{23.2}{.90} = 25.8 \text{ watt-hours}$$

Since the batteries are to be discharged no greater than 35%, their capacity must be

$$C = \frac{23.2}{.35 \times 28} = 2.37 \text{ amp-hours}$$

The average discharge voltage of Ni-Cd batteries is 1.1 volts, therefore 26 batteries are needed.

$$26 = \frac{28}{1.1}$$

F.2.4 Weight Analysis

Batteries .344 lb/battery x 26 batteries = 8.94 lb

Solar Cells 1.545×10^{-3} lb/cell x 5,256 cells = 8.12 lb

Regulators and electronics

Panel voltage regulator	3.9 lb
28-26 v DC converter	1.2 lb
Battery power regulator	1.9 lb
Power distribution unit	1.0 lb
Charge and mode controls	1.0 lb

The total weight is approximately 26.1 pounds

F.3 POWER AVAILABLE PROFILE

The power output of SCOPE's solar paddles is shown in Figure F.3. Since the greatest daylight power demand is 60.8 watts, the paddles must be able to produce a minimum of 88.6 watts taking all efficiencies into consideration.

$$88.6 = \frac{60.8}{.93 \times .95 \times .96 \times .90 \times .90}$$

By numerically integrating the area between the curves of power available and the power required, the power available for charging the Ni-Cd batteries is 33.7 watt-hours. Since 25.8 watt-hours are necessary to charge the batteries, there is an excess of 7.9 watt-hours.

Figure F.3 takes into consideration the angle of impinging solar radiation and the temperature variation of the paddles. The theoretical temperature was calculated at five points in the light portion of the orbit and was assumed to vary linearly between points as a first approximation.

APPENDIX G
THERMAL CONTROL

G. 1 This appendix will discuss the method and details of thermal control on SCOPE. The basic equationsgoverning thermal control are

Energy Balance Equation.

(energy Absorbed) + (Internal Energy) = (energy Radiated)

Thermal Conduction Equation

(Energy to be Transmitted) = (Difference in Temperature)/ (Thermal Resistivity)

Each of these terms in these quations will be defined as they are needed.

G. 2 THERMAL PARAMETERS*

$S = 130$ watts/ft^2	Solar radiation flux constant
$R = 38.67$ watts/ft^2	Reflected solar radiation flux const
$E = 18.67$ watts/ft^2	Earth radiation flux constant
$C_p = 0.22$ BTU/lb -^{o}F	Specific heat of aluminum
$K^p = 109.2$ BTU/hr/ft -^{o}F	Thermal conductivity of aluminum
$W = 188$ lbs	Weight of SCOPE
$= 0.1718 \times 10^{-8}$ BTU/ft^2-hr-^{o}R^4	Stefan-Boltzman constant
$Q = \begin{matrix} 83.0 \text{ watts (light side)} \\ 48.0 \text{ watts (dark side)} \end{matrix}$	Power to be dissipated as heat
$A_{panel} = (10.04'')(40'')1/144 = 2.78$ ft^2	Area of 1 side panel
$A^e = (10.04)(12.5)1/2(8)(1/144) = 3.49$ ft^2	Area of 1 end panel
$A_{total} = 29.19$ ft^2	Total surface area of SCOPE
$A^{ps} = /3.49 \cos\theta/ + /6.95 \sin\theta/$	Area projected to sun
$A^{ps}_{pe} = 3.49$ ft^2	Area projected to Earth
$\theta = 0^o$	SCOPE's angular position at the equ
$\theta = 90^o$	SCOPE's angular position at the South Pole
$\theta = 270^o$	SCOPE's angular position at the North Pole
$\alpha = .10$	Absorbtivity of thermal coatings
$\epsilon = .154$	Emissivity of thermal coatings

*These values were found in various handbooks and references (3, 7, 8, 9 & 11, Sec. 9).

G. 3 DELTA V MOTOR

Thermal consideration must be given to the heat conduction into the satellite from the delta V motor which will be used during orbital corrections. During the burning of the motor the flame temperature reaches a maximum of 5000°F. To reduce the heat conduction to a negligible value insulation must be wrapped around the nozzle of the engine. The type of insulation and its thickness can be found by first considering the amount of heat that can be transferred from the nozzle into the satellite without the use of insulation. This is done by the following equation.

The amount of heat conducted into the satellite is:

$$q_2 = \frac{T_1 - T_2}{R} = \Delta T \text{ watts}/^{o}F$$

where

$R = \frac{L}{AK}$ = 16.5 $-^{o}F/BTU$

T_1 = temperature of flame = 5000 ^{o}F

T_2 = temperature inside the satellite = 60 ^{o}F

A = conducting area = .125 inches^2

L = length of conduction path = 12 inches

K = conductivity of aluminum bottom surface = 70 BTU/hr/ft $-^{o}F$

Now an insulation must be found to stop this heat from transferring into the satellite. Various types were considered, however, the type needed must have a conductivity of at least 2×10^{-4} BTU/hr/ft $-^{o}F$ and must be easy to use. For this reason a composite type of multilayer insulation, Al Mylar, has been chosen. With this insulation heat conduction can be reduced to a negligible value.

The amount of heat conducted into the satellite with insulation installed around the nozzle is

$$q_2 = \frac{T_1 - T_2}{R} = .0000021\ \Delta T \text{ watts}/^{o}F$$

where, $R = 4.8 \times 10^{5}$ hr $-^{o}F/BTU$

This quantity of heat being transferred into SCOPE does not represent a serious problem.

G.4 SOLAR PANELS

The maximum temperature the solar panels reach is found by studying the panels when they are exposed to direct solar radiation. This condition is shown in the following diagram

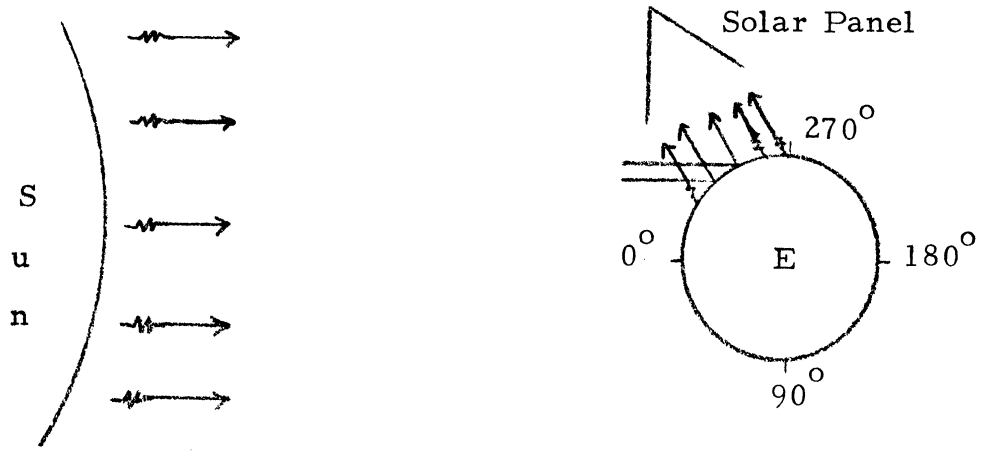

The quantities of radiation abosrbed by the panels are

Solar $q_{in} = (A)(\alpha)(S)$
$= (6.0)(.70)(130) =$ 545 watts

Earth $q_{in} = (A)(\epsilon)(E)$
$= (3.0 \text{ in}^2)(.20)(18.67 \text{ watts/ft}^2) = 11.2$ watts

Solar Reflected $q_{in} = (A)(\alpha)(R)$
$= (3.0 \text{ in}^2)(.20)(38.67 \text{ watts/ft}^2) = 81.2$ watts

Using the energy equation to find the temperature of the panels

$$Q_{out} = q_{in} = FA\epsilon_1 \sigma T_p^4 + FA\epsilon_2 \sigma T_p^4 = q_S + q_E + q_R = 637.4 \text{ watts}$$

where

F = the view factor of the solar panels = 1.0 - .78
α = absorbtivity of the front of the panels = .20
ϵ_1 = emissivity of the front of the panels = .84
ϵ_2 = emissivity of the back of the solar panels = .90

Thus

$$FA\epsilon_1 \sigma T_p^4 + FA\epsilon_2 \sigma T_p^4 = 637.4 \text{ watts}$$

or

$$T = 610\ ^\circ R = 150\ ^\circ F$$

Thus the maximum temperature which the solar panels reach will be 150^{o}F. Other temperatures have been calculated in a similar manner for other positions in the orbit. The results have been plotted in Figure 9.2. As can be seen the temperatures in the orbit are well within requirements.

G.5 AVERAGE TEMPERATURE

After several orbits SCOPE's temperature will stablize at some average temperature and remain very near this temperature for the remainder of its life time. In order to calculate this average temperature the energy balance equation will be used

(Energy absorbed) + (Internal energy) = (Energy radiated).

To find the energy absorbed by SCOPE each type of radiation it is exposed to must be considered

Solar radiation	$q_s = SA_{ps} F_s \alpha$
Earth radiation	$q_E = RA_{pe} F_E \epsilon$
Reflected solar radiation	$q_{ir} = EA_{pe} F_E \alpha$

To receive an average temperature these quantities must be averaged over one orbit. This gives:

$$q_s = 55.05 \text{ watts}$$
$$q_e = 9.8 \text{ watts}$$
$$q_{ir} = 29.4 \text{ watts}$$
$$q_{absorbed} = 94.25 \text{ watts}$$

The internal energy is simply the average value of Q, the internal energy or,

$$q_i = 75.0 \text{ watts}$$

Finally the energy radiated term is defined as,

$$q_{out} = \epsilon A_t \sigma T_{av}^4$$

or

$$q_{out} = 4.5 \sigma T_{av}^4$$

Thus the formula for average temperature becomes

$$T_{av}^4 = \frac{(94.25 + 75.0)}{4.5} \quad \text{watts/ft}^2$$

or

$$T_{av} = 63^{\circ}F$$

G.6 THERMAL TIME CONSTANT

To determine the temperature variation of the satellite during each orbit it will be necessary to determine the thermal time constant.

For this purpose this formula will be used

$$\frac{T_1 - T_2}{t_1 - t_2} = \frac{A_t \epsilon (\sigma T^4)}{C_p W}$$

or

$$\frac{T_1 - T_2}{t_1 - t_2} = \frac{(29.2)(.154)(37.6)}{(.22)(188)} \quad {}^{\circ}F/hr$$

or finally

$$\frac{T_1 - T_2}{t_1 - t_2} = 4.1\ {}^{\circ}F/hr$$

This value signifies that the satellite's temperature will vary only $4.1\ ^{\circ}F/hr$ from the average temperature. It should be noted, however, that to speak of the thermal time "constant" is misleading since this time "constant" depends upon the instaneous temperature and therefore is not a constant. Fortunately, for this case the variation of the temperature of the satellite from one point to the next is so slight that the change in the thermal time constant can be neglected, initially.

G.7 ACTUAL TEMPERATURE FLUCTUATION OF SCOPE

Culminating the proceeding discussions the actual temperature of SCOPE was calculated at each point of the orbit. To accomplish this task, a computer program was developed by members of University of Michigan's Project OBSERVER design group. This program is given in Figure (G.3) of this appendix. The result of

this study is pictorially represented in Figure G. 1 and a few of the results are shown in chart G. 1 as can be seen a maximum temperature of 66°F is reached at θ =85°F, the satellite then enters the shadow of the Earth and begins cooling down until, at θ = 250°F and at a temperature of 63°F, the satellite returns to the sun side of the orbit. These results are well within the limits of the satellite systems.

G. 8 HEAT CONDUCTION

All of the calculations derived thus far for SCOPE were based on the assumption that the satellite will be isothermal. That is, enough energy will be conducted through out the satellite such that the temperature at each point can be assumed to be the same. A study was conducted to determine whether this assumption was reasonable. To do this first, the heat on each panel was calculated at some characteristic point in the orbit in order to find the necessary heat conduction rates. These values can be found in chart G. 2. The panel notation is defined in Figure G. 2. Once these values have been ascertained the next step would be to determine the amount of energy which can be transferred around the satellite. The amount of heat which can be transferred from a side panel to an end panel is given by

$$q_1 = (T_1 - T_2)\, A\, K/L$$

where

L = Length of conduction
A = Cross sectional area
K = Thermal conductivity

for q_1

L = 12. 2 in
A = . 31 in^2
K = 2. 67 watts/°F-in

Thus

$$q_1 = .068\ \Delta T \text{ watts/}^{\circ}F$$

The amount of heat which can get transferred from side panel to side panel is

$$q_2 = (T_1 - T_2)\, AK/L$$

where

L = 10. 02 in
A = . 4 in^2
K = 2. 67 (watts/°F-in)

or

$$q_2 = .11\ \Delta T \text{ watts}/^{o}F$$

And the amount of heat which can be transferred from side panel to side panel to means of the support collar is

$$q_3 = (T_o - T_2)\ AK/L$$

where

$L = 10.00$ in
$A = .502$ in^2
$K = 2.67$ watts/^{o}F in

or

$$q_3 = .134\ \Delta T \text{ watts}/^{o}F$$

These values of heat conduction appear to be sufficient to transfer the desired amounts of energy in order to achieve an isothermal condition. Therefore, the assumption made in calculating the satellite's temperatures were reasonable, and the calculation, valid. It should be noted that these values must be thoroughly tested on a full scale mockup of SCOPE before launch for verification and final adjustment of variables.

Figure G. 1

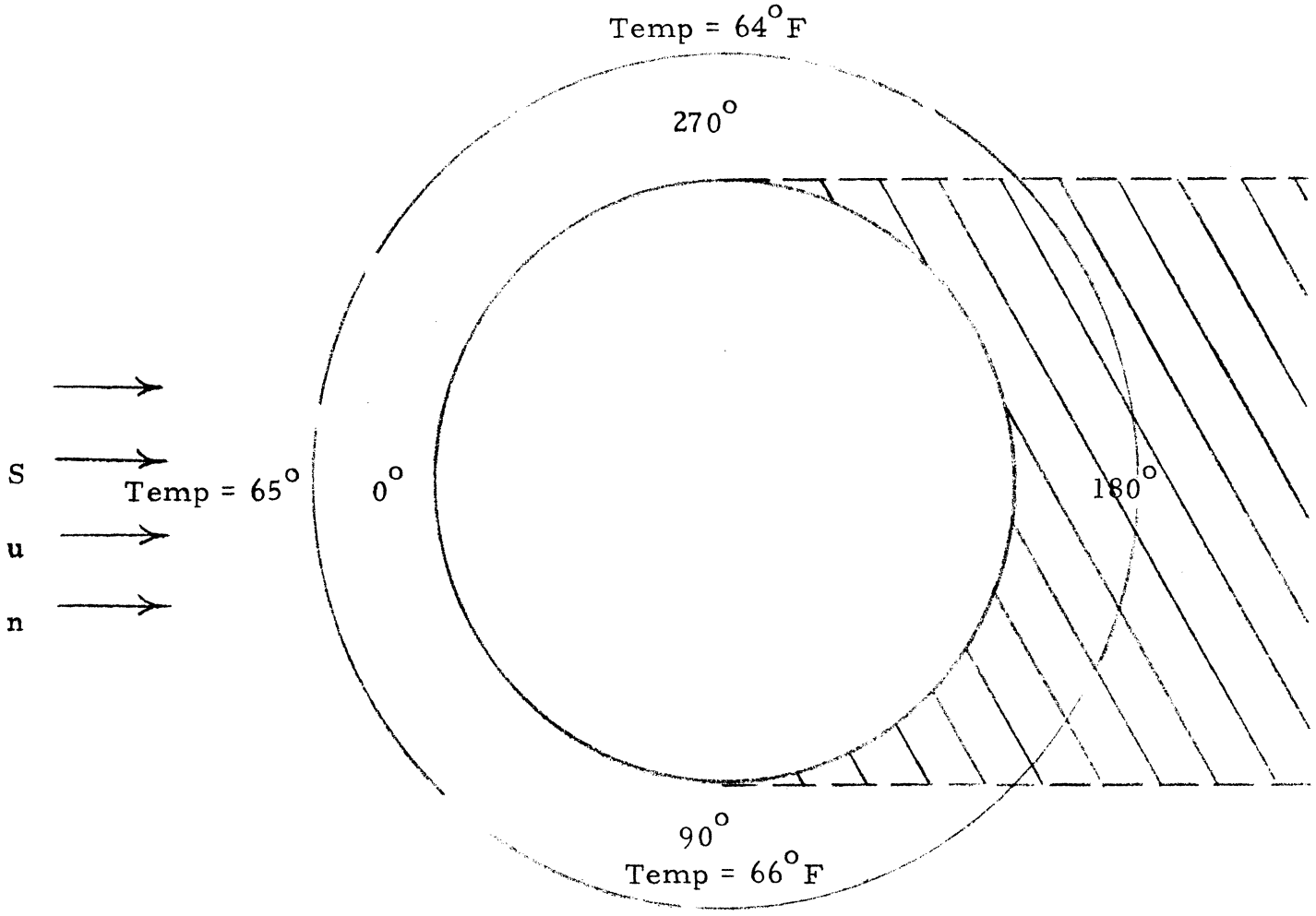

Chart G. 1

Angle (θ^{o})	Temp (^{o}F)
240°	63°
270°	64°
300°	64°
330°	64°
360°	65°
330°	65°
60°	65°
90°	66°

Figure G. 2 Energy Gradient at $\theta = 270^{o}$ (North Pole)

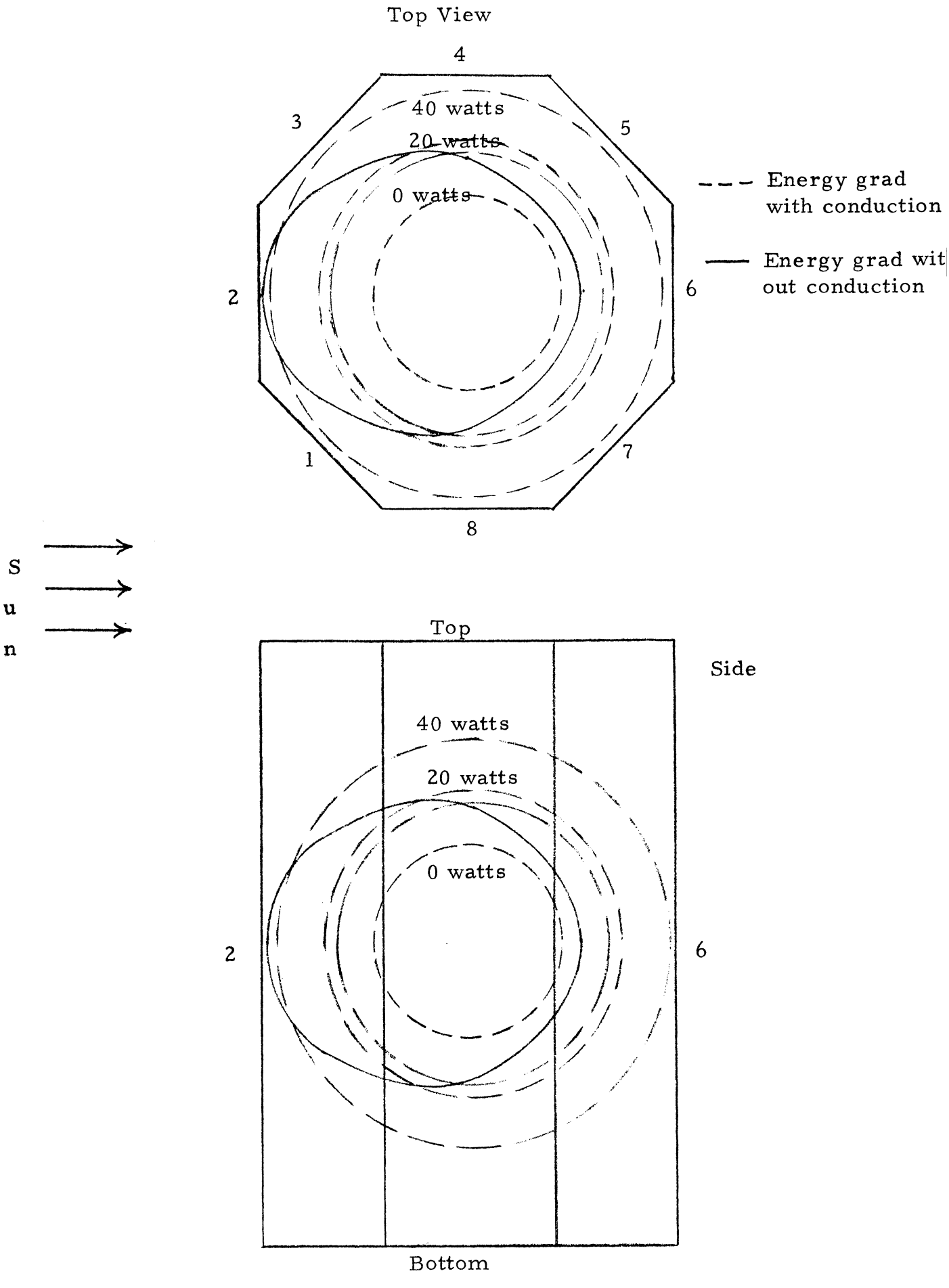

Side	θ^{o}	1	2	3	4	5	6	7	8	T	B
Total	0^{o}	13.7	13.7	13.7	13.7	13.7	13.7	13.7	13.7	55.4	33.3
Energy	180	7.0	7.0	7.0	7.0	7.0	7.0	7.0	7.0	5.8	15.8
Absorbed	90	10.42	10.42	10.42	10.42	36.02	46.62	36.02	10.42	10.0	20.0
(watts)	270	36.02	46.62	36.02	10.42	10.42	10.42	10.42	10.42	10.0	20.0
Ideal Energy (watts)						15.7					19.7
Heat	0^{o}	+2.0	+2.0	+2.0	+2.0	+2.0	+2.0	+2.0	+2.0	-45.4	-13.6
Transfer	90^{o}	5.3	5.3	5.3	5.3	5.3	5.3	5.3	5.3	9.7	-.3
Out	180^{o}	5.28	5.28	5.28	5.28	-20.3	-30.9	-20.3	+5.3	9.7	-.3
(watts)	270^{o}	-20.32	-30.42	-20.32	+5.28	5.28	5.28	5.28	9.7	9.7	-.3

Chart G.2 SCOPE Energy Flux

Figure G. 3 A Program for Determining Actual Temperature of SCOPE

```
$COMPILE
C TO FIND THE AREA PROJECTED TOWARD THE SUN
      DIMENSION C(360)
      C(360) = 3.49
      DO 10 I= 5,120,5
      Z = .0174*I
      APS = ABS(3.49*COS(Z))+ABS(6.95*SIN(Z))
      C(I) = APS
      J = 360-I
      C(J) = APS
 10   CONTINUE
C
C TO FIND TEMPERATURE EVERY 5 DEGREES OF ORBIT
      READ (5,100) TEMP,A,E,ENUM,ENUM 2,ENUM 3,ENUM 4,ENUM 5
 100  FORMAT (8F8.0)
C 250≤Θ≤270°
      DO 59 K = 240,270,30
      Q=84.0
      T1 = TEMP
      T2 = TEMP
      PAS = C(K)
      SUM = PAS*130.*A+105.9*E+Q
 52   D = (T1-T2)*602.1+SUM-26.7*E*5.0E-10*T2**4
      IF (ABS(D) .LE.ENUM) GO TO 58
      IF (D) 53,58,54
 53   T2 = T2-.07
      GO TO 52
 54   T2 = T2+.05
      GO TO 52
 58   TEMP = T2
      WRITE (6,200) K, TEMP
 200  FORMAT ('0K= 'I3' TEMP = 'F5.0)
 59   CONTINUE
C
C 275°≤ Θ ≤ 360°
      DO 69 KK = 300,360,30
      Q = .0174*KK
      Q = 84
      T1 = TEMP
      T2 = TEMP
      PAS = C(KK)
      SUM = PAS*130.*A+150.9*E+Q+41.4*3.49*A
 62   D = (T1-T2)*602.1+SUM-26.7*E*5.E-10*T2**4
      IF (ABS(D) .LE.ENUM 2) GO TO 68
      IF (D) 63,68,64
 63   T2 = T2-.07
      GO TO 62
 64   T2 = T2+.05
      GO TO 62
 68   TEMP = T2
      WRITE (6,200) KK, TEMP
 69   CONTINUE
C
C 0°≤ Θ ≤ 85°
      DO 79 KKK = 30,90,30
      Q = .0174*KKK
      Q = 84.
      T1 = TEMP
      T2 = TEMP
      PAS = C(KKK)
```

```
      SUM = PAS*130.*A+150.9*E+Q+41.4*3.49*A
 72   D = (T1-T2)*602.1+SUM-26.7*E*5.E-10*T2**4
      IF (ABS(D) .LE.ENUM 3) GO TO 78
      IF (D) 73, 78, 74
 73   T2 = T2-.07
      GO TO 72
 74   T2 = T2+.05
      GO TO 72
 78   TEMP = T2
      WRITE (6,200) KKK,TEMP
 79   CONTINUE
C
C 90° ≤ θ ≤ 110°
      Q = 84.
      T1 = TEMP
      T2 = TEMP
      PAS = C(120)
      SUM = PAS*130.*A+150.9*E+Q
 82   D = (T1-T2)*602.1+SUM-26.7*E*5.E-10*T2**4
      IF (ABS(D) .LE.ENUM 4) GO TO 88
      IF (D) 83, 88, 84
 83   T2 = T2-.07
      GO TO 82
 84   T2 = T2+.05
      GO TO 82
 88   TEMP = T2
      WRITE (6,200) K2,TEMP
C
C 115°≤ θ°≤ 245°
      DO 99 KDARK = 150,210,30
      Q = 48
      T1 = TEMP
      T2 = TEMP
 92   D = (T1-T2)*602.1+105.9*E+16.-26.7*E*5.E-10*T2**4+Q
      IF (ABS(D) .LE.ENUM 5) GO TO 98
      IF (D) 93, 98, 94
 93   T2 = T2-.07
      GO TO 92
 94   T2 = T2 +.05
      GO TO 92
 98   TEMP = T2
      WRITE (6,200) KDARK, TEMP
 99   CONTINUE
      END
```

ACKNOWLEDGMENTS

We wish to extend appreciation to those persons whom have helped make Project SCOPE a success. They are

Dr. Fred L. Bartman, Prof. of Meterology and Oceanography, U of M

Dr. E. A. Bortner, General Electric Co., Space Division

Dr. Harold Goldstein, General Electric Co., Space Division

Prof. Harm Buning, Prof. of Aerospace Engineering, U of M

Mr. James Florek, Bendix Aerospace Division

Mr. R. C. Gibson, Bendix Aerospace Division

Mr. William R. Polye, Bendix Navigation and Control Division

Mr. John Horvath, Space Physics Lab., U of M

Mr. Don Lowe, Bendix Aerospace Division

Dr. William F. Powers, Prof. of Aerospace Engineering, U of M

Dr. Lawrence L. Rauch, Prof. of Inf. and Control Eng., U of M

Dr. Marlin Ristenbatt, Res. Eng., Elec. and Comp. Eng., U of M

Mr. John J. Pacey, Vought Missiles and Space Company

Dr. David L. Sikarskie, Prof. of Aerospace Engineering, U of M

Mr. Richard Simms, Bendix Aerospace Division

Mr. Robert H. Pickard, NASA Goddard Space Flight Center

Mr. William S. West, NASA Goddard Space Flight Center

We wish to extend deep appreciation to Prof. Wilbur C. Nelson of The University of Michigan for his guidance throughout the project. Sincere thanks go to the Aerospace Engineering Departmental Secretaries for their assistance, especially to Caroline Rehberg for her efforts in the typing of this report.

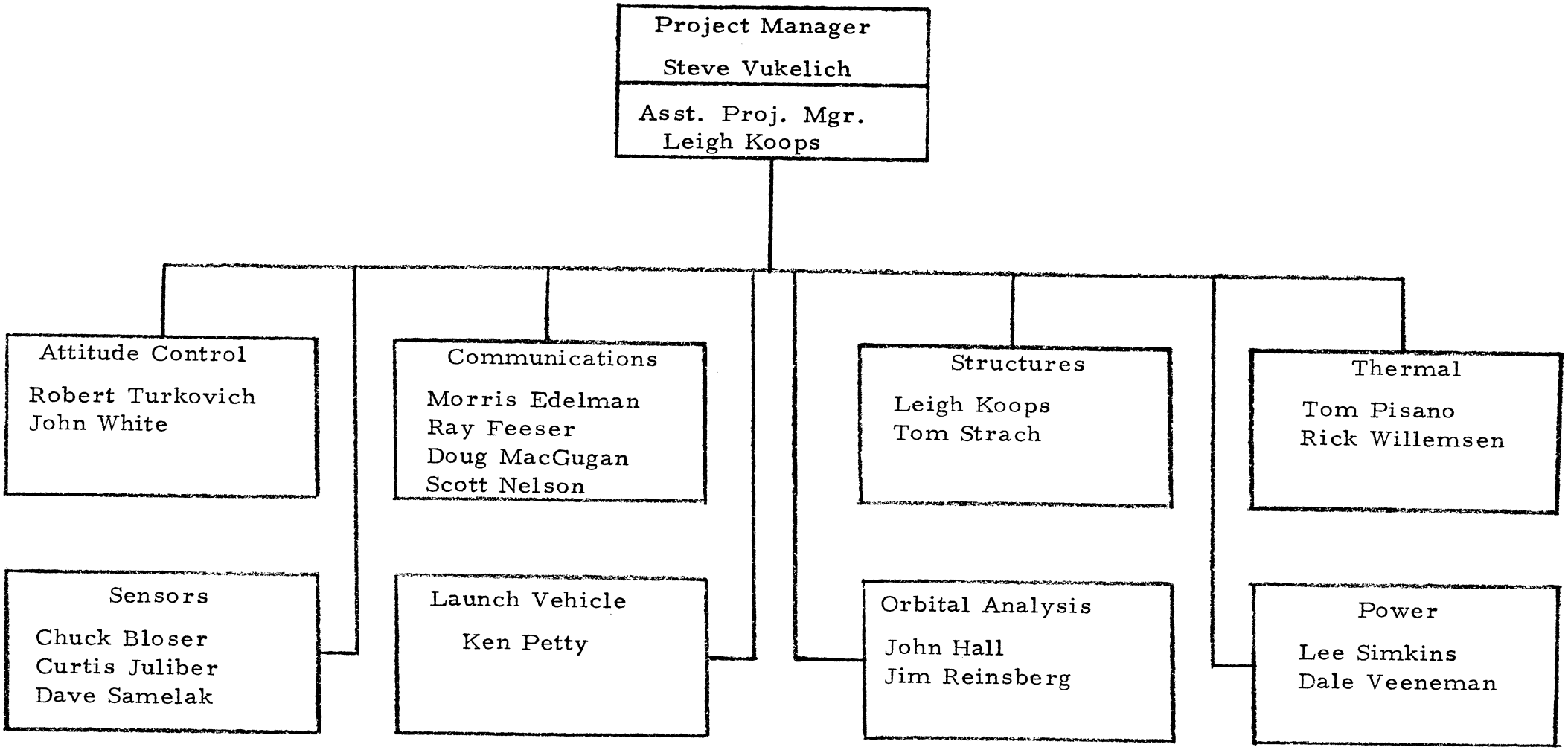
Project Manager
Steve Vukelich
Asst. Proj. Mgr.
Leigh Koops
Attitude Control
Robert Turkovich
John White
Communications
Morris Edelman
Ray Feeser
Doug MacGugan
Scott Nelson
Structures
Leigh Koops
Tom Strach
Thermal
Tom Pisano
Rick Willemsen
Sensors
Chuck Bloser
Curtis Juliber
Dave Samelak
Launch Vehicle
Ken Petty
Orbital Analysis
John Hall
Jim Reinsberg
Power
Lee Simkins
Dale Veeneman

UNIVERSITY OF MICHIGAN
3 9015 03483 8022